UNIVERSITY OF CALIFORNIA
RIVERSIDE

Noise-Induced Hearing Loss Leads to Cortical Region-Specific Central Gain and Temporal Processing Recovery

A Dissertation submitted in partial satisfaction
of the requirements for the degree of

Doctor of Philosophy

in

Neuroscience

by

Jamiela Kokash

December 2022

Dissertation Committee:
Dr. Khaleel Abdulrazak, Chairperson
Dr. Iryna Ethell
Dr. Peter Hickmott

The Dissertation of Jamiela Kokash is approved:

_____

_____

_____

Committee Chairperson

University of California, Riverside

Acknowledgements

Part of the text of this dissertation, Chapter 2, is a reprint of the material as it appears in Kokash, et al., 2018. The co-author, Khaleel Razak, directed and supervised the research. Co-authors Erin M. Alderson and Sarah M. Reinhard helped with experiments. Co-authors Cynthia A. Crawford, Devin K. Binder, and Iryna M. Ethell provided input on the manuscript.

To my parents - thank you for supporting all the decisions that led me to this point. Your advice, guidance, and faith in me was unparalleled. To my siblings – Tammy, Freddie, and Khaurontha – thank you for your unconditional support. Your persistence and insistence that I take breaks and hang out with you has helped immensely during grad school, even if I could not see it at the time. All of your cheering, love, and support has been heard and acknowledged, and I hope to continue to make you all proud.

From the earlier Razak era, thank you to all of my labmate friends who were there to inspire me – Teresa, Anna, Dustin, Sarah, Jonny, Jeff, and Katherine. Your own journeys and roles in lab set me on this path and I would not have continued without your advice. Thank you for all the laughs, late nights, experiments, conversations, and adventures we had on and off campus. You all made the basement a brighter and warmer place to be in. I was sad when you all left to tackle bigger and better things, but you continue to inspire me with the directions you chose. To my current Razak labmates – Mawaheb, Xin, Kati, and Anjum – I couldn't have asked for a better team in getting past the pandemic hardships. Thank you for letting me into your lab lives and passing on our lab expertise, your constancy and friendships made it easier to get through these past couple years.

To the friends outside of lab that I have made along the way, school would have been much quieter and lonelier without you. My Floobes – Quynh and Susan – your acceptance and encouragement has truly helped me grow. My Squadge – Q, S, Andrea, and Anjum – thank you for all the laughs and cuddles, and for pushing me to experience new adventures and getting me out of my comfort zone. I would be remiss if I didn't mention the Neuroscience Graduate Student Association (NGSA). To everyone who I have worked with through this capacity, thank you for your support of our endeavors and for making our visions become reality.

Most importantly, thank you to my advisor – Dr. Khaleel Razak. Thank you taking me into your lab as a technician all those years ago, and for believing that I could do more as a graduate student. Your guidance, advice, and mentorship as a neuroscientist and teacher are more than I could have asked for.

Funding sources received was the UC President's Pre-Professoriate Fellowship from 2021-2022.

Dedication

I would like to dedicate this dissertation to my parents, Mahmoud and Chanpim. Your unwavering faith in me has kept me going in furthering my education and endeavors. Shukran jazeelan for your constant support, love, and sacrifices to get me where I am today. I love you both to the moon and back.

To my nieces – Avery and Amirah – my little munchkins: this is also for you. I want to show you that the sky is the limit. You can do anything you put your mind to and achieve your wildest dreams.

ABSTRACT OF THE DISSERTATION

Noise-Induced Hearing Loss Leads to Cortical Region-Specific Central Gain and Temporal Processing Recovery

by

Jamiela Kokash

Doctor of Philosophy, Graduate Program in Neuroscience
University of California, Riverside, December 2022
Dr. Khaleel A. Razak, Chairperson

Noise-induced hearing loss (NIHL) is a major cause of auditory processing impairment and major cognitive impairment. Peripherally, cochlear hair cell damage has been studied extensively in NIHL. Fewer studies have looked at effects more centrally, but these studies have led to the emerging theory of 'central gain'. The lack of peripheral input (deafferentation) following NIHL increases gain in central auditory regions, leading to exaggerated spontaneous and sound evoked responses. These responses may lead to tinnitus and hyperacusis, for which currently there are no treatment to reduce these comorbidities following NIHL. The cellular mechanisms underlying the increased gain is unclear, however we hypothesize that neuroinflammation and matrix-metalloproteinase-9 (MMP-9) are upregulated following NIHL causing disruption in population level activity ultimately leading to enhanced central gain and temporal processing. To address this gap, we designed a series of experiments to identify the effects of NIHL in the brain. We have made several key findings. Firstly, there is a cortical-region specific difference in temporal processing, but not in sound detection and recovery following NIHL. Second, MMP-9

activity is not upregulated at 1-day post-NIHL. Last, minocycline enhances sound detection amplification after hearing loss, but does not affect temporal processing or auditory brainstem thresholds. Our data provides insight into longitudinal modulations of sound detection and temporal processing in auditory cortical regions with potential time course and therapeutic targets.

Table of Contents

Chapter 6

List of Tables

List of Figures

Chapter 1

Introduction

Noise induced hearing loss (NIHL) is a leading form of sensorineural hearing loss where exposure time and intensity determine the amount of hearing loss. Loud and sudden sounds like explosions or long-term exposure like heavy machinery can have lasting detrimental effects (Rabinowitz 2000) on the auditory system, both peripherally and centrally. Quality of life can be affected, where the consequences may bleed into daily activities and interactions (Chepesiuk 2005; Seidman and Standring 2010; Alamgir et al. 2016), and even may become comorbid with phenomena like tinnitus and hyperacusis (Attias et al. 1993; Henderson et al. 2011; Möhrle et al. 2019; Sun et al. 2012). Preventative measures can be taken (Lynch and Kil 2005; Martin 2008; Prasher 1998), but potential therapeutic approaches have yet to put forth a standard treatment (Le Prell et al. 2007; Prasher 1998) to address the many effects stemming from NIHL. Many studies have found the amount and type of damage that occurs in peripheral auditory structures (Kujawa and Liberman 2009), but the lack of regeneration abilities after cochlear structure ablation inhibits restoration options outside of preventative measures. Central auditory consequences are also being identified and could provide possible targets for alleviation of the cascading effects of NIHL, especially for long-term and comorbid consequences of NIHL. The cellular mechanisms underlying increased central auditory responses is unclear, but our hypothesis is that following NIHL, an endopeptidase called matrix metalloproteinase-9 (MMP-9) activity is upregulated in the auditory cortex which leads to perineuronal net (PNN) degradation. This degradation in turn can lead to reduced

parvalbumin-positive inhibitory neurons (PV+) excitability which could cause an imbalanced cortical network to skew towards hyperexcitable.

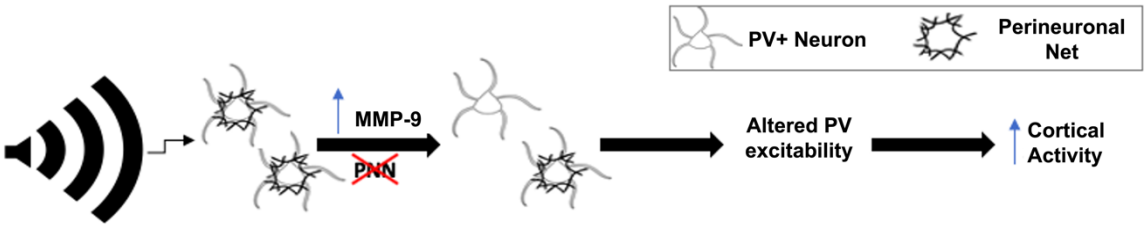

Figure 1. Diagram of working hypothesis on central gain mechanism following NIHL. High intensity sound stimulus will cause molecular and neuronal firing changes in the auditory cortex.

NIHL leads to central gain throughout the auditory pathway

'The central gain model' has emerged to link the peripheral deafferentation to exaggerated responses in the central auditory system following NIHL. A common finding is a lack of auditory brainstem responses (ABRs), but enhanced responses in the auditory cortex (Chambers et al. 2016; Resnik and Polley 2021). The central gain model is an emerging theory that may provide a basis for central auditory effects after NIHL. Many studies have compared enhanced gain control in the auditory cortex and inferior colliculus, but the temporal dynamics and recovery of responses is determined by the paradigm of sound exposure (R. J. Salvi et al. 1990; Syka, Rybalko, and Popelář 1994). Dynamic gain control has been implicated throughout the auditory lemniscal pathway, where long-term increases in spontaneous activity was seen in the dorsal cochlear nucleus (Zhang and Kaltenbach 1998) of rats and elevated inferior colliculus sound-evoked activity due to long-term low level sound-exposure although there was a recovery one week later (Sheppard et al. 2017). Decreases in auditory nerve compound potentials (R. Salvi et al. 2017) lead to

increased auditory cortex spontaneous activity following noise-exposure (Auerbach, Rodrigues, and Salvi 2014; Sun et al. 2012). A series of cat studies reported higher spontaneous activity and burst firing in primary auditory cortex (Eggermont and Komiya 2000; Noreña and Eggermont 2003; Seki and Eggermont 2003) as a neural correlate of tinnitus. Hyperactivity in the auditory cortex may manifest as increased spontaneous activity, where the balance between excitation and inhibition is altered. Ultimately this outcome may serve as a compensatory mechanism after deafferentation from the cochlea or sensory deprivation, where normal auditory input is unable to be transmitted due to peripheral damage or lack of connection coming from the cochlea (Cody and Robertson 1983; Haragopal et al. 2020; Kujawa and Liberman 2009).

Potential mechanism underlying central gain

Noise-exposure in guinea pigs compromised the blood-labyrinth barrier allowing for increased permeability in the stria vascularis of the cochlea that coincided with increased MMP-9 expression (Wu et al. 2017). This may trigger an inflammatory response along the auditory system that induces cytokines to synthesize and secrete MMP-9 (Gordon et al. 2009), further increasing protease activity and causing a cascade that eventually induces cortical plasticity. The result of which triggers extracellular degradation and altered cellular activity, particularly in inhibitory transmission. The output of the cortical response will lean towards homeostatic balance, but the lack of input reduces its ability to do so. Compensatory gain increases were found to be beneficial for sensory processing in the auditory cortex (Chambers et al. 2016), however if left unimpeded the compensation of excessive spontaneous firing may push past homeostasis and manifest as

hyperactivity (Möhrle et al. 2019; Rüttiger et al. 2013) that may underlie tinnitus and hyperacusis. Other factors like synaptic zinc has been implicated in regulating cortical gain and plasticity (Nakashima and Dyck 2009; McAllister and Dyck 2017), recently found to modulate inhibitory (Anderson et al. 2017; Kouvaros, Kumar, and Tzounopoulos n.d.) alongside excitatory (Anderson et al. 2015; Kalappa et al. 2015) transmission. However, the mechanism for which increased central gain and cortical responses after NIHL are not well understood. This may be a result of the interaction between PNNs and MMP-9 of the proposed hypothesis (Figure 1), where MMP-9 leads to the molecular changes that are linked to abnormal cortical function.

MMP-9 as a key upstream effector following trauma

MMP-9 is a zinc-dependent protease, known to cleave extracellular matrix. It is synthesized and secreted as a zymogen, which is an inert form of the protein. It must have its prodomain cleaved, as its active site that contains the catalytic zinc ion is blocked by a cysteine and histidine coordination (Van Den Steen et al. 2002). One way in which MMP-9 is activated is by another matrix-metalloproteinase – MMP-3. Ogata et al (Ogatas, Enghildp, and Nagasesll 1992) discovered that MMP-3 acts upon proMMP-9 in a stepwise manner, initially cleaving it from its 92kDa form to the 86kDa intermediate form by removing several amino acids, to its final 82kDa form of the active enzyme by making additional necessary amino acids accessible for removal. Once in its active form, it can cleave various types of extracellular matrix components, shown to target PNNs in particular (Alaiyed et al. 2019). Genetic manipulations reducing MMP-9 expression in a mouse model of Fragile X Syndrome revealed recovered PNN expression and cortical

activity compared to wild type (Wen, Afroz, et al. 2018). Inhibiting MMP-9 proteolytic activity rescued normal PV/PNN maturation in a schizophrenia model (Dwir et al. 2019) and introduces structural plasticity in light reintroduction after dark exposure (Murase, Lantz, and Quinlan 2017). In human patients diagnosed with epilepsy, MMP-9 was found to be at higher concentrations in obtained cerebrospinal fluid indicating a disrupted blood brain barrier and leukocyte infiltration into the central nervous system(Li et al. 2013). In the rodent model, MMP-9 facilitated seizure induction (Szklarczyk et al. 2002) and dendritic remodeling in the hippocampus (Wilczynski et al. 2008). This connection is promising in that there appears to be a link between the rescue of PNN and the downregulation of MMP-9, where the current set of studies will test the link between them following NIHL.

PNNs are experience-dependent and plastic

The extracellular matrix is made of many diverse components, but the one of particular interest is the perineuronal net. This structure is composed of a few key conserved components – chondroitin sulfate proteoglycans (CSPGs), hyaluronan, tenascin, and link proteins (Wen, Binder, et al. 2018). The hyaluronan are long polysaccharide chains that attach to the cell surface as well as CSPGs. These proteoglycans are part of the lectican family, of which 4 have been found to be constituents of PNNs. They are composed of a core protein with various number of repeating glycosaminoglycan chains. This allows for the diversity of the lectican family – aggrecan, brevican, versican, and neurocan (Yamaguchi 2000). Together, these components make up PNN structures that ensheath cell bodies and proximal dendrites of various cell types (Fader et al. 2016;

Reichelt et al. 2019). A main feature of PNNs are its association with critical period plasticity. Pizzorusso (2002) found that sensory deprived rodents' slower development in the visual cortex that coincided with delayed PNN congregation. In relation to this study, the question builds upon the notion of sensory deprivation and plasticity of the auditory system. For auditory sensory deprivation caused by NIHL, will there be a sort of experience-dependent plasticity that underlies cortical dysregulation? This will harm the integrity of the structure, causing it to lose its ability to filter out detrimental factors that may target the neurons they are protecting, in particular PV+ neurons.

PV+ interneurons are important in cortical circuitry

PV+ interneurons are a subset of GABAergic cells that provide mainly inhibitory input to cortical pyramidal cells. The interneurons make up about 20% of cell types in the cortex, of which 10-20% are PV-positive (Oviedo 2017). Yet, these specific neurons provide an important role for normal cortical excitation/inhibition balance and oscillatory maintenance due to their unique intrinsic properties. PV+ cells have been characterized as fast-spiking and have rapid repolarization that allow them to fire rapid trains of action potentials (Kawaguchi et al. 1987). This allows them to regulate cortical output by projecting onto pyramidal cell bodies and proximal dendrites in the cerebral cortex (Ferguson et al. 2018). They modulate feedforward inhibition and dynamic gain control (Ferguson et al. 2018; Moore and Wehr 2013). Specific properties in the auditory cortex include temporal resolution (Wehr and Zador 2003), regulate cortical responses to intensity and frequency(Moore and Wehr 2013), and shape receptive fields (Wang et al. 2002) through inhibitory input. PV+ has been posited to act as a gating mechanism for

feedforward activity in cortical circuits, modulating local connectivity (Hamilton et al. 2013). In the case of PV dysfunction, the overall cortical output would lean towards hyperactivity with the lack of inhibition to regulate excitatory output. This may be the underlying mechanism of the central gain theory. Another output of PV neurons is generating and modulating cortical oscillations, particularly at the gamma frequencies (30-80Hz) (Chen et al. 2017; Sohal et al. 2009), to provide synchronous neuronal interactions (Womelsdorf et al. 2007) important for information processing (Bartos, Vida, and Jonas 2007). The consequences of NIHL then would posit to be reduced gamma power as well as increased gain as manifested by increased spontaneous activity, seen in the last two parts of the working hypothesis (Figure 1).

NIHL could lead to a molecular cascade in the AC

PNNs are primarily found to be associated with inhibitory interneurons. PNNs are an integral structure to enhance excitatory output of PV neurons (Balmer 2016), where the degradation of PNNs reduced the gain and excitation of cortical fast-spiking interneurons. Another role these encapsulating structures have been to provide protection from oxidative stress (Cabungcal et al. 2013), in order for the enwrapped neurons to function normally. This is harmful because noise-exposure causes an increase in oxidative stress throughout the auditory system (Evans and Halliwell 1999; Henderson et al. 2006) as well as cognitive associated regions like the hippocampus (Cheng et al. 2011; Liu et al. 2018; Shukla et al. 2019). Maintaining the integrity of the extracellular architecture surrounding PV cells may mitigate the effects of NIHL. While other MMPs and zinc-dependent proteases cleave various components of PNNs (Bozzelli et al. 2018), MMP-9 proves to be a promising

candidate to target as a central upstream effector, as the cascade following NIHL in the auditory cortex can be blocked before degradation occurs.

Minocycline as an NIHL treatment by targeting MMP-9

Minocycline is a tetracycline derived antibiotic drug that also acts as an MMP-9 inhibitor. Despite its main function of antimicrobial properties, it has been prescribed as a treatment for many other cases. Clinically, minocycline has been used to treat acne as opposed to other tetracyclines, with some success (Eady et al. 1993; Hubbell et al. 1982). The drug has also been found to work against inflammatory activity, as reported in studies focused on cerebral (Chaturvedi and Kaczmarek 2014; Yrjänheikki et al. 1999), liver (Jiang, Desjardins, and Butterworth 2009), renal (Kelly et al. 2004), and retinal ischemia (Abcouwer et al. 2013). As a therapeutic pharmacological treatment, its merits include crossing the blood-brain barrier (Saivin and Houin 1988), anti-inflammatory capabilities (Abcouwer et al. 2013; Garwood et al. 2010), and ion chelating properties such as iron (Grenier, Huot, and Mayrand 2000) and calcium (Antonenko et al. 2010). In relation to MMP-9, several studies have determined the effectiveness of minocycline as an inhibitor, more potent than other tetracyclines and antibiotics (Modheji et al. 2016; Vandooren et al. 2017). Cancer drug administrations have also been tested for efficacy in reducing MMP-9, with diverse results of either no MMP-9 specific effect (Vandooren et al. 2017) or decreasing expression (Shi, Zhang, and Yin 2015). Different drug treatments affect MMP-9 in multiple ways, where azithromycin was found to decrease gene and mRNA expression while minocycline decreased MMP-9 activity (Vandooren et al. 2017). As this study is aiming to determine the trajectory of MMP-9 activity following noise-exposure,

minocycline as an inhibitor appears to be a leading choice in reversing the effects of NIHL in the auditory cortex. Minocycline is an FDA approved antibiotic drug that reduces MMP-9 activity (Dziembowska et al. 2013; Chaturvedi and Kaczmarek 2014; Siller and Broadie 2012). If minocycline proves to be effective, it can be readily available for human use or testing as a potential treatment for NIHL.

In chapter 2, we examined electroencephalography (EEG) recordings used in this study to allow for obtaining and analyzing various measurements from the auditory cortex at a population level in a within-subject design. Specifically, this study looked at auditory evoked potentials (ERPs) and intertrial phase coherence (ITPC) to measure changes in the auditory and frontal cortex at different timepoints after noise-induced hearing loss. The benefit of using EEGs was that we were able to design a longitudinal experiment that allowed us to record from the AC and FC over a longer period in awake mice.

Chapter 3 looks at molecular changes after NIHL in the AC. Wang et al. (2019) found that neuroinflammation in the auditory cortex following NIHL was upregulated, specifically various proinflammatory cytokine expression at different times – 12 hours, 1-, 3-, and 10 days. We targeted specific time points to determine if changes in MMP-9 activity or PNN degradation had occurred after NIHL. For MMP-9, we chose 1 day after NIHL to measure activity within the AC across cortical layers. PNN density and intensity was measured around the time points from Nguyen, Khaleel, and Razak (2017), specifically 23-65 days post-NIHL.

For Chapter 4, we administered an acute minocycline treatment after NIHL and recorded EEGs. Beginning immediately after noise-exposure, mice were given either saline or minocycline (45mg/kg, i.p.) daily for 5 days. We recorded ERPs, resting EEG power, 40-Hz ASSR, and gap-ASSR at 5-, 10-, and 23 days after NIHL.

Chapter 5 was written and published in 2019, titled *Genetic reduction of MMP-9 in the Fmr1 KO mouse partially rescues prepulse inhibition of acoustic startle response* (Kokash et al. 2019). This study showed how MMP-9 regulation alters behavioral output in a Fragile X Syndrome (FXS) mouse model. We found that MMP-9 expression was increased in the FXS KO group compared to wild-type in the inferior colliculus, which is an integral region in the central auditory and pre-pulse inhibition (PPI) pathways. By genetically reducing MMP-9 in a heterozygous adult mouse model, the PPI deficit was reversed.

The underlying mechanism that leads to increased central auditory hyperactivity following NIHL, often associated with tinnitus and hyperacusis, has yet to be determined. Many studies outlining the consequences of NIHL in the cochlea and auditory nerve fibers have been identified as well as increased central gain. This dissertation aims to identify changes in the auditory and frontal cortex (AC, FC) over time via electrophysiological and molecular assays. These deficits may not be immediate and may accumulate over specific time courses. The proposed study will identify the trajectory of changes at both the molecular and population activity level within the auditory cortex that may lead to increased spontaneous activity and altered temporal processing underlying the central gain theory. Matrix metalloproteinase-9 may be the initial catalyst that leads to overall cortical

hyperexcitability, potentially underlying central gain. The working hypothesis of this study is that MMP-9 activity is up-regulated as an outcome of NIHL that triggers a cascade of molecular and electrophysiological changes in the auditory cortex. As a result, perineuronal nets (PNNs) are degraded which compromises the structural integrity of the extracellular space surrounding integral neurons that modulate cortical activity. This pushes the auditory cortex towards a hyperactive state, as the parvalbumin-positive (PV+) inhibitory interneurons become dysfunctional and their inhibitory output onto pyramidal cells is disrupted. This would manifest as increased spontaneous firing, or gain (Figure 1), potentially at the expense of temporal processing capabilities.

1. Abcouwer, S. F., Lin, C. mao, Shanmugam, S., Muthusamy, A., Barber, A. J., & Antonetti, D. A. (2013). Minocycline prevents retinal inflammation and vascular permeability following ischemia-reperfusion injury. *Journal of Neuroinflammation*, *10*(1), 913. https://doi.org/10.1186/1742-2094-10-149

2. Alaiyed, S., Bozzelli, P. L., Caccavano, A., Wu, J. Y., & Conant, K. (2019). Venlafaxine stimulates PNN proteolysis and MMP-9-dependent enhancement of gamma power; relevance to antidepressant efficacy. *Journal of Neurochemistry*. https://doi.org/10.1111/jnc.14671

3. Alamgir, H., Turner, C. A., Wong, N. J., Cooper, S. P., Betancourt, J. A., Henry, J., … Packer, M. D. (2016). The impact of hearing impairment and noise-induced hearing injury on quality of life in the active-duty military population: Challenges to the study of this issue. *Military Medical Research*. BioMed Central Ltd. https://doi.org/10.1186/S40779-016-0082-5

4. Anderson, C. T., Kumar, M., Xiong, S., & Tzounopoulos, T. (2017). Cell-specific gain modulation by synaptically released zinc in cortical circuits of audition. *ELife*, *6*. https://doi.org/10.7554/eLife.29893

5. Anderson, C. T., Radford, R. J., Zastrow, M. L., Zhang, D. Y., Apfel, U. P., Lippard, S. J., & Tzounopoulos, T. (2015). Modulation of extrasynaptic NMDA receptors by synaptic and tonic zinc. *Proceedings of the National Academy of Sciences of the United States of America*, *112*(20), E2705–E2714. https://doi.org/10.1073/pnas.1503348112

6. Antonenko, Y. N., Rokitskaya, T. I., Cooper, A. J. L., & Krasnikov, B. F. (2010). Minocycline chelates Ca2+, binds to membranes, and depolarizes mitochondria by formation of Ca2+-dependent ion channels. *Journal of Bioenergetics and Biomembranes*, *42*(2), 151–163. https://doi.org/10.1007/s10863-010-9271-1

7. Attias, J., Urbach, D., Gold, S., & Shemesh, Z. (1993). Auditory event related potentials in chronic tinnitus patients with noise induced hearing loss. *Hearing Research*, *71*(1–2), 106–113. https://doi.org/10.1016/0378-5955(93)90026-W

8. Auerbach, B. D., Rodrigues, P. V., & Salvi, R. J. (2014). Central Gain Control in Tinnitus and Hyperacusis. *Frontiers in Neurology*, *5*. https://doi.org/10.3389/fneur.2014.00206

9. Balmer, T. S. (2016). Perineuronal Nets Enhance the Excitability of Fast-Spiking Neurons. *ENeuro*, *3*(4). https://doi.org/10.1523/ENEURO.0112-16.2016

10. Bartos, M., Vida, I., & Jonas, P. (2007, January). Synaptic mechanisms of synchronized gamma oscillations in inhibitory interneuron networks. *Nature Reviews*

Neuroscience. Nature Publishing Group. https://doi.org/10.1038/nrn2044

11. Bozzelli, P. L., Alaiyed, S., Kim, E., Villapol, S., & Conant, K. (2018). Proteolytic Remodeling of Perineuronal Nets: Effects on Synaptic Plasticity and Neuronal Population Dynamics. https://doi.org/10.1155/2018/5735789

12. Cabungcal, J. H., Steullet, P., Morishita, H., Kraftsik, R., Cuenod, M., Hensch, T. K., & Do, K. Q. (2013). Perineuronal nets protect fast-spiking interneurons against oxidative stress. *Proceedings of the National Academy of Sciences of the United States of America*, *110*(22), 9130–9135. https://doi.org/10.1073/pnas.1300454110

13. Chambers, A. R., Resnik, J., Yuan, Y., Whitton, J. P., Edge, A. S., Liberman, M. C., & Polley, D. B. (2016). Central Gain Restores Auditory Processing following Near-Complete Cochlear Denervation. *Neuron*, *89*(4), 867–879. https://doi.org/10.1016/j.neuron.2015.12.041

14. Chaturvedi, M., & Kaczmarek, L. (2014). MMP-9 inhibition: A therapeutic strategy in ischemic stroke. *Molecular Neurobiology*. Humana Press Inc. https://doi.org/10.1007/s12035-013-8538-z

15. Chen, G., Zhang, Y., Li, X., Zhao, X., Ye, Q., Lin, Y., … Zhang, X. (2017). Distinct Inhibitory Circuits Orchestrate Cortical beta and gamma Band Oscillations. *Neuron*, *96*(6), 1403-1418.e6. https://doi.org/10.1016/j.neuron.2017.11.033

16. Cheng, L., Wang, S. H., Chen, Q. C., & Liao, X. M. (2011). Moderate noise induced cognition impairment of mice and its underlying mechanisms. *Physiology & Behavior*, *104*(5), 981–988. https://doi.org/10.1016/J.PHYSBEH.2011.06.018

17. Chepesiuk, R. (2005). Decibel hell. *Environmental Health Perspectives*. Public Health Services, US Dept of Health and Human Services. https://doi.org/10.1289/ehp.113-a34

18. Cody, A. R., & Robertson, D. (1983). Variability of noise-induced damage in the guinea pig cochlea: Electrophysiological and morphological correlates after strictly controlled exposures. *Hearing Research*, *9*(1), 55–70. https://doi.org/10.1016/0378-5955(83)90134-X

19. Dwir, D., Giangreco, B., Xin, L., Tenenbaum, L., Cabungcal, J. H., Steullet, P., … Do, K. Q. (2019). MMP9/RAGE pathway overactivation mediates redox dysregulation and neuroinflammation, leading to inhibitory/excitatory imbalance: a reverse translation study in schizophrenia patients. *Molecular Psychiatry*, 1–16. https://doi.org/10.1038/s41380-019-0393-5

20. Dziembowska, M., Pretto, D. I., Janusz, A., Kaczmarek, L., Leigh, M. J., Gabriel, N.,

… Tassone, F. (2013). High MMP-9 activity levels in fragile X syndrome are lowered by minocycline. *American Journal of Medical Genetics, Part A*, *161*(8), 1897–1903. https://doi.org/10.1002/ajmg.a.36023

21. Eady, E. A., Jones, C. E., Gardner, K. J., Taylor, J. P., Cove, J. H., & Cunliffe, W. J. (1993). Tetracycline-resistant propionibacteria from acne patients are cross-resistant to doxycycline, but sensitive to minocycline. *British Journal of Dermatology*, *128*(5), 556–560. https://doi.org/10.1111/j.1365-2133.1993.tb00235.x

22. Eggermont, J. J., & Komiya, H. (2000). Moderate noise trauma in juvenile cats results in profound cortical topographic map changes in adulthood. *Hearing Research*, *142*(1–2), 89–101. https://doi.org/10.1016/S0378-5955(00)00024-1

23. Evans, P., & Halliwell, B. (1999). Free radicals and hearing: Cause, consequence, and criteria. In *Annals of the New York Academy of Sciences* (Vol. 884, pp. 19–40). New York Academy of Sciences. https://doi.org/10.1111/j.1749-6632.1999.tb08633.x

24. Fader, S., Imaizumi, K., Yanagawa, Y., & Lee, C. (2016). Wisteria Floribunda Agglutinin-Labeled Perineuronal Nets in the Mouse Inferior Colliculus, Thalamic Reticular Nucleus and Auditory Cortex. *Brain Sciences*, *6*(2), 13. https://doi.org/10.3390/brainsci6020013

25. Ferguson, B. R., Gao, W.-J., Maio, V. Di, Zaitsev, A. V, Palmer, L. M., Bern, U., & Bolkan, S. S. (2018). PV Interneurons: Critical Regulators of E/I Balance for Prefrontal Cortex-Dependent Behavior and Psychiatric Disorders. https://doi.org/10.3389/fncir.2018.00037

26. Garwood, C. J., Cooper, J. D., Hanger, D. P., & Noble, W. (2010). Anti-inflammatory impact of minocycline in a mouse model of tauopathy. *Frontiers in Psychiatry*, *1*(OCT). https://doi.org/10.3389/fpsyt.2010.00136

27. Gordon, G. M., Ledee, D. R., Feuer, W. J., & Fini, M. E. (2009). Cytokines and signaling pathways regulating matrix metalloproteinase-9 (MMP-9) expression in corneal epithelial cellsy. *Journal of Cellular Physiology*, *221*(2), 402–411. https://doi.org/10.1002/jcp.21869

28. Grenier, D., Huot, M. P., & Mayrand, D. (2000). Iron-chelating activity of tetracyclines and its impact on the susceptibility of Actinobacillus actinomycetemcomitans to these antibiotics. *Antimicrobial Agents and Chemotherapy*, *44*(3), 763–766. https://doi.org/10.1128/AAC.44.3.763-766.2000

29. Hamilton, L. S., Sohl-Dickstein, J., Huth, A. G., Carels, V. M., Deisseroth, K., & Bao, S. (2013). Optogenetic Activation of an Inhibitory Network Enhances Feedforward Functional Connectivity in Auditory Cortex. *Neuron*, *80*(4), 1066–1076.

https://doi.org/10.1016/j.neuron.2013.08.017

30. Haragopal, H., Dorkoski, R., Johnson, H. M., Berryman, M. A., Tanda, S., & Day, M. L. (2020). Paired measurements of cochlear function and hair cell count in Dutch-belted rabbits with noise-induced hearing loss. *Hearing Research*, *385*. https://doi.org/10.1016/j.heares.2019.107845

31. Henderson, D., Bielefeld, E. C., Harris, K. C., & Hu, B. H. (2006). The Role of Oxidative Stress in Noise-Induced Hearing Loss. *Ear and Hearing*, *27*(1), 1–19. https://doi.org/10.1097/01.aud.0000191942.36672.f3

32. Henderson, D., Bielefeld, E. C., Lobarinas, E., & Tanaka, C. (2011). Noise-induced hearing loss: Implication for tinnitus. In *Textbook of Tinnitus* (pp. 301–309). Springer New York. https://doi.org/10.1007/978-1-60761-145-5_37

33. Hubbell, C. G., Hobbs, E. R., Rist, T., & White, J. W. (1982). Efficacy of Minocycline Compared With Tetracycline in Treatment of Acne Vulgaris. *Archives of Dermatology*, *118*(12), 989–992. https://doi.org/10.1001/archderm.1982.01650240033017

34. Huetz, C., Guedin, M., & Edeline, J. M. (2014). Neural correlates of moderate hearing loss: Time course of response changes in the primary auditory cortex of awake guinea-pigs. *Frontiers in Systems Neuroscience*, *8*(APR). https://doi.org/10.3389/fnsys.2014.00065

35. Jiang, W., Desjardins, P., & Butterworth, R. F. (2009). Cerebral inflammation contributes to encephalopathy and brain edema in acute liver failure: Protective effect of minocycline. *Journal of Neurochemistry*, *109*(2), 485–493. https://doi.org/10.1111/j.1471-4159.2009.05981.x

36. Kalappa, B. I., Anderson, C. T., Goldberg, J. M., Lippard, S. J., & Tzounopoulos, T. (2015). AMPA receptor inhibition by synaptically released zinc. *Proceedings of the National Academy of Sciences of the United States of America*, *112*(51), 15749–15754. https://doi.org/10.1073/pnas.1512296112

37. Kawaguchi, Y., Katsumaru, H., Kosaka, T., Heizmann, C. W., & Hama, K. (1987). Fast spiking cells in rat hippocampus (CA1 region) contain the calcium-binding protein parvalbumin. *Brain Research*, *416*(2), 369–374. https://doi.org/10.1016/0006-8993(87)90921-8

38. Kelly, K. J., Sutton, T. A., Weathered, N., Ray, N., Caldwell, E. J., Plotkin, Z., & Dagher, P. C. (2004). Minocycline inhibits apoptosis and inflammation in a rat model of ischemic renal injury. *American Journal of Physiology-Renal Physiology*, *287*(4), F760–F766. https://doi.org/10.1152/ajprenal.00050.2004

39. Kokash, J., Alderson, E. M., Reinhard, S. M., Crawford, C. A., Binder, D. K., Ethell, I. M., & Razak, K. A. (2019). Genetic reduction of MMP-9 in the Fmr1 KO mouse partially rescues prepulse inhibition of acoustic startle response. *Brain Research*, *1719*(April), 24–29. https://doi.org/10.1016/j.brainres.2019.05.029

40. Kouvaros, S., Kumar, M., & Tzounopoulos, T. (n.d.). Synaptic Zinc Enhances Inhibition Mediated by Somatostatin, but not Parvalbumin, Cells in Mouse Auditory Cortex. https://doi.org/10.1093/cercor/bhaa005

41. Kujawa, S. G., & Liberman, M. C. (2009). Adding insult to injury: Cochlear nerve degeneration after "temporary" noise-induced hearing loss. *Journal of Neuroscience*, *29*(45), 14077–14085. https://doi.org/10.1523/JNEUROSCI.2845-09.2009

42. Le Prell, C. G., Yamashita, D., Minami, S. B., Yamasoba, T., & Miller, J. M. (2007). Mechanisms of noise-induced hearing loss indicate multiple methods of prevention. *Hearing Research*, *226*(1–2), 22–43. https://doi.org/10.1016/j.heares.2006.10.006

43. Li, Y. J., Wang, Z. H., Zhang, B., Zhe, X., Wang, M. J., Shi, S. T., … Zhao, H. (2013). Disruption of the blood-brain barrier after generalized tonic-clonic seizures correlates with cerebrospinal fluid MMP-9 levels. *Journal of Neuroinflammation*, *10*(1), 848. https://doi.org/10.1186/1742-2094-10-80

44. Liu, L., Xuan, C., Shen, P., He, T., Chang, Y., Shi, L., … Wang, J. (2018). Hippocampal mechanisms underlying impairment in spatial learning long after establishment of noise-induced hearing loss in CBA mice. *Frontiers in Systems Neuroscience*, *12*, 35. https://doi.org/10.3389/FNSYS.2018.00035/XML/NLM

45. Lynch, E. D., & Kil, J. (2005, October 1). Compounds for the prevention and treatment of noise-induced hearing loss. *Drug Discovery Today*. Elsevier Current Trends. https://doi.org/10.1016/S1359-6446(05)03561-0

46. Martin, W. H. (2008). Dangerous Decibels: Partnership for preventing noise-induced hearing loss and tinnitus in children. In *Seminars in Hearing* (Vol. 29, pp. 102–110). © Thieme Medical Publishers. https://doi.org/10.1055/s-2007-1021778

47. McAllister, B. B., & Dyck, R. H. (2017). A new role for zinc in the brain. *ELife*, *6*. https://doi.org/10.7554/eLife.31816

48. Modheji, M., Olapour, S., Khodayar, M. J., Jalili, A., & Yaghooti, H. (2016). Minocycline is more potent than tetracycline and doxycycline in inhibiting MMP-9 in vitro. *Jundishapur Journal of Natural Pharmaceutical Products*, *11*(2). https://doi.org/10.17795/jjnpp-27377

49. Möhrle, D., Hofmeier, B., Amend, M., Wolpert, S., Ni, K., Bing, D., … Rüttiger, L. (2019). Enhanced Central Neural Gain Compensates Acoustic Trauma-induced Cochlear Impairment, but Unlikely Correlates with Tinnitus and Hyperacusis. *Neuroscience*, *407*, 146–169. https://doi.org/10.1016/j.neuroscience.2018.12.038

50. Moore, A. K., & Wehr, M. (2013). Parvalbumin-expressing inhibitory interneurons in auditory cortex are well-tuned for frequency. *Journal of Neuroscience*, *33*(34), 13713–13723. https://doi.org/10.1523/JNEUROSCI.0663-13.2013

51. Murase, S., Lantz, C. L., & Quinlan, E. M. (2017). Light reintroduction after dark exposure reactivates plasticity in adults via perisynaptic activation of MMP-9. *ELife*, *6*. https://doi.org/10.7554/eLife.27345

52. Nakashima, A. S., & Dyck, R. H. (2009, March 1). Zinc and cortical plasticity. *Brain Research Reviews*. Elsevier. https://doi.org/10.1016/j.brainresrev.2008.10.003

53. Nguyen, A., Khaleel, H. M., & Razak, K. A. (2017). Effects of noise-induced hearing loss on parvalbumin and perineuronal net expression in the mouse primary auditory cortex. *Hearing Research*, *350*, 82–90. https://doi.org/10.1016/j.heares.2017.04.015

54. Noreña, A. J., & Eggermont, J. J. (2003). Changes in spontaneous neural activity immediately after an acoustic trauma: Implications for neural correlates of tinnitus. *Hearing Research*, *183*(1–2), 137–153. https://doi.org/10.1016/S0378-5955(03)00225-9

55. Ogatas, Y., Enghildp, J. J., & Nagasesll, H. (1992). *Matrix Metalloproteinase 3 (Stromelysin) Activates the Precursor for the Human Matrix Metalloproteinase 9". THE JOURNAL OF BIOLOGICAL CHEMISTRY* (Vol. 267).

56. Oviedo, H. V. (2017). Connectivity motifs of inhibitory neurons in the mouse Auditory Cortex. *Scientific Reports*, *7*(1). https://doi.org/10.1038/s41598-017-16904-2

57. Pizzorusso, T. (2002). Reactivation of Ocular Dominance Plasticity in the Adult Visual Cortex. *Science*, *298*(5596), 1248–1251. https://doi.org/10.1126/science.1072699

58. Prasher, D. (1998, October 17). New strategies for prevention and treatment of noise-induced hearing loss. *Lancet*. Elsevier Limited. https://doi.org/10.1016/S0140-6736(05)70483-9

59. Rabinowitz, P. M. (2000). Noise-Induced Hearing Loss - American Family Physician. Retrieved February 26, 2020, from https://www.aafp.org/afp/2000/0501/p2749.html

60. Reichelt, A. C., Hare, D. J., Bussey, T. J., & Saksida, L. M. (2019). Perineuronal Nets: Plasticity, Protection, and Therapeutic Potential. *Trends in Neurosciences*, *42*(7), 458–470. https://doi.org/10.1016/J.TINS.2019.04.003

61. Resnik, J., & Polley, D. B. (2021). Cochlear neural degeneration disrupts hearing in background noise by increasing auditory cortex internal noise. *Neuron*, *109*(6), 984-996.e4. https://doi.org/10.1016/J.NEURON.2021.01.015

62. Rüttiger, L., Singer, W., Panford-Walsh, R., Matsumoto, M., Lee, S. C., Zuccotti, A., … Knipper, M. (2013). The Reduced Cochlear Output and the Failure to Adapt the Central Auditory Response Causes Tinnitus in Noise Exposed Rats. *PLoS ONE*, *8*(3), 1–11. https://doi.org/10.1371/journal.pone.0057247

63. Saivin, S., & Houin, G. (1988, November 18). Clinical Pharmacokinetics of Doxycycline and Minocycline. *Clinical Pharmacokinetics*. Springer. https://doi.org/10.2165/00003088-198815060-00001

64. Salvi, R. J., Saunders, S. S., Gratton, M. A., Arehole, S., & Powers, N. (1990). Enhanced evoked response amplitudes in the inferior colliculus of the chinchilla following acoustic trauma. *Hearing Research*, *50*(1–2), 245–257. https://doi.org/10.1016/0378-5955(90)90049-U

65. Salvi, R., Sun, W., Ding, D., Chen, G.-D., Lobarinas, E., Wang, J., … Auerbach, B. D. (2017). Inner Hair Cell Loss Disrupts Hearing and Cochlear Function Leading to Sensory Deprivation and Enhanced Central Auditory Gain. *Frontiers in Neuroscience*, *10*(JAN), 621. https://doi.org/10.3389/fnins.2016.00621

66. Seidman, M. D., & Standring, R. T. (2010, October). Noise and quality of life. *International Journal of Environmental Research and Public Health*. Multidisciplinary Digital Publishing Institute (MDPI). https://doi.org/10.3390/ijerph7103730

67. Seki, S., & Eggermont, J. J. (2003). Changes in spontaneous firing rate and neural synchrony in cat primary auditory cortex after localized tone-induced hearing loss. *Hearing Research*, *180*(1–2), 28–38. https://doi.org/10.1016/S0378-5955(03)00074-1

68. Sheppard, A. M., Chen, G. Di, Manohar, S., Ding, D., Hu, B. H., Sun, W., … Salvi, R. (2017). Prolonged low-level noise-induced plasticity in the peripheral and central auditory system of rats. *Neuroscience*, *359*, 159–171. https://doi.org/10.1016/j.neuroscience.2017.07.005

69. Shi, C., Zhang, G. Bin, & Yin, S. W. (2015). Effect of bortezomib on migration and invasion in cervical carcinoma HeLa cell. *Asian Pacific Journal of Tropical Medicine*, *8*(6), 485–488. https://doi.org/10.1016/j.apjtm.2015.05.004

70. Shukla, M., Roy, K., Kaur, C., Nayak, D., Mani, K. V., Shukla, S., & Kapoor, N. (2019). Attenuation of adverse effects of noise induced hearing loss on adult neurogenesis and memory in rats by intervention with Adenosine A2A receptor agonist. *Brain Research Bulletin*, *147*, 47–57. https://doi.org/10.1016/J.BRAINRESBULL.2019.02.006

71. Siller, S. S., & Broadie, K. (2012). Matrix metalloproteinases and minocycline: Therapeutic avenues for fragile X syndrome. *Neural Plasticity*. Hindawi Publishing Corporation. https://doi.org/10.1155/2012/124548

72. Sohal, V. S., Zhang, F., Yizhar, O., & Deisseroth, K. (2009). Parvalbumin neurons and gamma rhythms enhance cortical circuit performance. *Nature*, *459*(7247), 698–702. https://doi.org/10.1038/nature07991

73. Sun, W., Deng, A., Jayaram, A., & Gibson, B. (2012). Noise exposure enhances auditory cortex responses related to hyperacusis behavior. *Brain Research*, *1485*, 108–116. https://doi.org/10.1016/J.BRAINRES.2012.02.008

74. Syka, J., Rybalko, N., & Popelář, J. (1994). Enhancement of the auditory cortex evoked responses in awake guinea pigs after noise exposure. *Hearing Research*, *78*(2), 158–168. https://doi.org/10.1016/0378-5955(94)90021-3

75. Szklarczyk, A., Lapinska, J., Rylski, M., McKay, R. D. G., & Kaczmarek, L. (2002). Matrix metalloproteinase-9 undergoes expression and activation during dendritic remodeling in adult hippocampus. *Journal of Neuroscience*, *22*(3), 920–930. https://doi.org/10.1523/jneurosci.22-03-00920.2002

76. Van Den Steen, P. E., Dubois, B., Nelissen, I., Rudd, P. M., Dwek, R. A., & Opdenakker, G. (2002). Biochemistry and molecular biology of gelatinase B or matrix metalloproteinase-9 (MMP-9). *Critical Reviews in Biochemistry and Molecular Biology*. Taylor & Francis. https://doi.org/10.1080/10409230290771546

77. Vandooren, J., Knoops, S., Buzzo, J. L. A., Boon, L., Martens, E., Opdenakker, G., & Kolaczkowska, E. (2017). Differential inhibition of activity, activation and gene expression of MMP-9 in THP-1 cells by azithromycin and minocycline versus bortezomib: A comparative study. *PLoS ONE*, *12*(4). https://doi.org/10.1371/journal.pone.0174853

78. Wang, J., McFadden, S. L., Caspary, D., & Salvi, R. (2002). Gamma-aminobutyric acid circuits shape response properties of auditory cortex neurons. *Brain Research*, *944*(1–2), 219–231. https://doi.org/10.1016/S0006-8993(02)02926-8

79. Wehr, M., & Zador, A. M. (2003). Balanced inhibition underlies tuning and sharpens

spike timing in auditory cortex. *Nature*, *426*(6965), 442–446. https://doi.org/10.1038/nature02116

80. Wen, T. H., Afroz, S., Reinhard, S. M., Palacios, A. R., Tapia, K., Binder, D. K., … Ethell, I. M. (2018). Genetic Reduction of Matrix Metalloproteinase-9 Promotes Formation of Perineuronal Nets Around Parvalbumin-Expressing Interneurons and Normalizes Auditory Cortex Responses in Developing Fmr1 Knock-Out Mice. *Cerebral Cortex*, *28*(11), 3951–3964. https://doi.org/10.1093/cercor/bhx258

81. Wen, T. H., Binder, D. K., Ethell, I. M., & Razak, K. A. (2018, August 3). The Perineuronal 'Safety' Net? Perineuronal Net Abnormalities in Neurological Disorders. *Frontiers in Molecular Neuroscience*. Frontiers Media S.A. https://doi.org/10.3389/fnmol.2018.00270

82. Wilczynski, G. M., Konopacki, F. A., Wilczek, E., Lasiecka, Z., Gorlewicz, A., Michaluk, P., … Kaczmarek, L. (2008). Important role of matrix metalloproteinase 9 in epileptogenesis. *Journal of Cell Biology*, *180*(5), 1021–1035. https://doi.org/10.1083/jcb.200708213

83. Womelsdorf, T., Schoffelen, J. M., Oostenveld, R., Singer, W., Desimone, R., Engel, A. K., & Fries, P. (2007). Modulation of neuronal interactions through neuronal synchronization. *Science*, *316*(5831), 1609–1612. https://doi.org/10.1126/science.1139597

84. Wu, J., Han, W., Chen, X., Guo, W., Liu, K., Wang, R., … Sai, N. (2017). Matrix metalloproteinase-2 and -9 contribute to functional integrity and noise-induced damage to the blood-labyrinth-barrier. *Molecular Medicine Reports*, *16*(2), 1731–1738. https://doi.org/10.3892/mmr.2017.6784

85. Yamaguchi, Y. (2000). *Review Lecticans: organizers of the brain extracellular matrix. CMLS, Cell. Mol. Life Sci* (Vol. 57).

86. Yrjänheikki, J., Tikka, T., Keinänen, R., Goldsteins, G., Chan, P. H., & Koistinaho, J. (1999). A tetracycline derivative, minocycline, reduces inflammation and protects against focal cerebral ischemia with a wide therapeutic window. *Proceedings of the National Academy of Sciences of the United States of America*, *96*(23), 13496–13500. https://doi.org/10.1073/pnas.96.23.13496

87. Zhang, J. S., & Kaltenbach, J. A. (1998). Increases in spontaneous activity in the dorsal cochlear nucleus of the rat following exposure to high-intensity sound. *Neuroscience Letters*, *250*(3), 197–200. https://doi.org/10.1016/S0304-3940(98)00482-0

Chapter 2

Cortical region-specific recovery of temporal processing following noise-induced hearing loss

Abstract

Noise-induced hearing loss (NIHL) is a major cause of auditory processing impairments. Studies of the central auditory system after NIHL suggest 'the central gain model' in which reduced peripheral input (deafferentation) following NIHL may lead to exaggerated responses, but with deficits in auditory temporal processing. These exaggerated responses may lead to tinnitus and hyperacusis following NIHL. Almost all NIHL studies have focused on the lemniscal auditory pathway, but very little is known about how different cortical regions recover response properties after NIHL. Here we studied response recovery trajectories in the auditory and frontal cortices (AC, FC) of adult mice following NIHL. We recorded electroencephalography (EEG) responses from awake, freely moving mice before and following NIHL to quantify response magnitude and temporal processing. NIHL was verified by measuring the auditory brainstem response (ABR) before and at 1-, 10-, 23-, and 45-days after noise-exposure. Resting EEG, event related potentials (ERP), auditory steady state responses (ASSR), and a novel gap-ASSR were recorded on the same days to perform within-subject analyses of the trajectory of EEG changes following NIHL. The inter-trial phase coherence (ITPC) of the ASSR quantified the ability of AC and FC to synchronize responses to short gaps of varying intervals embedded in noise, as a measure of temporal processing. Despite an absence of click-evoked ABRs up to 90 dB SPL and up to 45-days post-exposure – indicating permanent hearing loss – ERPs from the AC and FC

showed recovery in ~50% of the mice between 1- and 10 days post-NIHL, with full recovery to pre-NIHL levels in both AC and FC. This suggests that there is some residual signal that is received centrally and amplified in some of the mice. The ITPC of gap-ASSR was reduced following NIHL in both AC and FC in all the mice on day 1 after NIHL. Interestingly, the AC showed full recovery of temporal processing over the course of 45 days, but the FC did not. Despite ERP recovery, the FC does not show any recovery of ITPC in the gap-ASSR. These results suggest post-NIHL plasticity that emphasizes sound detection with strong cortical region-specific trajectories in temporal processing recovery. The lack of temporal processing recovery in the FC has implications for the interactions between hearing loss and cognitive decline.

Introduction

Noise induced hearing loss (NIHL) is a major cause of communication impairments that arises from occupational (Nelson et al. 2005) and recreational (Henderson, Testa, and Hartnick 2011; Chung et al. 2005) noise exposures. Previous studies have shown how noise exposure damages the cochlea (Liberman and Kujawa 2017), leading to deafferentation of central auditory regions. While extensive studies have been done to show the damage noise exposure causes in the periphery, it is also becoming clear that there are compensatory changes occurring in the central auditory system. The 'central gain model' may explain a number of central auditory processing changes after NIHL. The central gain model purports that compensatory changes emerge in higher auditory regions through amplification of residual inputs following NIHL (Noreña & Eggermont, 2003; Seki & Eggermont, 2003). The abnormal elevation in activity may be linked to tinnitus and hyperacusis (Eggermont

and Roberts 2004; Salvi et al. 2017; Sun et al. 2012). While a number of studies have quantified response magnitude changes following cochlear damage (Resnik and Polley 2021, 2017; Sun et al. 2012), few have looked at how temporal processing is affected, particularly within multiple cortical regions. Chambers et al. (2016) found that central gain is a mechanism that emphasizes sound detection following peripheral damage, at the expense of temporal processing. They found that temporal coding did not recover in the auditory cortex despite increases in response magnitude and improved sound detection over a number of days following peripheral damage. In the rat AC, sound evoked potentials increased 1 hour after noise exposure along with spike rate to a tone burst (Sun et al. 2012). Although ABR threshold shifts were temporary, cochlear synpatopathy was found to last 2 weeks after noise exposure and corticollicular response gain remained elevated after the same amount of time (Asokan et al. 2018). Spontaneous firing rates and bursting activity in the AC remained elevated up to 3 months in rats with putative tinnitus after blast exposure (Luo et al. 2014).

The main goal of the present study was to determine whether different cortical regions show a similar pattern of response gain and temporal processing changes in the auditory cortex. Another goal was to develop a pre-clinical NIHL model with outcomes measured using EEG recordings that can be relatively more easily translated to human work. To achieve these goals, we tracked response magnitude and temporal processing across the auditory cortex (AC) and frontal cortex (FC) of awake, freely moving mice over a number of days following NIHL using EEG recordings and a within-subject design. We chose to compare auditory with the frontal cortex because hearing loss is a major midlife

factor for increased age-related dementia (Livingston et al. 2020) and cognitive decline. It is possible that communication deficits associated with hearing loss leads to social isolation and cognitive decline in humans (Bernabei et al. 2014; Lin et al. 2013; Moore et al. 2014). Frontal cortex function and cognition are also impacted by hearing loss. The severity of hearing loss affects FC responses to visual stimuli measured by EEG and correlated with auditory behavioral measures (Campbell and Sharma 2020). Understanding speech in noise is difficult for older listeners with lower working memory capabilities and higher hearing thresholds (Giroud, Keller, and Meyer 2021). To understand the relationship between hearing loss and cognitive decline, studies in rodent models have examined behaviors such as working memory tasks and found deficits in spatial learning and memory in mice 3 months after noise exposure as well as in rats 15 days after noise exposure (Shukla et al. 2019). We recorded EEG signals from the FC, and compare those to AC responses, to obtain functional markers that may have implications for cognitive decline following hearing loss.

The acoustic steady state response (ASSR) is a measure used to evaluate speech perception, which relies on frequency and amplitude modulations (Zeng et al. 2005). Studies have linked ASSRs and speech processing through word recognition scores (Dimitrijevic, John, and Picton 2004) and phase-locking capabilities (Leigh-Paffenroth and Fowler 2006). We used the 40-Hz ASSR stimulus to provide insight to the relationship between NIHL and temporal processing in mice. More challenging tasks of speech understanding through varying degrees of noise negatively affected perceived effort in both young and old adults, particularly those with hearing impairments (Larsby et al. 2009). By

using a novel gap-ASSR stimulus, that inserts varying gap durations in continuous noise, we can understand if and how temporal processing in challenging conditions recover in the FC and AC after NIHL.

Permanent hearing loss was induced in mice using acute noise exposure and was tracked using auditory brainstem responses (ABRs) to clicks and cortical resting EEG, ERPs, and ASSRs for up to 45 days after noise exposure. Despite a persistent lack of ABRs, approximately half of the NIHL mice had recovered responses to noise bursts, as measured by ERP amplitudes in both the AC and FC. However, there was a cortical-region specific difference in recovery of temporal processing as evaluated by using the 40-Hz gap-ASSR stimuli. Recovery of pre-NIHL ASSR temporal fidelity was seen in only the AC, but not the FC. Together, these data suggest plasticity in a cortical region-specific manner to sound detection despite a diminished input from the periphery.

Methods

Overview.

A longitudinal, within-subject design was used to study the impact of NIHL on resting and sound evoked EEG responses in the auditory and frontal cortex (AC, FC). Recordings were obtained before the induction of NIHL ('pre-NIHL') and on a number of days post-NIHL (1, 10, 23, and 45 days after NIHL). Auditory brainstem responses (ABR) were recorded on the same days to ensure NIHL was present at least until the final day of EEG recordings.

Mice.

All procedures were approved by the Institutional Animal Care and Use Committee at the University of California, Riverside. Sighted FVB mice (FVB.129P2–Pde6b+Tyrc-ch/AntJ) were received from Jackson Laboratories, bred in-house and housed in an AALAC accredited vivarium with 12:12h light:dark cycle. One to four mice were housed in each cage with food and water available ad libitum. Male and female mice were used between postnatal day (P)74 and P120 (mean age: P102, s.d: 12 days).

Surgery.

The EEG electrode implant surgical procedures have been previously described in detail (Lovelace et al., 2018; Rumschlag et al., 2021). Briefly, mice were anesthetized with a ketamine/xylazine/acepromazine (80/10/1 mg/kg, i.p.) mixture and temperature was regulated (FHC, Inc., Maine) at ~37° throughout the procedure. Three ~1mm diameter burr holes were drilled (Foredom dental drill) in the skull above the frontal, auditory, and occipital cortex. The frontal hole was placed at the junction between the frontal sinus and sagittal suture over the right hemisphere and the occipital hole was placed just rostral to the lambdoid suture and lateral to the sagittal suture in the left parietal bone. The right hemispheric auditory hole was placed -2mm posteriorly and +5 laterally from Bregma. 1mm stainless steel screws were carefully inserted into the burr holes while attached to a 3-channel electrode post (P1 Technologies, Roanoke, VA) and held in place with cured dental cement. Post-operational care included one dose of analgesic injection of Ethiqa-XR (3.25 mg/kg body weight) (Fidelis Pharmaceuticals, NJ) and observation over the

course of 48 hours. Each mouse was singly housed after surgery to prevent damage to the implant.

Auditory Brainstem Response.

Hearing loss was measured using ABR recordings in response to clicks from mice anesthetized with ketamine/xylazine/acepromazine (80/10/1 mg/kg, i.p.). Once an anesthetic plane was verified via toe-pinch reflex test, the mouse was placed on a bite bar in an anechoic chamber (Gretch-Ken Industries, OR) and 3 Grass platinum needle electrodes (Grass Technologies, RI) were inserted subdermally. The recording electrode was placed at the vertex, the ground electrode in the left cheek, and reference electrodes were placed in the right cheek. The MF1 Multi-Field Magnetic Speaker (Tucker-David Technologies, FL) was placed 10cm away from the left ear and the TDT RZ6 multi I/O processor delivered the sound stimulus during the recording. The TDT software BioSigRZ was used to generate 512 click presentations at a 21Hz repetition rate of alternating +/- 1.4V (duration 0.1ms) at each sound level. Each protocol began at 90dB SPL and decreased in 5dB steps to 10dB SPL. Click ABRs were used to verify hearing loss and were recorded pre-NIHL and after each subsequent EEG recording. Hearing threshold was defined as a visible waveform at the lowest sound level within the first 7ms of the ABR.

Noise-exposure paradigm.

NIHL was caused using a noise-exposure paradigm in which a narrowband noise (6-12kHz) at ~120 dB SPL was played continuously over 3 hrs to awake mice. The NIHL stimulus was generated using Tucker Davis Technologies (TDT) software RPvdsEx and

delivered via the RZ6 multi I/O processor. The NIHL stimulus was presented using a Fostex FT96H horn tweeter that was suspended 6 inches above the cage. NIHL stimulus was presented immediately after the pre-NIHL EEG recording.

Auditory Stimuli.

Auditory stimulus presentation procedures were similar to those described in Rumschlag and Razak (2021). A TDT MF1 speaker was mounted 20cm above the plastic arena and used to present noise stimuli that was generated with a TDT RZ6. All sound stimuli were presented at 90dB SPL for all time points. For ERPs, a train of noise bursts (100ms, 5ms rise/fall time, 0.25Hz repletion rate, 120 repetitions) was presented. The ASSR was evoked at 40Hz using a pulsed noise stimulus (200 repetitions, 8ms duration, 2ms rise/fall time, 40Hz, 1-2 s random inter-stimulus interval) for a total duration of 12 minutes.

A 40 Hz gap-ASSR stimulus was used to measure the ability of the cortex to consistently respond to rapid short gaps in noise. The gap-ASSR is elicited by presenting 10 gaps repeated at 40 Hz (25 msec period) in continuous noise. The duration of the gap is varied randomly between 3 and 9 msec (1 msec resolution). A 75% modulation depth was used. A single stimulus began with 250 ms of continuous noise, followed by 250 ms of gap-interrupted noise, followed by continuous noise, and so on, for a total of 10 presentations of the gap-interrupted noise. The stimulus ended with 250 ms of continuous noise, followed by a silent ISI of 500 ms. For each 250 ms segment, the gap width was randomly selected from a parameter space, consisting of 3-9 ms gaps. Each stimulus was

presented at least 200 times over the 30-minute presentation period. If each gap in a 250 ms stimulus elicits a measurable response, then the recording will show a robust 40 Hz oscillatory signal. The strength of the gap-ASSR varies with gap width (Rumschlag and Razak, 2021).

Electroencephalography (EEG) recording.

Mice were awake and freely moving during the EEG recordings while tethered via the EEG implant that was connected to a freely rotating commutator. The TDT RA4LI/PA headstage and preamplifier was connected to the TDT RZ6 I/O device via optic fiber cable. Clean bedding was used for each mouse in a plastic arena during each recording placed inside a wire mesh Faraday cage. The entire set up was housed in an anechoic, sound attenuating chamber (Gretch-Ken Indusrtries, OR). The signal was recorded at 24.414 kHz and down-sampled to 1024 Hz using linear interpolation.

Data Analysis.

All EEG analyses were done using custom MATLAB (Math-Works, Natick, MA) scripts (Rumschlag and Razak, 2021). Graphpad Prism was used for statistical analysis. The specific statistical tests used are described in the sections below. Each comparison was done separately in the AC and FC.

Resting EEG Spectral Analysis.

To quantify changes after NIHL in EEG power spectral distribution, we measured resting EEG power across canonical frequency bands in both AC and FC across the various time points from 1- to 45 days post-NIHL, and compared with pre-NIHL values. The

phrase ‘resting EEG’ is used to describe data collected when there was no specific auditory stimulation. Five minutes of resting EEG was recorded from each mouse. The traces from each condition were split into Hanning-windowed 1-second segments with 50% overlap, which were then transformed to the frequency domain via Fourier transform. The average power spectrum was calculated by averaging the spectra from each of the 1-second segments. Each average power spectrum was then split into EEG frequency bands (theta: 3– 7 Hz, alpha: 8–13 Hz, beta: 14–29 Hz, low gamma: 30–59 Hz, high gamma: 61–100 Hz, and high-frequency oscillations (HFO): 101–250 Hz). Delta band power was not analyzed because the pre-amplifier had a built-in high-pass filter at 2.2 Hz. The average power from each frequency band was calculated. One-way ANOVA mixed-effects repeated measures was used to compare for spectral power at each time point for each of the frequency bands (Graphpad Prism) with the resulting p-values adjusted for multiple comparisons within each region.

ERP analysis.

To measure ERPs, the EEG trace was split into trials, using TTL pulses marking the sound onset. Each trial was baseline-corrected, such that for each trial, the mean of the 250 ms baseline period was subtracted from the trial trace. Each trial was then de-trended (MATLAB detrend function). To extract the ERP, all of the trials were averaged together. ERPs recorded from mice have distinct peaks, which are analogous to those seen in human ERPs (Umbricht et al., 2004). For each mouse, the peak magnitudes and latencies were measured as the local minimum or maximum within a physiologically relevant range, e.g. the P1 component was the local maximum between 15 ms and 30 ms following stimulus

onset. Each NIHL group was compared via mixed-effect analysis for P1 and N1 amplitude and latency with the time point as a factor in each region (AC and FC).

Pulse-ASSR analysis.

The pulse-ASSR was analyzed by calculating the average consistency of the 40 Hz response during the last 1000 ms of the 2000 ms stimulus. This was done to capture the steady-state response while avoiding the onset response. To that end, the trace was transformed to the time-frequency domain via dynamic complex Morlet wavelet transform. The ASSR can be characterized using multiple measurements, including the amplitude of the oscillation frequency in the frequency transform (FFT) of the signal (Parthasarathy et al., 2010), the amplitude of the Hilbert transform of the filtered signal, the vector strength of the signal with the original oscillatory stimulus, the phase-locking of FFTs (PLI) (Yokota and Naruse, 2015), or the inter-trial phase clustering (ITPC) at the oscillation frequency (Lovelace et al., 2020). ITPC provides both time and frequency information, and it is a direct measure of the degree of response consistency across trials, so it was used to assess ASSRs in this study. ITPC was calculated for each time-frequency point as the average vector of phase unit vectors across trials. If the phase response is consistent at a particular time- frequency point, it will have a high ITPC value. The ITPC calculations showed a high degree of phase consistency at 40 Hz during the pulse-ASSR stimulus. The ITPC values at 40 Hz were averaged to extract one value for each mouse, representing the phase consistency of the 40 Hz ASSR. A mixed-effects model was used to examine main effects of each time point for AC and FC.

Gap-ASSR analysis. The gap-ASSR was analyzed similarly to the pulse-ASSR, in which the consistency of the 40 Hz response was calculated using the ITPC. For the gap-ASSR, the consistency was calculated for each of the stimuli (7 gap widths, 3-9 msec). The EEG trace was transformed using a dynamic complex Morlet wavelet transform. The trials corresponding to each gap were grouped together, and the ITPC was calculated. A band of high ITPC appears at 40 Hz. The average ITPC value at 40 Hz during the stimulus was extracted for each stimulus for each mouse. The gap-ASSR compared ITPC mean using the mixed-effect model with gap-width (3-9 ms) and time point (pre, 1-, 10-, 23-, 45 days) were used as factors, for each region. By reducing gap duration, the temporal processing ability of the auditory system can be quantified.

Results

i. NIHL mice had increased thresholds up to 45 days after noise-exposure

Click ABRs were measured from all mice before and on multiple days after NIHL. The pre-NIHL ABR threshold was on average ~45 dB SPL, consistent with prior studies in the FVB strain (Rumschlag and Razak, 2022; Rumschlag et al., 2022). Following NIHL, none of the mice showed any click ABR responses up to 90 dB SPL on the day after NIHL and up to 45 days after NIHL, suggesting a permanent threshold shift, or permanent hearing loss (Figure 1).

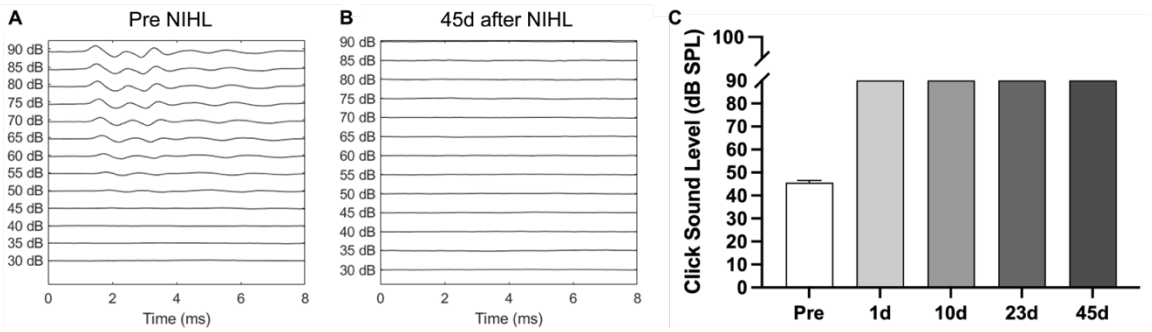

Figure 1. None of the NIHL mice showed any ABR up to 90dB SPL and hearing loss lasted at least 45 days after noise exposure. A) Example of ABR traces from one mouse before NIHL, threshold is ~50 dB SPL. B) Example of ABR traces from the same mouse 45 days after NIHL showing threshold has increased to above 90 dB SPL. C) Across the population, the average ABR threshold increased from ~45 dB SPL to >90dB SPL at all post-NIHL days tested.

ii. Approximately half the NIHL mice fully recovered auditory ERPs despite the lack of ABR

ERPs were recorded from the AC and FC from all mice showing NIHL. Although no click ABRs were apparent, in 16 of 29 mice, robust ERPs appeared in response to 90 dB SPL at 1-10 days after NIHL. Representative ERP traces spanning the recording timeline show from one mouse there is robust and enhanced recovery over time (Figure 2A-B). The remaining 13 mice had diminished ERPs up to 45 days after NIHL, with another representative set of ERP traces from a mouse with no recovery illustrating the difference of no recovery of sound detection in this group (Figure 2C-D). Due to differences in recovery of ERP, the NIHL mice were separated into two subgroups – response recovery (RR) and no response recovery (NR).

In the RR group, AC P1 peak amplitude significantly decreased from baseline (pre) to 1 day after NIHL ($F(2.063, 27.85) = 10.90$, $p=0.0003$; pre vs 1d: $p=0.0007$), but returned

to baseline values by 10 days and stayed at that that level at 23 and 45 days after NIHL (Figure 3A). FC P1 peak amplitude significantly decreased 1 day after NIHL ($F(2.050, 27.68) = 9.314$, $p=0.0007$; pre vs 1d: $p<0.0001$), but returned to baseline by 10 days after NIHL (Figure 3B). The N1 amplitude in the AC significantly decreased at 1 day after NIHL and returned to baseline within 10 days after NIHL and stayed at that level for up to 45 days ($F(3.152, 63.04) = 6.924$, $p=0.0003$) (Figure 3C). The N1 amplitude in the FC also decreased significantly 1 day after NIHL, but returned to baseline by 10 days after NIHL ($F(2.901, 58.60) = 5.554$, $p=.0022$) (Figure 3D). Auditory cortex ($F(2.332, 31.48) = 14.90$, $p <0.0001$) and FC ($F(2.775, 47.88) = 12.91$, $p<0.0001$) P1 latency significantly increased beginning 1 day after NIHL and persisted up to 45 days after NIHL (Figure 3E-F). The N1 latency in the AC ($F(2.519, 34.01) = 6.190$, $p=0.0029$) and FC ($F(2.749, 37.11) = 10.38$, $p<.0001$) increased and remained elevated beginning 1 day after NIHL (Figure 3G-H). These data indicate that although no ABR was present up to 90 dB SPL, robust cortical evoked responses to 90 dB noise stimuli were present within 10 days after NIHL in approximately 50% of the mice. However, ERP component latencies did not recover to pre-NIHL levels.

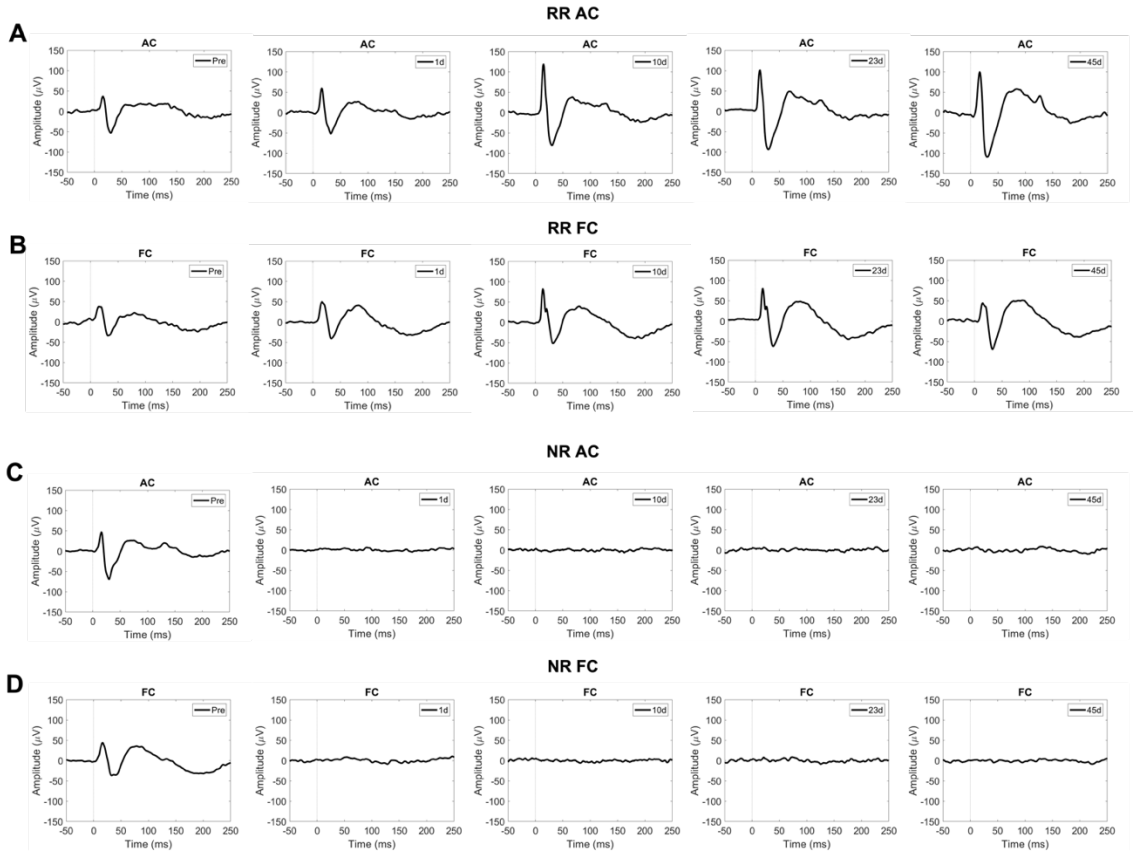

Figure 2. Example ERP traces of an illustrative RR mouse and illustrative NR mouse recorded before and on multiple days after NIHL. These mice showed no ABRs at levels up to 90 dB SPL post-NIHL. (A, B) The ERP amplitudes in this mouse increased above pre-levels at 10-, 23-, and 45 days post-NIHL in both AC (A) and FC (B). (C, D) The ERPs showed no recovery in this NR mouse example in the AC (C) or FC (D) up to 45 days after NIHL.

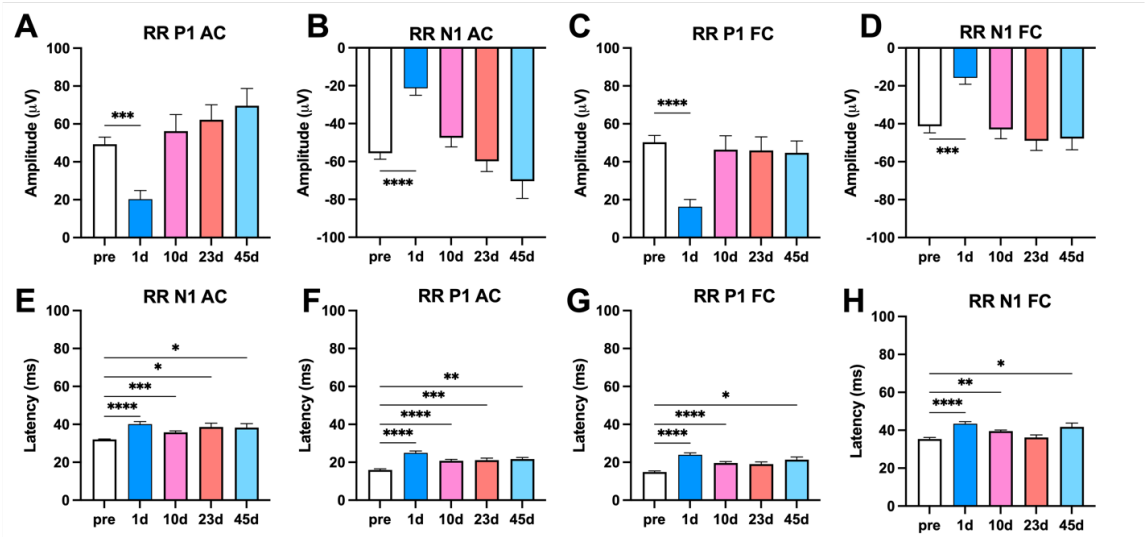

Figure 3. In mice that showed ERP response recovery after NIHL, P1 and N1 amplitude return to baseline in the AC and FC, but latency does not. The P1 and N1 peak amplitudes and latencies were extracted for each RR mouse and averaged (with +/- SEM) at each time point. A-D) RR P1 and N1 amplitudes decreased significantly after 1 day, but returned to baseline by 10 days in both AC and FC. E-H) RR P1 and N1 latencies increased significantly after NIHL and remained elevated. *, $p<0.05$; **, $p<0.01$; ***, $p<0.001$; ****, $p < 0.0001$

In the NR group, NIHL reduced both P1 and N1 amplitudes in the AC (P1: $F(1.176, 11.17) = 28.79$, $p=0.0001$; N1: $F(1.731, 21.64) = 70.93$, $p<0.0001$)) and FC (P1:$F(1.187, 11.28) = 50.99$, $p<0.0001$; N1: $F(1.467, 13.94) = 36.04$, $p<0.0001$)) (Figure 4A-D). The amplitudes did not recover up to 45 days post-NIHL. These data indicate that in a subset of mice experiencing NIHL, no response recovery was evident based on ERPs.

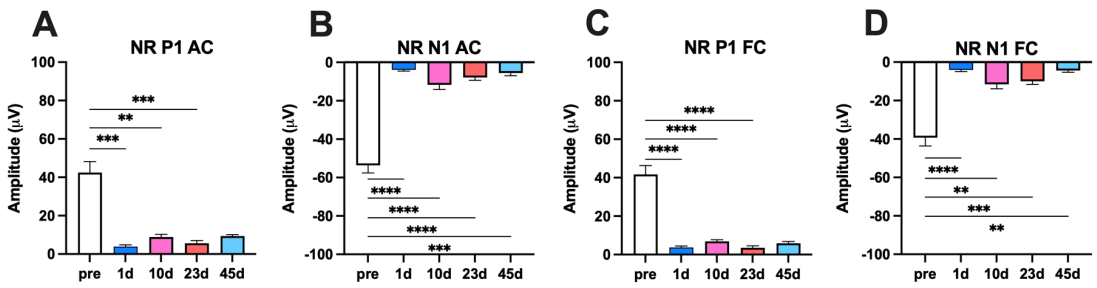

Figure 4. ERP P1 and N1 amplitudes remained diminished after noise-exposure in the NR group. P1 and N1 latency remained elevated. The P1 and N1 amplitudes and latencies maximum peaks decreased after NIHL and did not recover. This was used as the criterion for categorizing this subset of mice into the no recovery group. A-D) At each time point after NIHL, there was significant decrease in P1 and N1 amplitude compared to pre-NIHL in AC and FC. **, p<0.01; ***, p<0.001; ****, p < 0.0001

Directly comparing RR and NR group ERP peak amplitudes showed a clear difference in enhancement after NIHL between the two groups. A ratio of post- to pre- was calculated for 1- and 45 days after NIHL for both groups. The RR group had higher responses post-NIHL compared to NR, indicating there was more residual responses and input from the periphery. A two-way ANOVA was performed for all ratio comparisons. AC P1 amplitude had a main effect of group ($F(1, 40) = 29.44$; $p<0.0001$) and timepoint ($F(1, 40) = 21.71$; $p<0.0001$) as well as interaction between the two factors ($F(1, 40) = 11.01$; $p=0.0019$) with RR group significantly increased at 45 days after NIHL compared to NR (Bonferroni's: 45-day, $p<0.0001$) (Figure 5A). FC P1 amplitude group comparisons showed similar differences in regards to group comparison ($F(1, 40) = 22.48$; $p<0.0001$), time point ($F(1, 40) = 13.07$; $p=0.0008$), and interaction ($F(1, 40) = 8.068$; $p=0.0071$) with RR amplitude larger than NR at 45 days (Bonferroni's: 45-day, $p<0.0001$) (Figure 5B). There was a group effect ($F(1, 40) = 57.00$, $p<0.0001$) for AC N1 amplitude and effect of time point ($F(1, 40) = 22.93$, $p<0.0001$) as well as interaction ($F(1, 40) = 20.35$, $p<0.0001$)

with significant differences in amplitude between RR and NR at both time points (Bonferroni's: 1-day, p=0.0204; 45-day, p<0.0001) (Figure 5C). Lastly, FC N1 amplitude was different between groups (F (1, 27) = 46.26; p<0.0001) and time points (F (1, 13) = 27.85; p=0.0001) with an interaction between them (F (1, 13) = 21.16; p=0.0005) where the enhancement was seen in RR group (Bonferroni's: 45-day, p<0.0001) (Figure 5D). This data highlights the response enhancement of the AC and FC post-NIHL in the RR group.

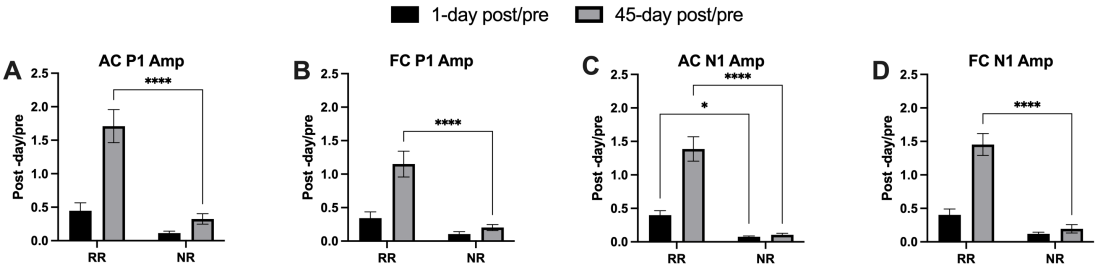

Figure 5. RR group P1 and N1 amplitude increased past baseline by 45 days after NIHL, but NR group did not. A ratio of post-NIHL day ERP amplitude was calculated compared to pre-NIHL amplitude. A value of 1 indicates equal post- and pre-NIHL values equal to pre-NIHL. A-B) AC P1 and N1 amplitudes were significantly increased by 45-days in RR compared to NR group. C) AC N1 amplitude was significantly different at 1- and 45-days between RR and NR groups. D) RR FC N1 amplitude was significantly enhanced compared to NR. $p < 0.0001$.

iii. EEG spectral power distribution differences between the RR and NR groups

Resting EEG power was quantified from 5 minutes EEG recordings in the absence of auditory stimuli. This analysis was performed to probe spontaneous neural oscillations after NIHL. Figure 6 shows the RR and NR group power spectral density pre-NIHL in comparison to 1- and 45-days post-NIHL. Figure 7 shows the ratio of absolute power for all the post-NIHL timepoints in comparison to pre-NIHL and 1-day post-NIHL, with mixed effects analysis one-way ANOVA used to analyze across the time points. In the RR group,

the low and high gamma spectral bands in the AC showed significant differences with time as a factor. In the post-hoc analysis with Bonferroni's multiple comparisons test, 23-day post-NIHL was significantly increased from 1-day post-NIHL in the low and high gamma frequency bands. There was also a significant increase in the beta band in the FC. This may indicate that there was an increase in spontaneous activity over time in the AC following NIHL. (See Table 1 and Table 2 for full statistical comparisons).

Figure 8 shows the NR group resting EEG spectral power in AC and FC. Nearly all frequency bands showed a main effect of time. Not all the significant differences in frequency bands and time point comparisons were similar between the two cortical regions. Both regions showed significant increases in beta, high gamma, and HFO. Theta was increased only in the AC while low gamma was increased only in the FC (See Table 1 and Table 2 for full statistical comparisons). These changes indicate that there was an overall increase in absolute power in both cortices.

In summary, RR group had few changes in power over time with the main effects seen mainly in the gamma frequency bands in AC. NR resting EEG spectral power was increased in both cortical regions over time in a non-specific manner.

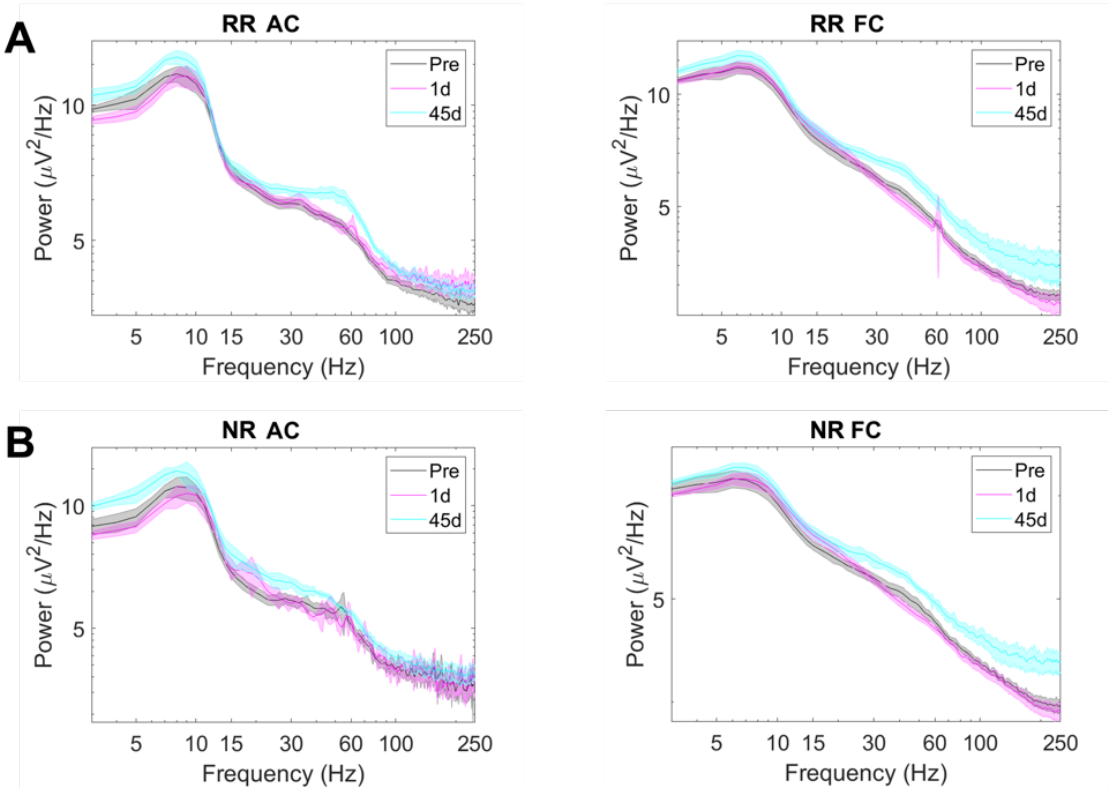

Figure 6. Power spectral density of response recovery (RR) and no recovery (NR) groups show changes in EEG power over time. Mice were divided into 2 groups: RR and NR, based on whether ERPs recovered over time after NIHL. Each panel shows the average power spectral density in the pre-NIHL and 1-, 45-day post-NIHL AC or FC.

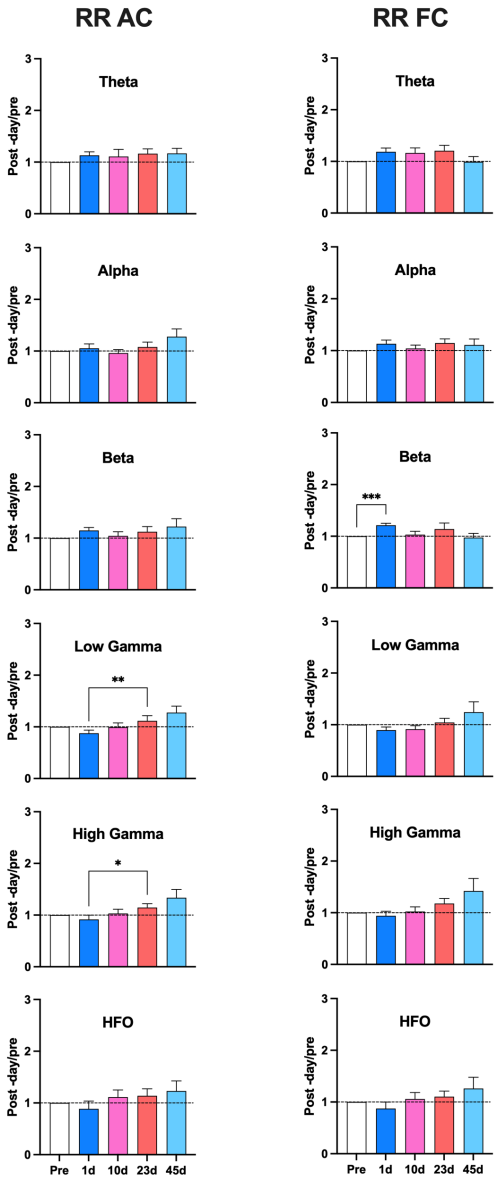

Figure 7. The power spectral density in the RR group showed few significant changes over time. Each panel shows the power in a frequency band at a specific day after NIHL as a ratio of the pre-NIHL power for the same frequency band. A ratio of 1 indicates no change. Ratios higher than 1 indicate an increase in the post-NIHL recorded timepoint in comparison to pre-NIHL. The only significant change was in beta power 1 day after NIHL. *p<0.05; **p<0.01, ***, p < 0.0001.

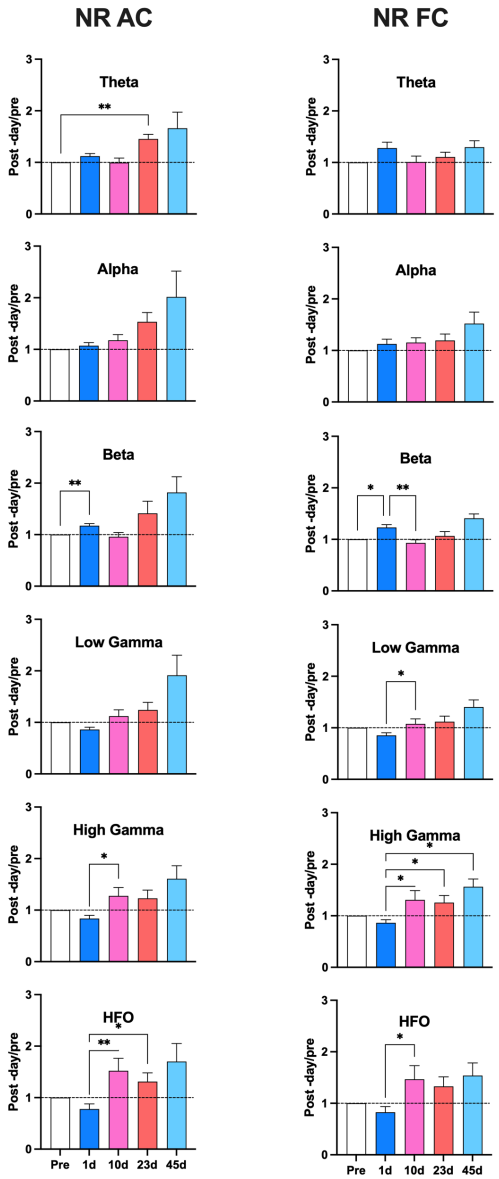

Figure 8. The power spectral density in the NR group showed a number of significant region-specific changes over post-NIHL time with increasing power being the main direction of change. *p<0.05; **p<0.01

Mixed-effects One-way ANOVA

RR AC	Main Effect of Time	p
Theta (3 – 7 Hz)	F (2.328, 29.68) = 0.5756	0.5936
Alpha (8 – 13 Hz)	F (2.242, 28.58) = 1.984	0.1518
Beta (14 – 29 Hz)	F (2.910, 37.11) = 1.313	0.2845
Low Gamma (30 – 59 Hz)	F (1.989, 24.86) = 5.728	**0.0091**
High Gamma (60 – 100 Hz)	F (1.889, 24.56) = 4.521	**0.0229**
HFO (101 – 250 Hz)	F (2.404, 31.25) = 1.438	0.2525

RR FC	Main Effect of Time	p
Theta	F (3.098, 40.28) = 1.874	0.1478
Alpha	F (2.303, 29.94) = 1.133	0.3418
Beta	F (2.170, 28.21) = 2.123	0.1350
Low Gamma	F (1.465, 19.04) = 3.025	0.0852
High Gamma	F (1.556, 20.22) = 3.356	0.0654
HFO	F (1.885, 24.51) = 1.383	0.2689

NR AC	Main Effect of Time	p
Theta	F (1.419, 16.68) = 8.735	**0.0050**
Alpha	F (1.590, 14.31) = 7.147	**0.0099**
Beta	F (2.121, 19.09) = 4.167	**0.0296**
Low Gamma	F (1.810, 16.29) = 11.84	**0.0009**
High Gamma	F (2.049, 17.93) = 7.815	**0.0035**
HFO	F (2.118, 19.06) = 7.692	**0.0032**

NR FC	Main Effect of Time	p
Theta	F (2.621, 23.59) = 2.185	0.1230
Alpha	F (1.929, 17.36) = 5.934	**0.0115**
Beta	F (2.423, 21.81) = 7.932	**0.0016**
Low Gamma	F (2.391, 21.52) = 8.955	**0.0009**
High Gamma	F (1.820, 16.38) = 7.623	**0.0054**
HFO	F (1.996, 17.96) = 5.586	**0.0130**

Table 1. Full statistical results table from EEG resting power analysis. Mixed-effects analysis one-way ANOVA compared the effect of time within each cortical region for RR and NR groups. Bold values indicate significance.

Bonferroni's Multiple Comparisons Test

RR AC	Pre vs 1d	Pre vs 10d	Pre vs 23d	Pre vs 45d	1d vs 10d	1d vs 23d	1d vs 45d
Theta (3 – 7 Hz)	0.4911	>0.9999	0.6144	0.6307	>0.9999	>0.9999	>0.9999
Alpha (8 – 13 Hz)	>0.9999	>0.9999	>0.9999	0.4695	>0.9999	>0.9999	>0.9999
Beta (14 – 29 Hz)	0.1432	>0.9999	>0.9999	0.9510	>0.9999	>0.9999	>0.9999
Low Gamma (30 – 59 Hz)	0.3944	>0.9999	>0.9999	0.2609	0.5178	**0.0099**	0.0939
High Gamma (60 – 100 Hz)	>0.9999	>0.9999	0.5221	0.3116	0.8133	**0.0258**	0.3386
HFO (101 – 250 Hz)	>0.9999	>0.9999	>0.9999	>0.9999	0.3092	0.9016	>0.9999

RR FC	Pre vs 1d	Pre vs 10d	Pre vs 23d	Pre vs 45d	1d vs 10d	1d vs 23d	1d vs 45d
Theta	0.1444	0.8396	0.4706	>0.9999	>0.9999	>0.9999	0.5615
Alpha	0.6231	>0.9999	0.6103	>0.9999	>0.9999	>0.9999	>0.9999
Beta	**0.0005**	>0.9999	>0.9999	>0.9999	0.1179	>0.9999	0.1757
Low Gamma	0.7033	>0.9999	>0.9999	>0.9999	>0.9999	0.4062	0.8318
High Gamma	>0.9999	>0.9999	0.5938	0.5938	>0.9999	0.2156	0.6490
HFO	>0.9999	>0.9999	>0.9999	>0.9999	0.5454	>0.9999	>0.9999

NR AC	Pre vs 1d	Pre vs 10d	Pre vs 23d	Pre vs 45d	1d vs 10d	1d vs 23d	1d vs 45d
Theta	0.2268	>0.9999	**0.0029**	0.5679	>0.9999	0.0554	>0.9999
Alpha	>0.9999	>0.9999	0.0884	0.6181	>0.9999	0.0750	0.9048
Beta	**0.0078**	>0.9999	0.7433	0.3217	0.2484	>0.9999	0.6456
Low Gamma	0.0876	>0.9999	0.9290	0.4464	0.1089	0.0663	0.2620
High Gamma	0.1561	0.8083	>0.9999	0.4251	**0.0242**	0.0818	0.2248
HFO	0.3527	0.3903	0.6824	0.6370	**0.0073**	**0.0261**	0.2979

NR FC	Pre vs 1d	Pre vs 10d	Pre vs 23d	Pre vs 45d	1d vs 10d	1d vs 23d	1d vs 45d
Theta	0.2241	>0.9999	>0.9999	0.4297	0.6728	>0.9999	>0.9999
Alpha	>0.9999	0.8313	>0.9999	0.4515	>0.9999	>0.9999	>0.9999
Beta	**0.0111**	>0.9999	>0.9999	0.0698	**0.0094**	**0.4867**	**0.9656**
Low Gamma	0.0917	>0.9999	>0.9999	0.2538	**0.0333**	0.0720	0.0849
High Gamma	0.3030	0.7868	0.6135	0.1321	**0.0464**	**0.0401**	**0.0408**
HFO	0.9842	0.7575	0.7339	0.5203	**0.0347**	0.0796	0.2150

Table 2. Post-hoc analysis from EEG resting power analysis. Bonferroni's multiple comparisons test was used to compare post-NIHL time points with pre-NIHL timepoints in the first four columns. The last three columns compare 1-day post-NIHL with later time points. Significant adjusted p-values are in bold.

iv. 40 Hz Auditory Steady State Response recovers in the AC, but not FC, in the RR group

A 40 Hz pulsed noise stimulus was presented at 90 dB SPL to generate an auditory steady state response (ASSR). The inter-trial phase coherence (ITPC) measured the cortex's ability to consistently phase lock to the stimulus across trials, with mean ITPC compared between timepoints in the RR (Figure 9) and NR groups. The mean ITPC showed that the FC did not recover after NIHL, but the AC did. In the RR group, the AC ITPC decreased significantly 1 day after NIHL ($F(2.123, 19.11) = 9.813$, $p=0.001$; Dunnett's multiple comparisons test – pre vs 1-day: $p=0.0422$) (Figure 10A). The FC had reduced ITPC mean values beginning at 1 day after NIHL and remained lowered up to 45 day ($F(1.286, 11.57) = 29.17$, $p<0.0001$; Dunnett's multiple comparisons test – pre vs 1-day: $p=0.0001$, pre vs 10-day: $p=0.0017$, pre vs 23-day: $p=0.0029$, pre vs 45-day: $p=0.0028$) (Figure 10B). ITPC group averages were compared across timepoints by repeated measures 1-way ANOVA. These data show cortical-region specific differences in recovery of ASSR post-NIHL.

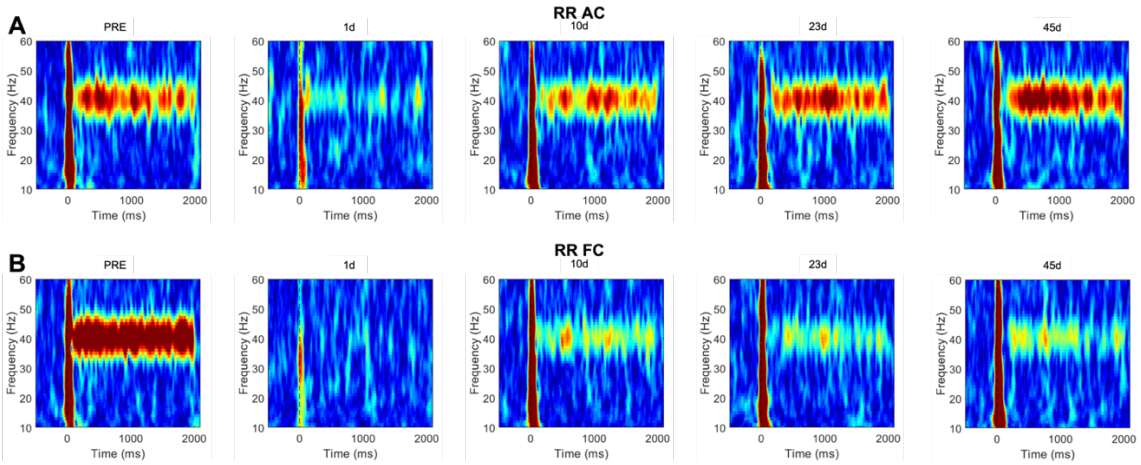

Figure 9. Example 40 Hz ASSR from one RR mouse shows recovery in the AC, but not the FC. Each panel shows after ITPC across trials from each region (AC, FC) for the RR mouse across a number of time points relative to NIHL. While the ASSR consistency clearly recovered after NIHL in the AC (A), there was no significant recovery in the FC (B) even up to 45 days after NIHL.

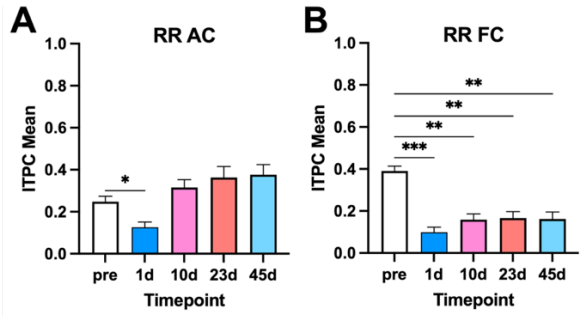

Figure 10. The ITPC mean remained diminished over time in the frontal cortex, but recovered in the auditory cortex by 10 days after NIHL. The group average ITPC was compared at each timepoint with +/- SEM. A) Auditory cortex ITPC mean for RR group showing ITPC mean returns to baseline levels by 10 days. B) RR frontal cortex ITPC mean does not recover over time.

v. Temporal processing recovers above pre-NIHL levels in the AC, but not FC, after NIHL

Gap-ASSR is a more challenging stimulus for the cortex to follow and consistently synchronize to, particularly as gap-width is reduced. Prior to NIHL, the AC in the RR group responds robustly at 9ms and the ITPC steadily decreases as the gap widths decreased (Figure 11). There was a significant decrease in ITPC at 1 day ($F(1.310, 11.79) = 9.921$,

p=0.006) after NIHL compared to baseline particularly at the longer gap durations (F (2.284, 20.56) = 58.71, p<0.0001) (gap duration x timepoint: F (4.338, 37.78) = 3.683, p=0.011); Dunnett: pre vs 1 day after NIHL; 5-, 7-, 8-, 9 ms; p<.001), but the mean ITPC was only significantly different from pre-NIHL values at 3- and 4 ms at 45 days after NIHL (Dunnet: p=0.03; p=-.0036, respectively) but not at the longer gap durations (Figure 12A).

In the FC of the RR group, however, the gap-ASSR did not recover after NIHL at any of the gap durations (F (1.599, 14.39) = 23.57, p<0.0001) or time points (F (1.243, 11.19) = 33.94, p<0.0001). The FC of the RR group showed that ITPC mean remained diminished over time after NIHL across gap widths (gap duration x timepoints: F (4.835, 42.11) = 7.980, p<0.0001; Dunnett: all gap widths and time points, p=<0.01) (Figure 12B). These data show that there is a cortical-region specific difference in recovery of temporal processing after NIHL.

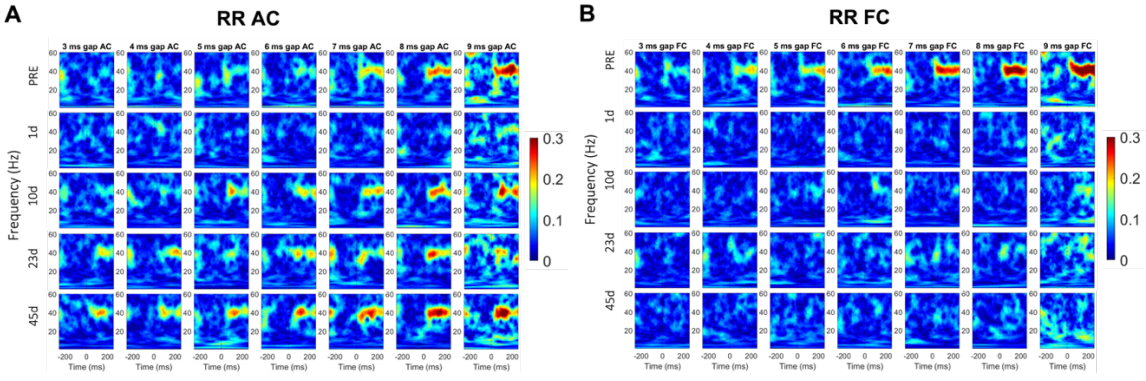

Figure 11. Example Gap-ASSR ITPC from one RR mouse from pre- to 45 days after NIHL. A) Auditory cortex gap durations increasing from 3 ms to 9 ms (right to left) from pre-NIHL (top row) shows an enhancement by 45 days after NIHL (bottom row). B) Frontal cortex gap-ASSR shows that ITPC does not recover to baseline (top row) even by 45 days after NIHL (bottom row) even at 9 ms gap duration (left columns). Heatmap scale warmer color indicates greater ITPC.

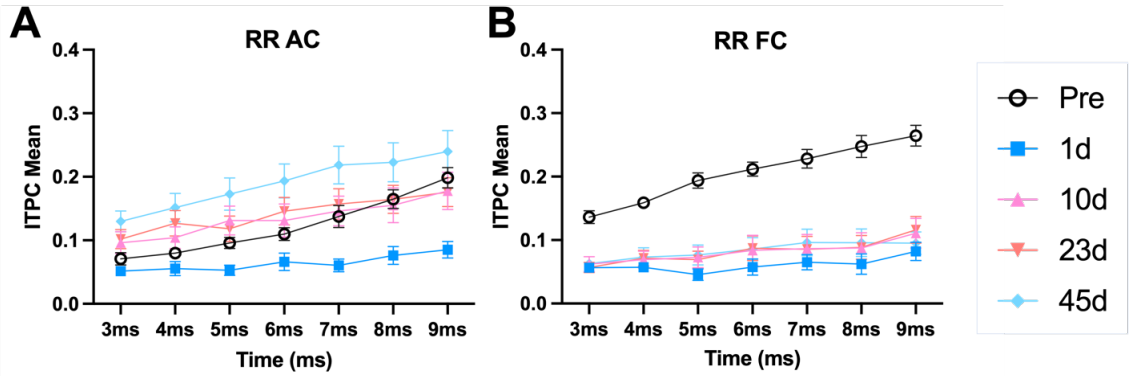

Figure 12. Average gap-ASSR ITPC values across gap-widths and post-NIHL time points show region-specific differences in recovery. In the AC (A), the ITPC values decrease considerably the day after NIHL, but recover above pre-NIHL levels at 45 days post-NIHL. On the other hand, average ITPC values in the FC (B) do no recover after NIHL even though the ERPs in this region were back to pre-NIHL levels.

Discussion

This study examined the longitudinal effects of NIHL on resting power and sound evoked responses in adult FVB mice. We found changes that indicate central gain after noise-exposure. Key findings over 45 days post-NIHL were as follows: 1) all mice had increased ABR thresholds >90 dB SPL at every time point measured post-NIHL, 2) despite the lack of ABRs, approximately half of the mice showed response recovery (RR group) to noise stimuli at 90 dB as measured by ERPs in both AC and FC, 3) resting EEG spectral power density was relatively more affected in the NR group AC and FC than the RR group, 4) there was a cortical region-specific recovery in the AC ITPC for 40 Hz ASSR and gap-ASSR, but not FC. We interpret the recovery of ERP amplitude as evidence for some residual hearing in the RR group, undetected by click ABR, that is amplified post-NIHL. This is supported by ERP amplitudes that were ~40% of pre-NIHL levels on day 1 post-

NIHL in the RR group. The pre-NIHL ERPs were also recorded at 90 dB SPL, but this sound level was ~45 dB above ABR thresholds. The post-NIHL ERPs were also recorded at 90 dB SPL, which is likely closer to the threshold of any residual hearing that was undetected by click ABRs. The post-NIHL ERP amplitudes, however, recovered to pre-NIHL amplitudes despite the relative sound levels being considerably different pre- vs post-NIHL. The recovery of ERPs therefore suggests central amplification of the residual signal, consistent with central gain models. This is also supported by the improved auditory cortex ITPC for ASSR for the RR group, which showed a larger ITPC at 45 days post-NIHL compared to pre-NIHL. However, despite the ERPs recovering in the FC, there was no recovery of ITPC in the ASSR and gap-ASSR paradigms in this cortical region. Taken together, our data provide support for the central gain model, with regional differences in recovery of temporal processing after NIHL.

Although our NIHL paradigm induced permanent threshold shifts and non-detectable click ABRs, some mice had residual hearing which indicate some residual hearing remained that may have been amplified at the level of the cortex. Schrode et al. (2018) tested adult CBA/CaJ click and tone ABRs following 2 hours of broadband 100 dB SPL sound exposure and reported elevated threshold shifts with no strong effect of frequency likely due to the broadband exposure stimulus. This potentially explains why approximately half of our mice showed sound evoked responses despite the absence of click ABRs, we predict that the tone ABRs would have showed responses at higher intensities. Many studies have compared enhanced gain in the auditory cortex and inferior colliculus (IC), but the temporal dynamics and recovery of responses often show there is

stronger enhancement in the AC (Chambers et al., 2016; Resnik & Polley, 2021). We chose to focus on the AC as it has been shown that there was persistent gain for long periods of time and descending projections from the cortex could underlie the compensatory plasticity that manifests after hearing loss (Asokan et al. 2017). Gap-detection was found to be impaired in C57BL/6 mice up to 10 days after noise exposure, but not in FVB mice (Zinsmaier et al. 2020). In line with these findings, our FVB mice only showed recovered ITPC to both ASSR protocols, which can be used as a way to measure temporal processing, in the AC of the RR group. Our data may provide weight to central gain as seen in the sound evoked responses, but temporal processing recovers but is not enhanced in the AC. Mechanistically, it is likely that reduced inhibition because of NIHL may underlie enhanced central gain. Hyperactivity has been attributed to an imbalanced cortical circuit, with inhibition being impacted after NIHL. Fast-spiking inhibitory interneurons are a prime suspect to be causing the skew towards hyperexcitability. Parvalbumin inhibitory interneurons (PV) had limited sound evoked recovery after cochlear nerve degeneration whereas putative pyramidal cells had near-complete recovery in the AC, netting in hyperexcitability (Resnik & Polley, 2021). At the synaptic level, NIHL also impacts vesicular glutamate transporters (VGLUT) by decreased expression of VGLUT1 in rat AC, while PV + perineuronal net (PNN) stained cells also decreased (S. Park et al. 2020). This further implicates E/I imbalance post-NIHL as a potential cause of central gain.

Hearing loss has been linked with cognitive decline and other neurological pathologies, though the mechanisms and implications of disconnecting AC and FC are not as well understood. Humans with hearing loss are more likely to be diagnosed with

dementia and cognitive decline (Lin, 2011; Uhlmann, Larson, Rees, Koepsell, & Duckert, 1989). Lin (2011) suggested that hearing loss may be related to cognitive decline through exhaustion of cognitive reserves. Under difficult listening conditions (hearing loss and gaps in noise), more cognitive resources may be allocated to basic auditory processing at the expense of frontal cortex executive functions. That is, there is a reallocation of cortical resources possibly leading to reduced cognition at the expense of sensory detection. Our data supports this interpretation in that the auditory cortex provides the substrates for improved detection and temporal processing following NIHL, but the frontal cortex is unable to phase lock reliably to short gaps in noise. To the extent that temporal processing in the frontal cortex is linked to cognitive functions (Emmons et al., 2017; Kim et al., 2017; Olton, Wenk, Church, & Meck, 1988), active listening (Hall et al., 2000), and descending control of sensory cortices, these data predict abnormal cognition following NIHL. Future studies should include NIHL and gap detection tasks under active and passive listening conditions to determine if the absence of frontal cortex recovery has implications for temporal processing.

In a rodent model of NIHL, Wieczerzak et al. (2021) found a clear cortical region-specific increase was found in sound evoked activity in the AC of awake rats compared to prefrontal cortex after noise exposure. Although their rat model had smaller threshold shifts than the mice in the present study, they also showed decreases in intertrial phase coherence of the 40 Hz steady state response only in the prefrontal cortex as well as impaired spatial learning. Moreover, they reported reduced phase-locking value between the AC and prefrontal cortex speculating that the functional connectivity between the two cortical

regions was impacted after NIHL. Despite the difference in animal model and hearing loss induction, these temporal processing findings were consistent with the cortical region-specific differences we found in the ASSR and gap-ASSR data. Further, prefrontal cortex has been speculated to be involved with sensory gating of auditory information and can be disrupted following hearing loss (Barry, Robertson, and Mulders 2017; De Vis, Barry, and Mulders 2022). It is unknown whether the mechanistic changes are occurring in the AC are similar to what is occurring in the FC. We speculate that the clear difference in cortical-region recovery during temporal processing post-NIHL could indicate a disruption between AC and FC communication and connectivity. Phase-amplitude or phase-phase coupling between AC and FC may more clearly find the disruption between the two regions. Deficits in other regions may also link hearing loss to cognitive decline. For example, moderate noise exposure led to impaired learning and memory of mice along with oxidative stress in the AC, IC, and hippocampus (Cheng et al. 2011). NIHL was induced in young mice and recognition memory was permanently impacted along with increased p-tau expression in the hippocampus, indicating a link to hearing-related cognitive decline (S. Y. Park et al. 2018). A longitudinal study of young mice showed cognitive impairment through lower performance during memory tasks after moderate hearing loss (S. Y. Park et al. 2016). In rats, spatial working memory was impaired along with increased ABR thresholds, diminished outer hair cells and synaptic ribbons (Shukla et al. 2019). Taken together, NIHL impacts not just the AC and auditory centers, but cognitive regions as well with the connectivity between AC and FC may be damaged leading to impaired top-down regulation of sensory input.

Hyperactivity in the auditory cortex may manifest as increased spontaneous activity, where the balance between excitation and inhibition is altered. Increased internal noise within the AC may underlie perceptual difficulties, preventing the system from detecting targets in noise (Resnik & Polley, 2021). Noise exposure was found to increase spike firing rate in AC neurons of rats soon after noise exposure as well as increased auditory cortex sound evoked potentials (Sun et al., 2012). Decreases in auditory nerve compound potentials (Salvi et al. 2017) lead to increases in auditory cortex spontaneous activity following noise-exposure (Auerbach, Rodrigues, and Salvi 2014). These findings are somewhat consistent with our resting EEG data, which show that in the RR group there are differences mainly in the low and high gamma frequency ranges in the AC. Wieczerzak et al. (2021) reported no changes in spontaneous activity in either AC or FC across the frequency spectrum, which may be different from our findings due to the difference in rodent model and pattern of hearing loss. They also only tested up to 7 days post-NIHL, which may not have been enough time to see any compensatory changes in the rat cortex. Ray and Maunsell (2011) correlate "high gamma (80-200 Hz)" with spiking activity. Spontaneous activity following NIHL could manifest as enhanced cortical activity in the absence of stimulus, which we see occurring at the purported frequency ranges linked to spiking and hyperactivity. Additionally, this is in line with our hypothesis that NIHL ultimately affects PV+ cells, for which these interneurons are purported to be highly linked with gamma oscillations (Bartos, Vida, and Jonas 2007; Guyon et al. 2021; Sohal et al. 2009). Guyon et al. (2021) reported deficient PV+ inhibition was linked to enhanced broadband gamma power indicating asynchronous excitatory firing. We report that there is

a broadband gamma band enhancement in the AC from deafferentation leading to increased spontaneous activity. In the NR group, almost all the frequency bands are affected by NIHL in resting EEG power in both cortical regions recorded indicating an increase in spectral power across the board. This may skew the auditory system from detecting external stimuli. We speculate this to mean that there is an indiscriminatory circuit dysfunction. In the absence of peripheral input, absolute power goes up in a non-specific manner post-NIHL. Taken together with our data, resting EEG spectral power is differentially affected post-NIHL depending on whether mice had residual hearing. In both cases, network activity is disrupted but further studies should test at the synaptic and cellular level to investigate how excitatory and inhibitory activity and expression are remaining.

Conclusions

Ultimately these outcomes may serve as a compensatory mechanism after deafferentation from the cochlea or sensory deprivation, where normal auditory input is unable to be transmitted due to peripheral damage or lack of connection coming from the cochlea (Cody and Robertson 1983; Haragopal et al. 2020; Kujawa and Liberman 2009). Compensatory gain increases were found to be beneficial for sensory processing in the auditory cortex (Chambers et al. 2016), however if left unimpeded the compensation of excessive spontaneous firing may push past homeostasis and manifest as hyperactivity (Möhrle et al. 2019; Rüttiger et al. 2013) that may underlie tinnitus and hyperacusis (Auerbach et al., 2014; Roberts et al., 2010), at the expense of fine temporal processing.

1. Asokan, M. M., Williamson, R. S., Hancock, K. E., & Polley, D. B. (2017, July 13). Dynamic gain adjustments in descending corticofugal outputs from auditory cortex compensate for cochlear nerve synaptic damage. *BioRxiv*. bioRxiv. https://doi.org/10.1101/162909

2. Asokan, M. M., Williamson, R. S., Hancock, K. E., & Polley, D. B. (2018). Sensory overamplification in layer 5 auditory corticofugal projection neurons following cochlear nerve synaptic damage. *Nature Communications 2018 9:1*, *9*(1), 1–10. https://doi.org/10.1038/s41467-018-04852-y

3. Auerbach, B. D., Rodrigues, P. V., & Salvi, R. J. (2014). Central Gain Control in Tinnitus and Hyperacusis. *Frontiers in Neurology*, *5*. https://doi.org/10.3389/fneur.2014.00206

4. Barry, K. M., Robertson, D., & Mulders, W. H. A. M. (2017). Medial geniculate neurons show diverse effects in response to electrical stimulation of prefrontal cortex. *Hearing Research*, *353*, 204–212. https://doi.org/10.1016/J.HEARES.2017.07.002

5. Bartos, M., Vida, I., & Jonas, P. (2007, January). Synaptic mechanisms of synchronized gamma oscillations in inhibitory interneuron networks. *Nature Reviews Neuroscience*. Nature Publishing Group. https://doi.org/10.1038/nrn2044

6. Bernabei, R., Bonuccelli, U., Maggi, S., Marengoni, A., Martini, A., Memo, M., … Lin, F. R. (2014). Hearing loss and cognitive decline in older adults: questions and answers. *Aging Clinical and Experimental Research 2014 26:6*, *26*(6), 567–573. https://doi.org/10.1007/S40520-014-0266-3

7. Campbell, J., & Sharma, A. (2020). Frontal Cortical Modulation of Temporal Visual Cross-Modal Re-organization in Adults with Hearing Loss. *Brain Sciences 2020, Vol. 10, Page 498*, *10*(8), 498. https://doi.org/10.3390/BRAINSCI10080498

8. Chambers, A. R., Resnik, J., Yuan, Y., Whitton, J. P., Edge, A. S., Liberman, M. C., & Polley, D. B. (2016). Central Gain Restores Auditory Processing following Near-Complete Cochlear Denervation. *Neuron*, *89*(4), 867–879. https://doi.org/10.1016/j.neuron.2015.12.041

9. Cheng, L., Wang, S. H., Chen, Q. C., & Liao, X. M. (2011). Moderate noise induced cognition impairment of mice and its underlying mechanisms. *Physiology & Behavior*, *104*(5), 981–988. https://doi.org/10.1016/J.PHYSBEH.2011.06.018

10. Chung, J. H., Des Roches, C. M., Meunier, J., & Eavey, R. D. (2005). Evaluation of Noise-Induced Hearing Loss in Young People Using a Web-Based Survey Technique. *Pediatrics*, *115*(4), 861–867. https://doi.org/10.1542/PEDS.2004-0173

11. Cody, A. R., & Robertson, D. (1983). Variability of noise-induced damage in the guinea pig cochlea: Electrophysiological and morphological correlates after strictly controlled exposures. *Hearing Research*, *9*(1), 55–70. https://doi.org/10.1016/0378-5955(83)90134-X

12. De Vis, C., Barry, K. M., & Mulders, W. H. A. M. (2022). Hearing Loss Increases Inhibitory Effects of Prefrontal Cortex Stimulation on Sound Evoked Activity in Medial Geniculate Nucleus. *Frontiers in Synaptic Neuroscience*, *14*, 6. https://doi.org/10.3389/FNSYN.2022.840368/XML/NLM

13. Dimitrijevic, A., John, M. S., & Picton, T. W. (2004). Auditory Steady-State Responses and Word Recognition Scores in Normal-Hearing and Hearing-Impaired Adults. *Ear and Hearing*, *25*(1), 68–84. https://doi.org/10.1097/01.AUD.0000111545.71693.48

14. Eggermont, J. J., & Roberts, L. E. (2004). The neuroscience of tinnitus. *Trends in Neurosciences*, *27*(11), 676–682. https://doi.org/10.1016/J.TINS.2004.08.010

15. Emmons, E. B., De Corte, B. J., Kim, Y., Parker, K. L., Matell, M. S., & Narayanan, N. S. (2017). Rodent Medial Frontal Control of Temporal Processing in the Dorsomedial Striatum. *The Journal of Neuroscience : The Official Journal of the Society for Neuroscience*, *37*(36), 8718–8733. https://doi.org/10.1523/JNEUROSCI.1376-17.2017

16. Giroud, N., Keller, M., & Meyer, M. (2021). Interacting effects of frontal lobe neuroanatomy and working memory capacity to older listeners' speech recognition in noise. *Neuropsychologia*, *158*, 107892. https://doi.org/10.1016/J.NEUROPSYCHOLOGIA.2021.107892

17. Guyon, N., Zacharias, L. R., de Oliveira, E. F., Kim, H., Leite, J. P., Lopes-Aguiar, C., & Carlén, M. (2021). Network asynchrony underlying increased broadband gamma power. *Journal of Neuroscience*, *41*(13), 2944–2963. https://doi.org/10.1523/JNEUROSCI.2250-20.2021

18. Hall, D. A., Haggard, M. P., Akeroyd, M. A., Summerfield, A. Q., Palmer, A. R., Elliott, M. R., & Bowtell, R. W. (2000). Modulation and Task Effects in Auditory Processing Measured Using fMRI. *Hum. Brain Mapping*, *10*, 107–119. https://doi.org/10.1002/1097-0193

19. Haragopal, H., Dorkoski, R., Johnson, H. M., Berryman, M. A., Tanda, S., & Day, M. L. (2020). Paired measurements of cochlear function and hair cell count in Dutch-belted rabbits with noise-induced hearing loss. *Hearing Research*, *385*. https://doi.org/10.1016/j.heares.2019.107845

20. Henderson, E., Testa, M. A., & Hartnick, C. (2011). Prevalence of Noise-Induced Hearing-Threshold Shifts and Hearing Loss Among US Youths. *Pediatrics*, *127*(1), e39–e46. https://doi.org/10.1542/PEDS.2010-0926

21. Kim, Y. C., Han, S. W., Alberico, S. L., Ruggiero, R. N., De Corte, B., Chen, K. H., & Narayanan, N. S. (2017). Optogenetic Stimulation of Frontal D1 Neurons Compensates for Impaired Temporal Control of Action in Dopamine-Depleted Mice. *Current Biology*, *27*(1), 39–47. https://doi.org/10.1016/j.cub.2016.11.029

22. Kujawa, S. G., & Liberman, M. C. (2009). Adding insult to injury: Cochlear nerve degeneration after "temporary" noise-induced hearing loss. *Journal of Neuroscience*, *29*(45), 14077–14085. https://doi.org/10.1523/JNEUROSCI.2845-09.2009

23. Larsby, B., Hällgren, M., Lyxell, B., & Arlinger, S. (2009). Cognitive performance and perceived effort in speech processing tasks: effects of different noise backgrounds in normal-hearing and hearing-impaired subjects Desempeño cognitivo y percepción del esfuerzo en tareas de procesamiento del lenguaje: Efectos de las diferentes condiciones de fondo en sujetos normales e hipoacúsicos. *Http://Dx.Doi.Org/10.1080/14992020500057244*, *44*(3), 131–143. https://doi.org/10.1080/14992020500057244

24. Leigh-Paffenroth, E. D., & Fowler, C. G. (2006). Amplitude-modulated auditory steady-state responses in younger and older listeners. *Journal of the American Academy of Audiology*, *17*(8), 582–597. https://doi.org/10.3766/JAAA.17.8.5/BIB

25.

26. Liberman, M. C., & Kujawa, S. G. (2017). Cochlear synaptopathy in acquired sensorineural hearing loss: Manifestations and mechanisms. *Hearing Research*, *349*, 138–147. https://doi.org/10.1016/J.HEARES.2017.01.003

27. Lin, F. R. (2011). Hearing Loss and Cognition Among Older Adults in the United States. *The Journals of Gerontology Series A: Biological Sciences and Medical Sciences*, *66A*(10), 1131. https://doi.org/10.1093/GERONA/GLR115

28. Lin, F. R., Yaffe, K., Xia, J., Xue, Q. L., Harris, T. B., Purchase-Helzner, E., … Simonsick, E. M. (2013). Hearing Loss and Cognitive Decline in Older Adults. *JAMA Internal Medicine*, *173*(4), 293–299. https://doi.org/10.1001/JAMAINTERNMED.2013.1868

29. Livingston, G., Huntley, J., Sommerlad, A., Ames, D., Ballard, C., Banerjee, S., … Mukadam, N. (2020, August 8). Dementia prevention, intervention, and care: 2020 report of the Lancet Commission. *The Lancet*. Lancet Publishing Group. https://doi.org/10.1016/S0140-6736(20)30367-6

30. Luo, H., Pace, E., Zhang, X., & Zhang, J. (2014). Blast-Induced tinnitus and

spontaneous firing changes in the rat dorsal cochlear nucleus. *Journal of Neuroscience Research*, *92*(11), 1466–1477. https://doi.org/10.1002/jnr.23424

31. Möhrle, D., Hofmeier, B., Amend, M., Wolpert, S., Ni, K., Bing, D., … Rüttiger, L. (2019). Enhanced Central Neural Gain Compensates Acoustic Trauma-induced Cochlear Impairment, but Unlikely Correlates with Tinnitus and Hyperacusis. *Neuroscience*, *407*, 146–169. https://doi.org/10.1016/j.neuroscience.2018.12.038

32. Moore, D. R., Edmondson-Jones, M., Dawes, P., Fortnum, H., McCormack, A., Pierzycki, R. H., & Munro, K. J. (2014). Relation between Speech-in-Noise Threshold, Hearing Loss and Cognition from 40–69 Years of Age. *PLOS ONE*, *9*(9), e107720. https://doi.org/10.1371/JOURNAL.PONE.0107720

33. Nelson, D. I., Nelson, R. Y., Concha-Barrientos, M., & Fingerhut, M. (2005). The global burden of occupational noise-induced hearing loss. *American Journal of Industrial Medicine*, *48*(6), 446–458. https://doi.org/10.1002/ajim.20223

34. Noreña, A. J., & Eggermont, J. J. (2003). Changes in spontaneous neural activity immediately after an acoustic trauma: Implications for neural correlates of tinnitus. *Hearing Research*, *183*(1–2), 137–153. https://doi.org/10.1016/S0378-5955(03)00225-9

35. Olton, D. S., Wenk, G. L., Church, R. M., & Meck, W. H. (1988). Attention and the frontal cortex as examined by simultaneous temporal processing. *Neuropsychologia*, *26*(2), 307–318. https://doi.org/10.1016/0028-3932(88)90083-8

36. Park, S., Lee, D., Lee, S. M., Lee, C. H., & Kim, S. Y. (2020). Noise exposure alters MMP9 and brevican expression in the rat primary auditory cortex. *BMC Neuroscience 2020 21:1*, *21*(1), 1–10. https://doi.org/10.1186/S12868-020-00567-3

37. Park, S. Y., Kim, M. J., Kim, H. L., Kim, D. K., Yeo, S. W., & Park, S. N. (2018). Cognitive decline and increased hippocampal p-tau expression in mice with hearing loss. *Behavioural Brain Research*, *342*, 19–26. https://doi.org/10.1016/J.BBR.2018.01.003

38. Park, S. Y., Kim, M. J., Sikandaner, H., Kim, D. K., Yeo, S. W., & Park, S. N. (2016). A causal relationship between hearing loss and cognitive impairment. *Http://Dx.Doi.Org/10.3109/00016489.2015.1130857*, *136*(5), 480–483. https://doi.org/10.3109/00016489.2015.1130857

39. Ray, S., & Maunsell, J. H. R. (2011). Different origins of gamma rhythm and high-gamma activity in macaque visual cortex. *PLoS Biology*, *9*(4). https://doi.org/10.1371/journal.pbio.1000610

40. Resnik, J., & Polley, D. B. (2017). Fast-spiking GABA circuit dynamics in the auditory cortex predict recovery of sensory processing following peripheral nerve damage. *ELife*, *6*. https://doi.org/10.7554/eLife.21452

41. Resnik, J., & Polley, D. B. (2021). Cochlear neural degeneration disrupts hearing in background noise by increasing auditory cortex internal noise. *Neuron*, *109*(6), 984-996.e4. https://doi.org/10.1016/J.NEURON.2021.01.015

42. Roberts, L. E., Eggermont, J. J., Caspary, D. M., Shore, S. E., Melcher, J. R., & Kaltenbach, J. A. (2010). Ringing Ears: The Neuroscience of Tinnitus. *Journal of Neuroscience*, *30*(45), 14972–14979. https://doi.org/10.1523/JNEUROSCI.4028-10.2010

43. Rüttiger, L., Singer, W., Panford-Walsh, R., Matsumoto, M., Lee, S. C., Zuccotti, A., … Knipper, M. (2013). The Reduced Cochlear Output and the Failure to Adapt the Central Auditory Response Causes Tinnitus in Noise Exposed Rats. *PLoS ONE*, *8*(3), 1–11. https://doi.org/10.1371/journal.pone.0057247

44. Salvi, R., Sun, W., Ding, D., Chen, G.-D., Lobarinas, E., Wang, J., … Auerbach, B. D. (2017). Inner Hair Cell Loss Disrupts Hearing and Cochlear Function Leading to Sensory Deprivation and Enhanced Central Auditory Gain. *Frontiers in Neuroscience*, *10*(JAN), 621. https://doi.org/10.3389/fnins.2016.00621

45. Schrode, K. M., Muniak, M. A., Kim, Y. H., & Lauer, A. M. (2018). Central compensation in auditory brainstem after damaging noise exposure. *ENeuro*, *5*(4). https://doi.org/10.1523/ENEURO.0250-18.2018

46. Seki, S., & Eggermont, J. J. (2003). Changes in spontaneous firing rate and neural synchrony in cat primary auditory cortex after localized tone-induced hearing loss. *Hearing Research*, *180*(1–2), 28–38. https://doi.org/10.1016/S0378-5955(03)00074-1

47. Shukla, M., Roy, K., Kaur, C., Nayak, D., Mani, K. V., Shukla, S., & Kapoor, N. (2019). Attenuation of adverse effects of noise induced hearing loss on adult neurogenesis and memory in rats by intervention with Adenosine A2A receptor agonist. *Brain Research Bulletin*, *147*, 47–57. https://doi.org/10.1016/J.BRAINRESBULL.2019.02.006

48. Sohal, V. S., Zhang, F., Yizhar, O., & Deisseroth, K. (2009). Parvalbumin neurons and gamma rhythms enhance cortical circuit performance. *Nature*, *459*(7247), 698–702. https://doi.org/10.1038/nature07991

49. Sun, W., Deng, A., Jayaram, A., & Gibson, B. (2012). Noise exposure enhances auditory cortex responses related to hyperacusis behavior. *Brain Research*, *1485*, 108–116. https://doi.org/10.1016/J.BRAINRES.2012.02.008

50. Uhlmann, R. F., Larson, E. B., Rees, T. S., Koepsell, T. D., & Duckert, L. G. (1989). Relationship of Hearing Impairment to Dementia and Cognitive Dysfunction in Older Adults. *JAMA*, *261*(13), 1916–1919. https://doi.org/10.1001/JAMA.1989.03420130084028

51. Wieczerzak, K. B., Patel, S. V., MacNeil, H., Scott, K. E., Schormans, A. L., Hayes, S. H., … Allman, B. L. (2021). Differential Plasticity in Auditory and Prefrontal Cortices, and Cognitive-Behavioral Deficits Following Noise-Induced Hearing Loss. *Neuroscience*, *455*, 1–18. https://doi.org/10.1016/j.neuroscience.2020.11.019

52. Zeng, F. G., Nie, K., Stickney, G. S., Kong, Y. Y., Vongphoe, M., Bhargave, A., … Cao, K. (2005). Speech recognition with amplitude and frequency modulations. *Proceedings of the National Academy of Sciences of the United States of America*, *102*(7), 2293–2298. https://doi.org/10.1073/PNAS.0406460102/SUPPL_FILE/06460SUPPAUDIO.DOC

53. Zinsmaier, A. K., Wang, W., Zhang, L., Hossainy, N. N., & Bao, S. (2020). Resistance to noise-induced gap detection impairment in FVB mice is correlated with reduced neuroinflammatory response and parvalbumin-positive neuron loss. *Scientific Reports*, *10*(1), 20445. https://doi.org/10.1038/s41598-020-75714-1

Chapter 3

Matrix metalloproteinase-9 activity and perineuronal nets are not changed at specific time points after noise-induced hearing loss

Abstract

Noise induced hearing loss (NIHL) is a common form of hearing loss where exposure time and intensity determine the amount of hearing loss. Central auditory consequences are also being identified and could provide possible targets for alleviation of the cascading effects of NIHL, especially for long-term and comorbid consequences of NIHL. The central gain model purports that deafferentation following hearing loss amplifies residual signal causing increased spontaneous activity and response magnitudes. However, the cellular mechanisms underlying increased central gain is unclear. Here we test the hypothesis that following NIHL, an endopeptidase called matrix metalloproteinase-9 (MMP-9) activity is upregulated in the auditory cortex which leads to perineuronal net (PNN) degradation which has been associated with inhibitory interneuron activity. We found that in FVB mice, MMP-9 activity is unchanged 1 day after NIHL and PNN density and intensity did not decrease 23-45 days after NIHL.

Introduction

Noise-induced hearing loss (NIHL) is a major cause of auditory processing impairments. NIHL is an occupational hazard – with high incidence in individuals in construction (Oi Saeng Hong, 2005), mining (McBride, 2004), military (Yankaskas, 2013), and airline industries (O. S. Hong & Kim, 2001) – as well as a recreational hazard, with the increased use of in-ear devices (Mostafapour, Lahargoue, & Gates, 1998). The

consequences of NIHL in the inner ear include cochlear hair cell damage (Kujawa & Liberman, 2009) which leads to deafferentation, or a lack of input from the periphery to central auditory centers. This deafferentation results in central gain, which is a compensatory increase in central auditory responses, and may lead to tinnitus and hyperacusis. The hyperexcitability in the auditory cortex may emerge from circuit abnormalities, particularly abnormal balance of excitation and inhibition after NIHL.

Cortical plasticity in response to sensory deprivation has been seen in other sensory systems (Murase, Lantz, & Quinlan, 2017), so we hypothesize that deafferentation from the inner ear will lead to cellular changes that may affect normal circuit function. The cellular mechanisms of increased central gain are unclear. A previous study showed that perineuronal net (PNN) intensity is decreased at 1- and 10-days post-NIHL but recovered at 30-days to control levels, however the mechanism of increased PNN degradation is unknown (Nguyen, Khaleel, & Razak, 2017). MMP-9 is an activity-dependent protease that cleaves extracellular matrix (ECM) (Ethell & Ethell, 2007; Reinhard, Ethell, & Razak, 2015), particularly PNNs, which are specialized aggregates of ECM. PNNs encase various neurons, but have been highly associated with parvalbumin-positive inhibitory interneurons (PV+) (Härtig, Brauer, & Brückner, 1992) cells and are thought to provide stability for the PV+ neurons, increase PV+ cell excitability, and protect them from oxidative stress (Wen, Binder, Ethell, & Razak, 2018). PV+ cells are mainly inhibitory, and are thought to generate oscillations in the gamma band (40Hz) involved in sensory processing (Cardin et al., 2009). With disrupted PNNs, PV+ cells may exhibit reduced excitability (Balmer, 2016). One of the major aims of this study was to determine if MMP-

9 activity increased after NIHL leading to PNN degradation and enhanced responses in the auditory cortex. If this hypothesis is supported, therapeutic approaches such as MMP-9 inhibitors can be used to reduce NIHL-related central gain.

Therefore, we hypothesized that NIHL will cause an upregulation of MMP-9 that will lead to a degradation of PNNs which will affect inhibitory neurons activity resulting in cortical E/I imbalance. This study aims to determine if MMP-9 is upregulated after NIHL and if there is an associated change in PNNs. The PNN quantification time points in this study were at 23-day and 45-65 days post-NIHL. Presently, we found that 1-day post-NIHL did not capture any changes in MMP-9 activity. Additionally, PNN density or intensity remained unchanged at these later time points post-NIHL.

Methods

Auditory Brainstem Response.

Hearing loss was measured using ABR recordings from mice anesthetized with ketamine/xylazine/acepromazine (80/10/1 mg/kg, i.p.). Once an anesthetic plane was verified via toe-pinch reflex test, the mouse was placed on a bite bar in an anechoic chamber (Gretch-Ken Industries, OR) and 3 Grass platinum needle electrodes (Grass Technologies, RI) were inserted subdermally. The recording electrode was placed at the vertex, the ground electrode in the left cheek, and reference electrodes were placed in the right cheek. The MF1 Multi-Field Magnetic Speaker (Tucker-David Technologies, FL) was placed 10cm away from the left ear and the TDT RZ6 multi I/O processor delivered the sound stimulus during the recording. The TDT software BioSigRZ was used to generate

512 click presentations at a 21Hz repetition rate of alternating +/- 1.4V (duration 0.1ms) at each sound level. Each protocol began at 90dB SPL and decreased in 5dB steps to 10dB SPL. ABRs were used to verify hearing loss and were recorded before noise-exposure and after each subsequent EEG recording. Hearing threshold was defined as a visible waveform at the lowest sound level within the first 7ms of the ABR.

Noise-exposure paradigm.

NIHL was caused using a noise-exposure (NE) paradigm in which a narrowband noise (6-12kHz) at ~120 dB SPL was played continuously over 3 hrs to awake mice. The NE stimulus was generated using Tucker Davis Technologies (TDT) software RPvdsEx and delivered via the RZ6 multi I/O processor. The NE stimulus was presented using a Fostex FT96H horn tweeter that was suspended 6 inches above the cage. NE was presented immediately after the first (pre) EEG recording or 1-2 days after pre-ABRs (MMP-9 mice). A separate group of mice, termed 'control', went through all the same procedures, but without NIHL.

WFA Staining.

After NIHL and EEG recordings, mice were sacrificed and transcardially perfused with 4% paraformaldehyde. Whole brains were harvested and fixed overnight then cryoprotected in 30% sucrose. Tissue slices were obtained via cryostat at 40um thickness. The tissue was quenched in 50mM ammonium chloride for 15 minutes and rinsed with PBS. The incubation period in 1:500 wisteria floribunda agglutinin (WFA) (Thermo Fisher Scientific, Waltham, MA) lasted for 3 hours at room temperature. Slices were then blocked

with a 5% normal serum and 1% bovine serum albumin solution for an hour. Washes with 0.5% Tween-20 and PBS were done before slices were mounted onto slides and cover slipped.

Dye-quenched zymography.

A separate group of mice (n=18) were sacrificed and transcardially perfused with Accustain (Sigma-Aldrich, Burlington, MA) 1-day after NIHL. Whole brains were harvested and fixed overnight in Accustain. Tissue slices were obtained via microtome for 50um thickness. For zymography, slices were mounted onto charged slides and covered with DI water in a hydrophobic area surrounding the tissue. They were incubated at 37°C for 40 minutes. The Dye-Quenched (DQ) gelatinase (Thermo Fisher Scientific, Waltham, MA) substrate was prepared from a 1mL stock tube to make a 1:50 dilution and filtered prior to incubation. A specific MMP-9 blocker, SB3CT (Sigma-Aldrich, Burlington, MA), was used as a negative control (15.3ug/1mL). Slices were then incubated with the DQ working substrate at the same temperature for 40 minutes. Several rinses were done with DI water and then a 15 minute room temperature incubation was done with 4% paraformaldehyde. The last rinses were with PBS prior to mounting with DAPI Vectashield (Newark, CA) and cover slipped.

Statistical analysis.

Image quantification for MMP-9 and PNNs was done manually in Fiji. A 400um wide region of interest (ROI) was located from pia to bottom of layer VI in the auditory cortex. For PNN analysis, intensity was done with background subtraction by measuring

the mean intensity of a 40um^2 box in L1, which is a distinct area lacking PNNs and subtracting the value from the ROI total area. Superficial and deep layers are separated by measuring the length of the cortex and dividing in half. Putative PNNs are counted from LII to LVI. MMP-9 intensity is measured by taking the mean intensity from LII to LVI within the ROI.

All statistical analysis was done in Graphpad Prism (San Diego, CA). Mixed-effects ANOVA was performed for both MMP-9, and 1-way ANOVA for PNN intensity and density comparisons.

Results

i. Click ABR thresholds were decreased 1 day after NIHL and remained decreased over time

Click ABR thresholds were significantly increased post-NIHL for mice used in the MMP-9 quantification compared to control mice. A 2-way ANOVA was performed to compare time ($F(1, 26) = 833.5$, $p<0.0001$) and group ($F(1, 26) = 730.6$, $p<0.0001$), both had main effects and interaction ($F(1, 26) = 796.0$, $p<0.0001$). Bonferroni's multiple comparisons test showed a correct p-value for noise-exposed group ($p<0.0001$) (Figure 1). This data indicated that no peripheral hearing was present 1-day post-NIHL.

For mice used in PNN quantification, click ABRs remained elevated up as measured 45-65 days post-NIHL. There was a main effect of time ($F(2, 32) = 710.4$, $p<0.0001$) and group ($F(1, 32) = 2713$, $p<0.0001$) and interaction ($F(8, 128) = 694.1$, $p<0.0001$). A Tukey's post-hoc analysis indicates RR and NR groups are significantly

different from CTL groups at each corresponding time point ($p<0.0001$) (Figure 2). This data indicated no peripheral hearing was present in the RR or NR groups.

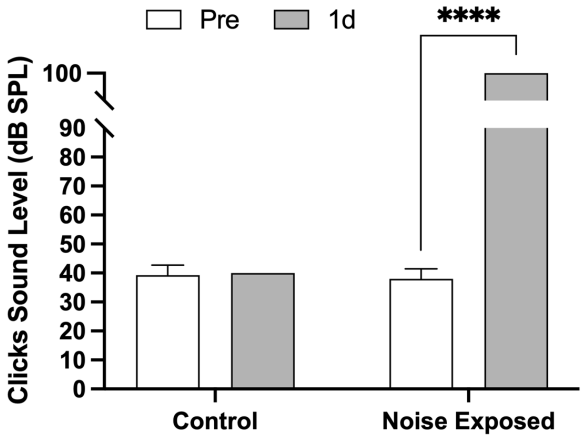

Figure 1. Click ABR thresholds are elevated 1-day post-NIHL in mice used for MMP-9 quantification. Compared to Control mice, noise-exposure significantly elevated threshold levels. ****, $p<0.0001$.

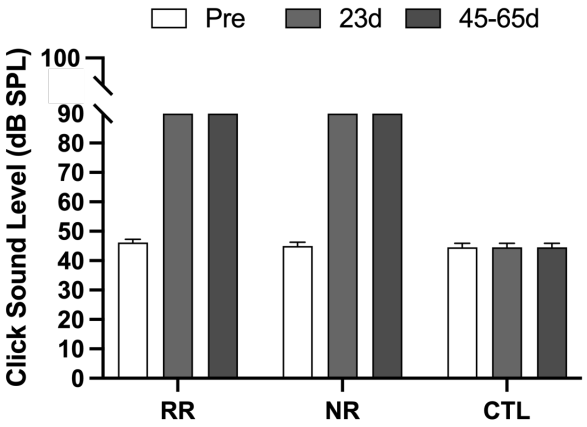

Figure 2. ABR thresholds remained elevated for mice used in PNN quantification. Both RR and NR groups' threshold levels increased over time. Control ABRs did not change.

ii. MMP-9 activity does not change 1 day after NIHL

MMP-9 activity was quantified by using a Dye-Quenched Gelatinase substrate. Once the enzyme is digested by MMP proteins, it releases an attached fluorophore that can

be measured (Figure 3). We used in vitro fixed tissue slices to quantify the intensity of MMP-9. SB3CT was used as negative control to block MMP-9 specific activity (Figure 4). We found that there was no difference in MMP-9 activity 1 day after 3 hours of silence or noise-exposure at any of the ROIs (Layers: $F(2.257, 15.80) = 22.78$, $p<0.0001$; ROI: $F(1.016, 7.114) = 47.88$, $p=0.0002$; Dunnett: LII-VI, CTL SB3CT vs NIHL 1d – $p=0.0164$; CTL SB3CT vs NIHL SB3CT – $p=0.0059$; L II-IV, CTL SB3CT vs NIHL 1d – $p=0.0087$; CTL SB3CT vs NIHL SB3CT – $p=0.0128$; L V-VI, CTL SB3CT vs NIHL 1d – $p=0.0394$; CTL SB3CT vs NIHL SB3CT – $p=0.0044$). In summary, MMP-9 activity does not change after 1 day of noise-exposure, a timepoint at which previous study (Nguyen et al., 2017) showed that PNN intensity is decreased.

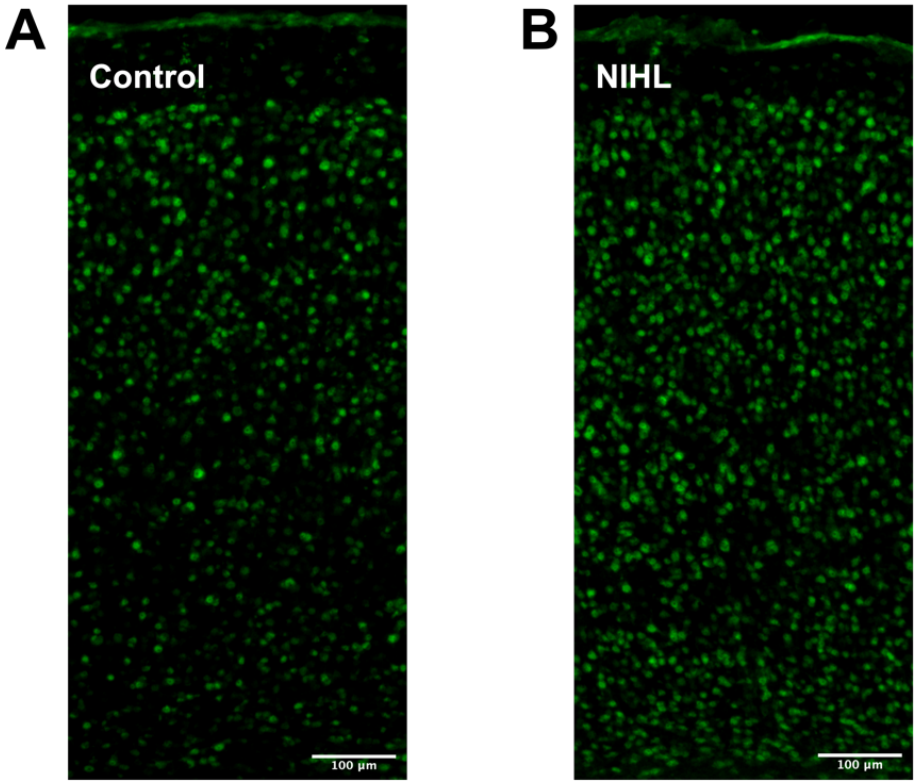

Figure 3. MMP-9 activity representative images. Auditory cortex region of interest spanning from superficial to deep layers for control (A) and NIHL (B) example slices.

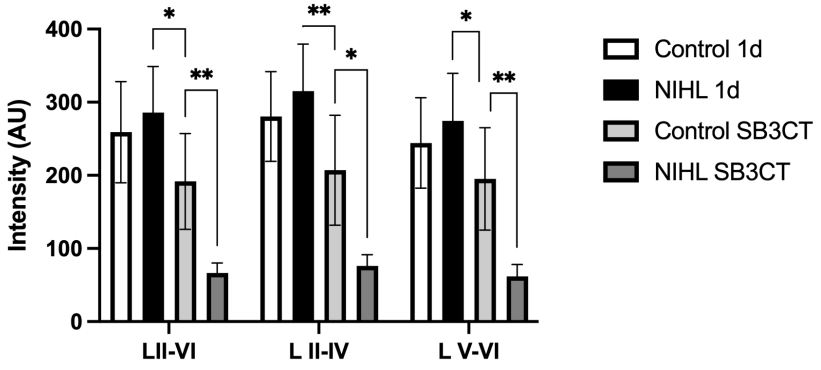

Figure 4. There is no difference in MMP-9 intensity between control and NIHL groups 1 day after noise-exposure. A 40um box was placed in L1 to measure background intensity. The whole slice ROI includes LII-LVI. The cortical layers were divided between superficial (L II-IV) and deep (L V-VI). The negative SB3CT control shows lower intensity in all measurements. *, $p<0.05$; **, $p<0.01$.

iii. PNN density and intensity is not changed long term after NIHL

PNN density and intensity was measured from mice that had undergone NIHL and EEG recordings and sacrificed after the last day of EEG recordings (See Chapter 3). All statistics performed for PNN measurements were 1-way ANOVAs. Layer specific quantification was done for density measurements (Figure 5).

There were no changes in PNN density at either 23- or 45–65-day post-NIHL across the cortical length (Fig. 6A). When looking into layer specific differences, superficial nor deep layers showed any changes in post-NIHL timepoints (Fig. 6B-C). There were no differences in PNN density in the NR group in any of the layers (Fig. 6D-F).

Intensity measurements across LI-VI for RR and NR did not show any changes. The RR group did not have any significant differences in either post-NIHL timepoints compared to control (Fig. 7A). The NR group did was not different at 23- or 45–65-day post-NIHL (Figure 7B). Taken together, PNN density and intensity are not different from controls at later timepoints post-NIHL.

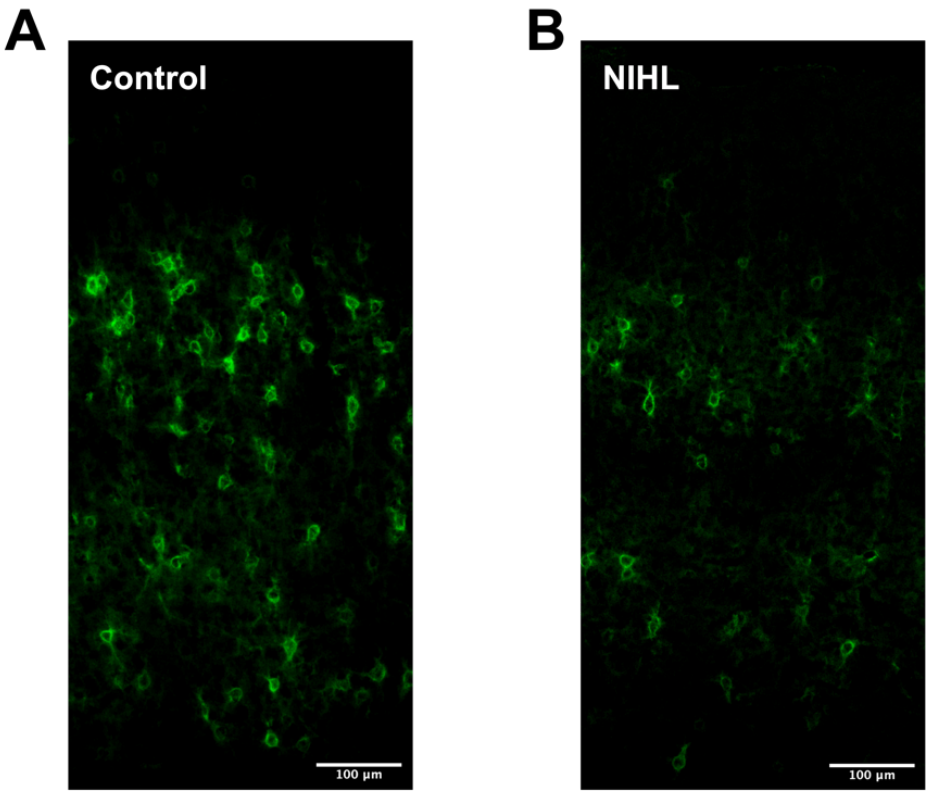

Figure 5. PNN representative images from the auditory cortex. Region of interest in the auditory cortex from LI-VI for control (A) and NIHL (B) slices used to measure density and intensity.

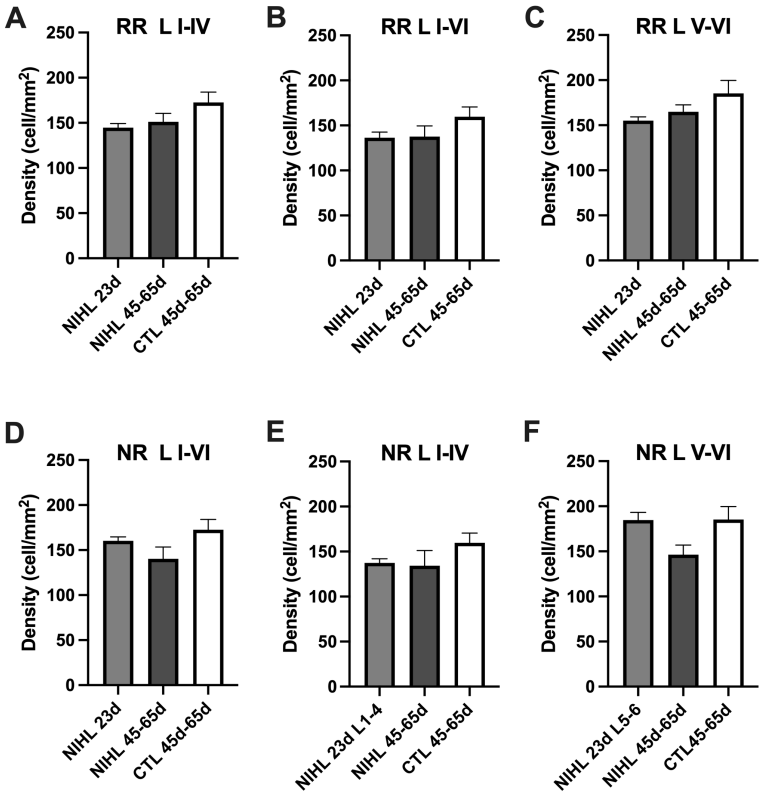

Figure 6. PNN density is not altered after 23-days or later post-NIHL in RR or NR group. RR and NR groups do not show any difference in PNN density across the cortical length (A, D) nor when splitting superficial (B, E) and deep layers (C, F).

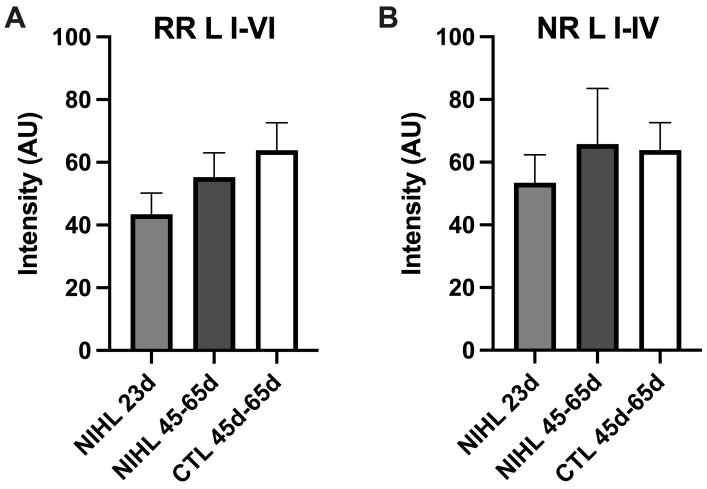

Figure 7. PNN intensity is not significantly different post-NIHL. Intensity across the cortical length is not different from controls in the RR (A) or NR (B) groups.

Discussion

This study examined whether MMP-9 activity is elevated and PNNs are altered after NIHL. We found that 1) at 1-day post-NIHL, MMP-9 activity was not different from controls, 2) at 23 or 45-65 days post-NIHL, PNN density or intensity was not different across cortical layers. Taken together, if there are any changes in MMP-9 activity or PNNs after NIHL, these timepoints did not capture them. There may be cellular recovery over time.

The intensity of PNNs may be associated with the level of degradation (Enwright et al., 2016) that is independent of PNN+ cell density. In Nguyen, Khaleel, and Razak (2017), PNN intensity was reduced beginning 1-day and up to 10-days post-NIHL, but no changes in density were seen. This led us to hypothesize that PNNs are degraded following NIHL but recover over time. Our current PNN findings align with Nguyen's in that PNN density and intensity are unchanged at later time points. Although the previous study used CBA/CaJ mice, our FVB strain is similar in their resistance to age-related hearing loss. Our 23-day time point may indicate that PNN recovery occurs between earlier than 3 weeks post-NIHL. Our 45–65-day post-NIHL timepoint is consistent with Nguyen's 30-day post-exposure recovery.

Due to the change in PNN intensity, we hypothesized that there must be a concurrent protease activated post-NIHL. MMP-9 is a prime suspect as it has been shown to cleave ECM (Ethell & Ethell, 2007) and its genetic reduction rescues PNN formation (Wen, Afroz, et al., 2018). Although it is not NIHL, one study showed that cerebral

ischemia caused a significant ABR threshold shift in conjunction with elevated MMP-9 expression levels 24-hours after injury (Kamat, Kalani, Metreveli, Tyagi, & Tyagi, 2015). Other neurological pathologies show central increases in MMP-9, therefore NIHL may also exert a similar effect on weakened extracellular matrices. Inconsistent with our findings, a study using rats showed that NIHL decreased brevican – a major component of PNNs – and PV+WFA cells in the auditory cortex of rats, along with elevated MMP-9 expression (Park, Lee, Lee, Lee, & Kim, 2020). This discrepancy may be due to the age and species used, where they targeted the precritical period that already has plasticity occurring in cortex.

For the timing of MMP-9 upregulation and activation, an earlier time point seemed the most reasonable to initially test. MMP-9 secretion and neuroinflammatory markers are highly interconnected after injury, even in the periphery (Nam & Kwon, 2014; Pathak, Goldofsky, Vivas, Bonagura, & Vambutas, 2011). Microglia is a secretor of matrix metalloproteinase-9 (MMP-9) (Kauppinen & Swanson, 2005; Könnecke & Bechmann, 2013) which subsequently acts as a second player in neuroinflammation. Zinsmaier et al. (2020) further reported that microglial activation is upregulated in C57BL6 mice after noise exposure in auditory cortex. Wang et al. (2019) found that neuroinflammation in the auditory cortex following NIHL was upregulated, specifically various proinflammatory cytokine expression at different times – 12 hours, 1-, 3-, and 10 days. Since PNN intensity was decreased at 1-day post-exposure, we asked if MMP-9 activity was upregulated at the same time. It seems that MMP-9 elevation can occur earlier than the time point we currently observed. Future studies should be done that targets 12-hours or earlier. In the auditory

cortex of rats 2 hours after NIHL, several neuroinflammatory markers were upregulated indicating that MMP-9 may also be upregulated almost immediately post-NIHL (Lee, Kim, Lee, Lee, & Kim, 2021).

SB3CT is a selective inhibitor of gelatinases MMP-2 and MMP-9 (Kleifeld et al., 2001). In cerebral ischemia, treatment with SB3CT rescued neuronal cell death and prevented increased levels of MMP-9 in mice (Cui et al., 2012). In rats, SB3CT was used to reverse behavioral deficits and secondary effects post-injury (Jia et al., 2014). In a rat NIHL model, Lee et al. (2021) reported that after NIHL MMP-9 protein expression was upregulated but reduced with SB3CT administration. Our results show that although there were no differences in MMP-9 intensity between control and NIHL, the SB3CT treated slices used as negative controls were significantly different from the experimental groups. Control group should have baseline levels of active MMP-9, so with SB3CT+Control, there should be little active gelatinases including MMP-2. This makes sense where we see the reduction in SB3CT+Control compared to NIHL, but not compared to Control alone as there should be no gelatinases in these conditions. However, the SB3CT+NIHL group was reduced the most – this indicates that the drug works and is impacting MMPs specifically. The marked reduction in SB3CT+NIHL should indicate that there was an increase in MMP-9 activity that the antagonist was able to work on inhibiting. Potentially the combination of MMP-2 and MMP-9 showed up as the enhanced reduction in intensity.

Alternatively, if MMP-9 is not directly or continuously degrading PNNs, another pathway may be involved after initiation. The receptor for advanced glycation end-products (RAGE) has been implicated in neuroinflammation in a schizophrenia model,

where MMP-9 triggered RAGE shedding leading to cytokine secretions ultimately impacting PV+ and PNN maturation (Dwir et al., 2019). In this study, MMP-9 inhibition rescued these changes despite additional oxidative stress. However, RAGE can also be activated by a disintegrin and metalloprotease (ADAM10) (Raucci et al., 2008). Potentially, MMP-9 may have a more direct role in activity dependent plasticity that is closer to critical period or at a younger age. The mice we used were adults (mean age: P102, s.d: 12 days). Future studies should not only investigate earlier time points post-NIHL, but also RAGE and ADAM10 expression.

Conclusions

We targeted specific time points to determine if changes in MMP-9 activity or PNN degradation had occurred after NIHL. We found that 1 day after NIHL, MMP-9 activity was not different from the control group and that several weeks after NIHL did not show significant PNN degradation. Future studies need to track both MMP-9 at multiple time points post-NIHL as well as other potential proteases that degrade PNNs. Neuroinflammation may be a secondary or indirect mediator following NIHL, immunohistochemistry studies should be performed to determine if any upregulation occurs in the AC as well.

1. Balmer, T. S. (2016). Perineuronal Nets Enhance the Excitability of Fast-Spiking Neurons. *ENeuro*, *3*(4). https://doi.org/10.1523/ENEURO.0112-16.2016

2. Cardin, J. A., Carlén, M., Meletis, K., Knoblich, U., Zhang, F., Deisseroth, K., … Moore, C. I. (2009). Driving fast-spiking cells induces gamma rhythm and controls sensory responses. *Nature*, *459*(7247), 663–667. https://doi.org/10.1038/nature08002

3. Cui, J., Chen, S., Zhang, C., Meng, F., Wu, W., Hu, R., … Gu, Z. (2012). Inhibition of MMP-9 by a selective gelatinase inhibitor protects neurovasculature from embolic focal cerebral ischemia. *Molecular Neurodegeneration*, *7*(1), 1–15. https://doi.org/10.1186/1750-1326-7-21/FIGURES/7

4. Dwir, D., Giangreco, B., Xin, L., Tenenbaum, L., Cabungcal, J. H., Steullet, P., … Do, K. Q. (2019). MMP9/RAGE pathway overactivation mediates redox dysregulation and neuroinflammation, leading to inhibitory/excitatory imbalance: a reverse translation study in schizophrenia patients. *Molecular Psychiatry*, 1–16. https://doi.org/10.1038/s41380-019-0393-5

5. Enwright, J. F., Sanapala, S., Foglio, A., Berry, R., Fish, K. N., & Lewis, D. A. (2016). Reduced Labeling of Parvalbumin Neurons and Perineuronal Nets in the Dorsolateral Prefrontal Cortex of Subjects with Schizophrenia. *Neuropsychopharmacology : Official Publication of the American College of Neuropsychopharmacology*, *41*(9), 2206–2214. https://doi.org/10.1038/NPP.2016.24

6. Ethell, I. M., & Ethell, D. W. (2007). Matrix metalloproteinases in brain development and remodeling: Synaptic functions and targets. *Journal of Neuroscience Research*, *85*(13), 2813–2823. https://doi.org/10.1002/JNR.21273

7. Härtig, W., Brauer, K., & Brückner, G. (1992). Wisteria floribunda agglutinin-labelled nets surround parvalbumin-containing neurons. *NeuroReport*, *3*(10), 869–872. https://doi.org/10.1097/00001756-199210000-00012

8. Hong, O. S., & Kim, M. J. (2001). Factors associated with hearing loss among workers of the airline industry in Korea. *ORL-Head and Neck Nursing : Official Journal of the Society of Otorhinolaryngology and Head-Neck Nurses*, *19*(1), 7–13.\

9. Hong, Oi Saeng. (2005). Hearing loss among operating engineers in American construction industry. *International Archives of Occupational and Environmental Health*, *78*(7), 565–574. https://doi.org/10.1007/s00420-005-0623-9

10. Jia, F., Yin, Y. H., Gao, G. Y., Wang, Y., Cen, L., & Jiang, J. Y. (2014). MMP-9 inhibitor SB-3CT attenuates behavioral impairments and hippocampal loss after traumatic brain injury in rat. *Journal of Neurotrauma*, *31*(13), 1225–1234. https://doi.org/10.1089/NEU.2013.3230/ASSET/IMAGES/LARGE/FIGURE8.JPEG

11. Kamat, P. K., Kalani, A., Metreveli, N., Tyagi, S. C., & Tyagi, N. (2015). A possible molecular mechanism of hearing loss during cerebral ischemia in mice. *Canadian Journal of Physiology and Pharmacology*, *93*(7), 505–516. https://doi.org/10.1139/CJPP-2014-0489/ASSET/IMAGES/LARGE/CJPP-2014-0489F11.JPEG

12. Kauppinen, T. M., & Swanson, R. A. (2005). Death Matrix Metalloproteinase-9-Mediated Neuron Microglial Activation, Proliferation, and Poly(ADP-Ribose) Polymerase-1 Promotes. *J Immunol References*, *174*, 2288–2296. https://doi.org/10.4049/jimmunol.174.4.2288

13. Kleifeld, O., Kotra, L. P., Gervasi, D. C., Brown, S., Bernardo, M. M., Fridman, R., … Sagi, I. (2001). X-ray Absorption Studies of Human Matrix Metalloproteinase-2 (MMP-2) Bound to a Highly Selective Mechanism-based Inhibitor. *Journal of Biological Chemistry*, *276*(20), 17125–17131. https://doi.org/10.1074/jbc.m011604200

14. Könnecke, H., & Bechmann, I. (2013). The Role of Microglia and Matrix Metalloproteinases Involvement in Neuroinflammation and Gliomas. *Clinical and Developmental Immunology*, *2013*. https://doi.org/10.1155/2013/914104

15. Kujawa, S. G., & Liberman, M. C. (2009). Adding insult to injury: Cochlear nerve degeneration after "temporary" noise-induced hearing loss. *Journal of Neuroscience*, *29*(45), 14077–14085. https://doi.org/10.1523/JNEUROSCI.2845-09.2009

16. Lee, C. H., Kim, K. W., Lee, D. hye, Lee, S. M., & Kim, S. Y. (2021). Overexpression of the receptor for advanced glycation end-products in the auditory cortex of rats with noise-induced hearing loss. *BMC Neuroscience*, *22*(1), 1–11. https://doi.org/10.1186/S12868-021-00642-3/FIGURES/8

17. McBride, D. I. (2004). Noise-induced hearing loss and hearing conservation in mining. *Occupational Medicine*, *54*(5), 290–296. https://doi.org/10.1093/occmed/kqh075

18. Mostafapour, S. P., Lahargoue, K., & Gates, G. A. (1998). Noise-induced hearing loss in young adults: The role of personal listening devices and other sources of leisure noise. *The Laryngoscope*, *108*(12), 1832–1839. https://doi.org/10.1097/00005537-199812000-00013

19. Murase, S., Lantz, C. L., & Quinlan, E. M. (2017). Light reintroduction after dark exposure reactivates plasticity in adults via perisynaptic activation of MMP-9. *ELife*, *6*. https://doi.org/10.7554/eLife.27345

20. Nam, S. Il, & Kwon, T. K. (2014). Dexamethasone inhibits interleukin-1β-induced matrix metalloproteinase-9 expression in cochlear cells. *Clinical and Experimental Otorhinolaryngology*, *7*(3), 175–180. https://doi.org/10.3342/CEO.2014.7.3.175

21. Nguyen, A., Khaleel, H. M., & Razak, K. A. (2017). Effects of noise-induced hearing loss on parvalbumin and perineuronal net expression in the mouse primary auditory cortex. *Hearing Research*, *350*, 82–90. https://doi.org/10.1016/j.heares.2017.04.015

22. Park, S., Lee, D., Lee, S. M., Lee, C. H., & Kim, S. Y. (2020). Noise exposure alters MMP9 and brevican expression in the rat primary auditory cortex. *BMC Neuroscience 2020 21:1*, *21*(1), 1–10. https://doi.org/10.1186/S12868-020-00567-3

23. Pathak, S., Goldofsky, E., Vivas, E. X., Bonagura, V. R., & Vambutas, A. (2011). IL-1β Is Overexpressed and Aberrantly Regulated in Corticosteroid Nonresponders with Autoimmune Inner Ear Disease. *The Journal of Immunology*, *186*(3), 1870–1879. https://doi.org/10.4049/JIMMUNOL.1002275

24. Raucci, A., Cugusi, S., Antonelli, A., Barabino, S. M., Monti, L., Bierhaus, A., … Bianchi, M. E. (2008). A soluble form of the receptor for advanced glycation endproducts (RAGE) is produced by proteolytic cleavage of the membrane-bound form by the sheddase a disintegrin and metalloprotease 10 (ADAM10). *FASEB Journal : Official Publication of the Federation of American Societies for Experimental Biology*, *22*(10), 3716–3727. https://doi.org/10.1096/FJ.08-109033

25. Reinhard, S. M., Ethell, I. M., & Razak, K. (2015). A delicate balance: role of MMP-9 in brain development and pathophysiology of neurodevelopmental disorders. https://doi.org/10.3389/fncel.2015.00280

26. Wang, W., Zhang, L. S., Zinsmaier, A. K., Patterson, G., Leptich, E. J., Shoemaker, S. L., … Bao, S. (2019). Neuroinflammation mediates noise-induced synaptic imbalance and tinnitus in rodent models. *PLOS Biology*, *17*(6), e3000307. https://doi.org/10.1371/journal.pbio.3000307

27. Wen, T. H., Afroz, S., Reinhard, S. M., Palacios, A. R., Tapia, K., Binder, D. K., … Ethell, I. M. (2018). Genetic Reduction of Matrix Metalloproteinase-9 Promotes Formation of Perineuronal Nets Around Parvalbumin-Expressing Interneurons and Normalizes Auditory Cortex Responses in Developing Fmr1 Knock-Out Mice. *Cerebral Cortex*, *28*(11), 3951–3964. https://doi.org/10.1093/cercor/bhx258

28. Wen, T. H., Binder, D. K., Ethell, I. M., & Razak, K. A. (2018, August 3). The Perineuronal 'Safety' Net? Perineuronal Net Abnormalities in Neurological Disorders. *Frontiers in Molecular Neuroscience*. Frontiers Media S.A. https://doi.org/10.3389/fnmol.2018.00270

29. Yankaskas, K. (2013, January). Prelude: Noise-induced tinnitus and hearing loss in the military. *Hearing Research*. https://doi.org/10.1016/j.heares.2012.04.016

30. Zinsmaier, A. K., Wang, W., Zhang, L., Hossainy, N. N., & Bao, S. (2020). Resistance to noise-induced gap detection impairment in FVB mice is correlated with reduced neuroinflammatory response and parvalbumin-positive neuron loss. *Scientific Reports*, *10*(1), 20445. https://doi.org/10.1038/s41598-020-75714-1

Chapter 4

Minocycline treatment reduces cortical central gain following noise-induced hearing loss

Abstract

Noise-induced hearing loss (NIHL) has been purported to enhance 'central gain' as a compensatory mechanism for decreased input from the peripheral auditory structures. The mechanism underlying this phenomenon is unknown, however we hypothesize that an activity dependent mediator – matrix metalloproteinase-9 (MMP-9) – as well as neuroinflammation, may be the beginning of the molecular cascade leading to enhanced cortical responses following NIHL. These upstream effectors may be prime targets to treat following NIHL. We measured sound evoked responses, resting spectral power, and acoustic steady state responses (ASSR) to 40 Hz and novel gap stimulus via electroencephalography. Mice were treated with 5 days of minocycline after hearing loss was induced. Minocycline did not affect auditory brainstem response thresholds but increased evoked response potentials in the auditory (AC) and frontal cortices (FC). There were cortical region-specific differences in 40 Hz ASSR and gap-ASSR, which were enhanced in the AC for both saline and minocycline treated groups, but FC did not recover. Taken together, minocycline may enhance sound detection responses but not temporal processing after NIHL.

Introduction

Noise-induced hearing loss (NIHL) can lead to compensatory enhanced responses in the central auditory regions, a phenomena termed 'central gain' (Eggermont & Komiya, 2000; Seki & Eggermont, 2003). Central gain may act as a compensatory mechanism after deafferentation to enhance sound detection, but aberrant activity in central auditory regions may underlie issues like tinnitus and hyperacusis (Auerbach, Radziwon, & Salvi, 2019; Radziwon et al., 2019; Salvi et al., 2017). However, because the underlying cellular mechanisms of central gain remain mostly unclear, there is no therapeutic avenue to reduce aberrant auditory activity resulting from NIHL. A previous study in our lab has shown PNN intensity was reduced beginning 1 day and lasted at least up to 10 days following NIHL (Nguyen, Khaleel, & Razak, 2017), indicating perineuronal net (PNN) integrity was impacted following sound exposure. Several studies have suggested loss of activity in fast-spiking inhibitory interneurons as mediators of central gain enhancement (Resnik & Polley, 2017) and reduced recovery following deafferentation (Resnik & Polley, 2021). Our working hypothesis is that an endopeptidase – matrix metalloproteinase-9 (MMP-9) – is upregulated causing PNN degradation which decreases parvalbumin-positive inhibitory interneurons (PV+) activity leading to circuit level excitatory/inhibitory (E/I) imbalance.

If enhanced central gain is the consequence of a cascade of changes occurring after NIHL, targeting an upstream effector may prevent the changes seen after sound exposure. We predict that by inhibiting MMP-9 activity following NIHL, electroencephalography (EEG) measurements to sound evoked-stimuli and acoustic steady state responses (ASSR) will be reversed. Minocycline is an FDA approved antibiotic that inhibits MMP-9

(Dziembowska et al., 2013; Machado et al., 2006; Modheji, Olapour, Khodayar, Jalili, & Yaghooti, 2016; Switzer et al., 2011), amongst other effects like neuroinflammatory protection (Elewa, Hilali, Hess, Machado, & Fagan, 2006; Schmidt, Raposo, Torres-Espin, Fenrich, & Fouad, 2021) and antiapoptosis (Chen, Yin, Hwang, Tang, & Yang, 2012; Mishra & Basu, 2008). Minocycline's anti-inflammatory function may also aid in reversing molecular and cellular effects of NIHL, if neuroinflammation acts as a possible second mediator after noise-exposure. Lin et al. (2020) reported that noise-exposure induced neuroinflammatory marker upregulation and cognitive impairment in adult mice but acute minocycline treatment attenuated these effects. In a number of Fragile-X syndrome (FXS) studies, acute and chronic minocycline treatment attenuates audiogenic seizures and other behavioral improvements (Bilousova et al., 2009; Dansie et al., 2013) as well as increased gamma band phase locking to auditory stimuli and reduced sound-evoked power (Lovelace, Ethell, Binder, & Razak, 2020). This drug was a prime candidate to initially test with NIHL due to its public accessibility and connection with other neurological pathologies linked to MMP-9 as well as its neuroprotective abilities.

In the present study, NIHL was achieved in a cohort of mice. Event related potentials (ERPs) and intertrial phase coherence (ITPC) were quantified before and after 5 days of minocycline administration. We found that acute minocycline treatment enhanced auditory (AC) and frontal cortex (FC) ERP amplitudes beginning 5 days and lasting up to 23 days post-NIHL but did not differently affect ITPC of ASSR or gap-ASSR compared to saline controls. However, there was a cortical-region specific difference between AC and FC in consistency to ASSR stimuli for both saline and minocycline treated groups.

Methods

Overview.

We used a longitudinal, within-subject design to study the impact of minocycline treatment on hearing loss and EEG responses recorded from the auditory and frontal cortex (AC, FC). Epidural EEG recordings were obtained to measure auditory event related potentials (ERP) and temporal processing before noise induced hearing loss (NIHL) and on a number of days post-NIHL (5, 10, and 23 days after NIHL). Mice either received 5 days of saline or minocycline administration. Auditory brainstem responses (ABR) were recorded before and after NIHL, at multiple time points to measure the time course of acute drug administration at least until the final day of EEG recordings.

Mice.

All procedures were approved by the Institutional Animal Care and Use Committee at the University of California, Riverside. Sighted FVB mice (FVB.129P2–Pde6b+Tyrc-ch/AntJ) were received from Jackson Laboratories, bred in-house and housed in an AALAC accredited vivarium with 12:12h light:dark cycle. One to four mice were housed in each cage with food and water available *ad libitum*. Male and female mice were used between postnatal day (P)63 and P98 (mean: 72, s.d: 9.7 days) between the two treatment groups.

Drug Administration.

Minocycline hydrochloride (45mg/kg) was prepared in 0.9% NaCl and frozen in aliquots until time of use. Minocycline or saline was administered through i.p. injections daily for 5 days after NIHL. The first dosage was given immediately after NIHL and post-NIHL ABR. No EEGs were recorded during drug administration and post-NIHL recordings were obtained after the last day of injections.

Surgery.

The aseptic EEG electrode implant surgical procedures have been previously described in detail (Lovelace, Ethell, Binder, & Razak, 2018; Rumschlag & Razak, 2021). Briefly, mice were anesthetized with a ketamine/xylazine/acepromazine (80/10/1 mg/kg, i.p.) mixture and temperature was regulated (FHC, Inc., Maine) at ~37° throughout the procedure Three ~1mm diameter burr holes were drilled (Foredom dental drill) in the skull above the frontal, auditory, and occipital cortex. The frontal hole was placed at the junction between the frontal sinus and sagittal suture over the right hemisphere and the occipital hole was placed just rostral to the lambdoid suture and lateral to the sagittal suture in the left parietal bone. The right hemispheric auditory hole was placed -2mm posteriorly and +5 laterally from Bregma. 1mm stainless steel screws were carefully inserted into the burr holes while attached to a 3-channel electrode post (P1 Technologies, Roanoke, VA) and held in place with cured dental cement. Post-operational care included one dose of analgesic injection of Ethiqa-XR (3.25 mg/kg body weight) (Fidelis Pharmaceuticals, NJ)

and observation over the course of 48 hours. Each mouse was singly housed after surgery to prevent damage to the implant.

Auditory Brainstem Response.

Hearing loss was measured using ABR recordings from mice anesthetized with ketamine/xylazine/acepromazine (80/10/1 mg/kg, i.p.). Once an anesthetic plane was verified via toe-pinch reflex test, the mouse was placed on a bite bar in an anechoic chamber (Gretch-Ken Indus- tries, OR) and 3 Grass platinum needle electrodes (Grass Technologies, RI) were inserted subdermally. The recording electrode was placed at the vertex, the ground electrode in the left cheek, and reference electrodes were placed in the right cheek. The MF1 Multi-Field Magnetic Speaker (Tucker-David Technologies, FL) was placed 10cm away from the left ear and the TDT RZ6 multi I/O processor delivered the sound stimulus during the recording. The TDT software BioSigRZ was used to generate 512 click presentations at a 21Hz repetition rate of alternating +/- 1.4V (duration 0.1ms) at each sound level. Each protocol began at 90dB SPL and decreased in 5dB steps to 10dB SPL. ABRs were used to verify hearing loss and were recorded before noise-exposure and after each subsequent EEG recording. Hearing threshold was defined as a visible waveform at the lowest sound level within the first 7ms of the ABR.

Noise-exposure paradigm.

NIHL was caused using a noise-exposure paradigm in which a narrowband noise (6-12kHz) at ~110-115 dB SPL was played continuously over 3 hrs to awake mice. The NIHL stimulus was generated using Tucker Davis Technologies (TDT) software RPvdsEx

and delivered via the RZ6 multi I/O processor. The NE stimulus was presented using a Fostex FT96H horn tweeter that was suspended 6 inches above the cage. Noise exposure stimulus was presented immediately after the first (pre) EEG recording.

Auditory Stimuli.

Auditory stimulus presentation procedures were similar to those described in Rumschlag and Razak (2021). A TDT MF1 speaker was mounted 20cm above the plastic arena and used to present noise stimuli that was generated with a TDT RZ6 with a sampling rate of 24.414kHz. All sound stimuli were presented at 90dB SPL for all timepoints. For event-related potentials (ERPs), a train of noise bursts (100ms, 5ms rise/fall time, 0.25Hz repletion rate, 120 repetitions) was presented. The auditory steady-state response (ASSR) was evoked at 40Hz using a pulsed noise stimulus (200 repetitions, 8ms duration, 2ms rise/fall time, 40Hz, 1-2 s random inter-stimulus interval) for a total duration of 12 minutes. A 40 Hz gap-ASSR stimulus was used to measure temporal processing before and after NIHL.

The gap ASSR is elicited by presenting gaps repeated at 40 Hz (25 msec period) in continuous noise. The duration of the gap is varied randomly between 3 and 9 msec (1 msec resolution). A 75% modulation depth was used. The gap-ASSR stimulus uses gaps in continuous noise to elicit an ASSR. The stimuli consisted of continuous noise periodically interrupted by 10 gaps placed 25 ms apart from onset to onset (for a presentation frequency of 40 Hz). A single stimulus began with 250 ms of noise, followed by 250 ms of gap-interrupted noise, followed by continuous noise, and so on, for a total of

10 presentations of the gap-interrupted noise. The stimulus ended with 250 ms of continuous noise, followed by a silent ISI of 500 ms. For each 250 ms segment, the gap width was randomly selected from a parameter space, consisting of 3-9 ms gaps (1 ms intervals). Each stimulus was presented at least 200 times over the 30-minute presentation period.

The gap-ASSR stimulus consisted of 5.75-second trains of noise, alternating between 250 ms of noise and 250 ms of noise interrupted by gaps spaced 25 ms apart, from onset to onset. These 250 ms periods of noise interrupted by gaps elicit an ASSR at 40 Hz, the strength of which varies with gap width and modulation depth. If each gap in a 250 ms stimulus elicits a measurable response, then the recording will show a robust 40 Hz oscillatory signal, and this response will be consistent across trials, yielding a high ITPC value. If some gaps in a stimulus fail to produce a response, then the ITPC value will be significantly lower. The gap-ASSR is a measurement of the ability of the cortex to consistently respond to rapid short gaps in noise.

Electroencephalography (EEG) recording.

Mice were awake and freely moving during the EEG recordings while tethered via the EEG implant that was connected to a freely rotating commutator. The TDT RA4LI/PA headstage and preamplifier was connected to the TDT RZ6 I/O device via optic fiber cable. Clean bedding was used for each mouse in a plastic arena during each recording placed inside a wire mesh Faraday cage. The entire set up was housed in an anechoic chamber

(Gretch-Ken Indusrtries, OR). The signal was recorded at 24.414 kHz and down-sampled to 1024 Hz.

Data Analysis.

Graphpad Prism was used for statistical analysis. Each comparison was done separately in auditory and frontal cortex. Rumschlag and Razak (2021) described in detail the auditory response analyses that was also used in the present study. All responses were measured using custom MATLAB (Math-Works, Natick, MA) scripts. The EEG signals were recorded at 24.414 kHz and down-sampled to 1024 Hz using linear interpolation. All analyses were performed on signals collected from both the AC and the FC.

ERP analysis.

To measure ERPs, the EEG trace was split into trials, using TTL pulses marking the sound onset. Each trial was baseline corrected, such that for each trial, the mean of the 250 ms baseline period was subtracted from the trial trace. Each trial was then detrended (MATLAB detrend function). To extract the ERP, all of the trials were averaged together. ERPs recorded from mice have distinct peaks, which are analogous to those seen in human ERPs (Umbricht et al., 2004). For each mouse, the peak magnitudes and latencies were measured as the local minimum or maximum within a physiologically relevant range, e.g. the P1 component was the local maximum between 15 ms and 30 ms following stimulus onset.

Each group was compared via mixed-effect analysis 2-way ANOVA for P1 and N1 amplitude and latency with the timepoint and treatment as a factor in each region (AC and

FC). With all timepoints factors and saline versus minocycline, we tested for main effects and interactions. Dunnett's multiple comparisons test compared pre-NIHL vs post-NIHL ERP values for each treatment group.

Resting EEG Spectral Analysis.

To quantify changes after NIHL in EEG power spectral distribution, we measured resting EEG power across canonical frequency bands in both AC and FC across the various time points from 5- to 23 days post-NIHL, and compared with pre-NIHL values. The phrase 'resting EEG' is used to describe data collected when there was no specific auditory stimulation. Five minutes of resting EEG was recorded from each mouse. The traces from each condition were split into Hanning-windowed 1-second segments with 50% overlap, which were then transformed to the frequency domain via Fourier transform. The average power spectrum was calculated by averaging the spectra from each of the 1-second segments. Each average power spectrum was then split into EEG frequency bands (theta: 3– 7 Hz, alpha: 8–13 Hz, beta: 14–29 Hz, low gamma: 30–59 Hz, high gamma: 61–100 Hz, and high-frequency oscillations (HFO): 101–250 Hz). Delta band power was not analyzed because the pre-amplifier had a built-in high-pass filter at 2.2 Hz. The average power from each frequency band was calculated. Two-way ANOVA mixed-effects repeated measures was used to compare for spectral power at each time point for each of the frequency bands (Graphpad Prism) with the resulting p-values adjusted for multiple comparisons within each region.

Pulse-ASSR analysis.

The pulse-ASSR was analyzed by calculating the average consistency of the 40 Hz response during the last 1000 ms of the 2000 ms stimulus. This was done to capture the steady-state response while avoiding the onset response. To that end, the trace was transformed to the time-frequency domain via dynamic complex Morlet wavelet transform. The ASSR can be characterized using multiple measurements, including the amplitude of the oscillation frequency in the frequency transform (FFT) of the signal (Parthasarathy, Cunningham, & Bartlett, 2010), the amplitude of the Hilbert transform of the filtered signal, the vector strength of the signal with the original oscillatory stimulus, the phase-locking of FFTs (PLI) (Yokota & Naruse, 2015), or the inter-trial phase clustering (ITPC) at the oscillation frequency (Lovelace et al., 2020). ITPC provides both time and frequency information, and it is a direct measure of the degree of response consistency across trials, so it was used to assess ASSRs in this study. ITPC was calculated for each time-frequency point as the average vector of phase unit vectors across trials. If the phase response is consistent at a particular time- frequency point, it will have a high ITPC value. The ITPC calculations showed a high degree of phase consistency at 40 Hz during the pulse-ASSR stimulus. The ITPC values at 40 Hz were averaged to extract one value for each mouse, representing the phase consistency of the 40 Hz ASSR.

A mixed-effects 2-way ANOVA analysis was used to examine interactions and main effects of each timepoint for AC and FC between saline and minocycline. Dunnett's

multiple comparisons test compared pre-NIHL vs post-NIHL ITPC values for each treatment group.

Gap-ASSR analysis.

The gap-ASSR was analyzed similarly to the pulse-ASSR, in which the consistency of the 40 Hz response was calculated. For the gap-ASSR, the consistency was calculated for each of the 40 stimuli (1 modulation depth x 7 gap widths). The EEG trace was transformed using a dynamic complex Morlet wavelet transform. The trials corresponding to each stimulus were grouped together, and the ITPC was calculated. A band of high ITPC appears at 40 Hz, which is clearly visible in the responses from all of the HL and CTL mice. The average ITPC value at 40 Hz during the stimulus was extracted for each stimulus for each mouse. The gap-ASSR compared ITPC mean using the mixed-effect model with gap-width (3-9 ms) and timepoint (pre, 5-, 10-, 23-days) were used as factors, for each region.

Results

i. A threshold shift was achieved

Click ABRs were tested in all mice pre-NIHL and after each EEG recording, including immediately after noise exposure. Click ABR threshold levels were significantly elevated post-NIHL threshold levels when compared to pre-NIHL with a main effect of time (2-way ANOVA: $F(1.712, 28.24) = 154.1$, $p<0.0001$; Dunnett's multiple comparisons test – all post-NIHL time points were different than pre-NIHL level, $p<0.0001$), but there was no effect of saline or minocycline treatment and no interaction

between the time and treatment (Figure 1). However, the threshold shifts at later time points were reduced compared to immediately post-NIHL indicating a threshold shift, but no effect of minocycline as they were not different from saline ABR thresholds.

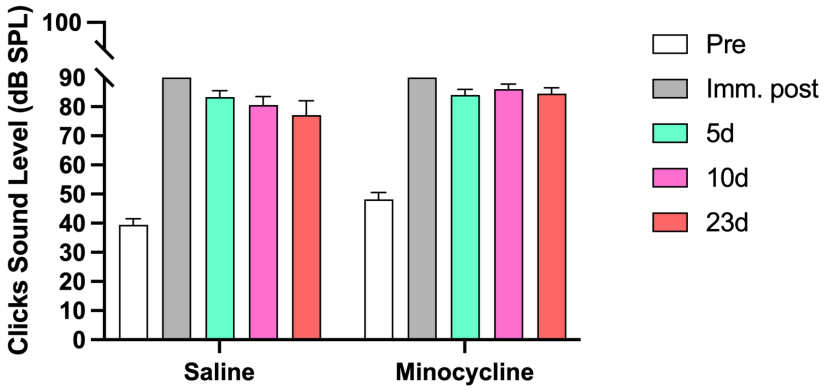

Figure 1. Click ABR thresholds remained elevated post-NIHL in saline and minocycline treated groups. All post-NIHL time points were significantly different from pre-NIHL.

ii. Minocycline enhances ERP P1 and N1 amplitudes in the AC and FC

The event related potential (ERP) was recorded from the auditory cortex and frontal cortex from all mice. Mice received either saline or minocycline administration daily for 5 days after NIHL.

A 2-way ANOVA was performed to compare time and treatment on sound-evoked responses following NIHL. There was a main effect of time ($F(3, 47) = 4.697$, $p=0.006$) in the AC P1 amplitude (Figure 2A) specifically in the minocycline treated group (Dunnett's: pre vs 5d – $p=0.0143$; pre vs 10d – $p=0.047$; pre vs 23d, $p=0.029$), but no effect of treatment. There were no differences in N1 AC amplitude in either saline or minocycline groups (Figure 2B). P1 FC amplitude (Figure 2C) had a main effect across timepoints (F

(3, 47) = 3.196, p=0.0319) with increased amplitudes in the minocycline group (Dunnett's: pre vs 5d, p=0.0273; pre vs 10d, p=0.0420). N1 FC amplitude (Figure 2D) remained elevated up to 23 days after NIHL (F (3, 47) = 3.079, p=.00364; Dunnett's: pre vs 5d, p=0.044; pre vs 10d, p=0.0382; pre vs 23d, p=0.0115). There were no changes in latency in AC or FC for either treatment groups (Figure 2E-H). Taken together, 5 days of acute minocycline administration increased most ERP amplitudes in the AC and FC after NIHL.

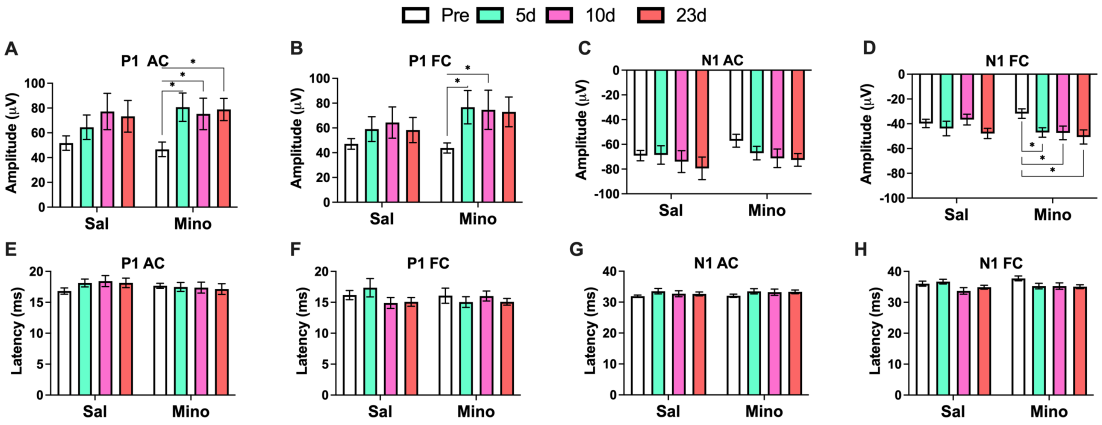

Figure 2. Minocycline treatment increased P1 and N1 amplitudes in the AC and FC. The P1 and N1 amplitudes and latencies maximum peaks were extracted for each RR mouse and averaged (with +/- SEM) at each time point. A) The P1 amplitude in the AC was significantly increased from baseline after minocycline administration, but saline did not show significant differences. B) There were no changes in either treatment group in N1 AC amplitude. C) Only 5d and 10d were significantly increased from pre-levels in P1 FC with minocycline. D) N1 FC amplitude remained elevated with minocycline up to 23 days post-NIHL. E-H) There were no changes in amplitude for either saline or minocycline treatment.

iii. Minocycline attenuates exaggerated spontaneous activity in the AC and FC

Absolute spectral power was quantified from 5 minutes resting EEG recordings in the absence of auditory stimuli. This analysis was performed to probe spontaneous neural oscillations after NIHL and minocycline treatment, with saline used as a control. Two-way

ANOVA mixed effects analysis was performed to compare drug treatment and time, with Bonferroni's multiple comparisons test used to discern significant differences over time for saline and minocycline in both cortical regions. In the AC (Figure 3A), there were only main effects of time in the lower frequency bands – theta and alpha, with significant decrease in spectral power from pre-NIHL at 10-days post-NIHL in both the saline treated and minocycline groups. This suggests that spectral power remains decreased in lower frequency ranges despite, with no effect of minocycline. However, both high gamma and HFO had main effects of time and treatment, with HFO having a significant interaction between the two factors (See Table 1 and Table 2 for detailed statistics). Over time, spectral power increases in the higher frequency ranges compared to pre-NIHL, but the main effect of treatment indicates a difference in enhanced power. These results suggest that spontaneous activity is enhanced after hearing loss, but minocycline attenuates these effects.

In the FC (Figure 3B), there is a main effect of treatment for low gamma, high gamma, and HFO. Only high gamma and HFO also had main effects of time, with HFO having a significant interaction between the two factors. There was a significant enhancement in spectral power in the saline group over time at the higher frequency ranges (See Table 1 and Table 2 for detailed statistics). This indicates that minocycline prevented increased resting EEG power in the FC over time. Both cortical regions had attenuated exaggerated spontaneous activity following NIHL.

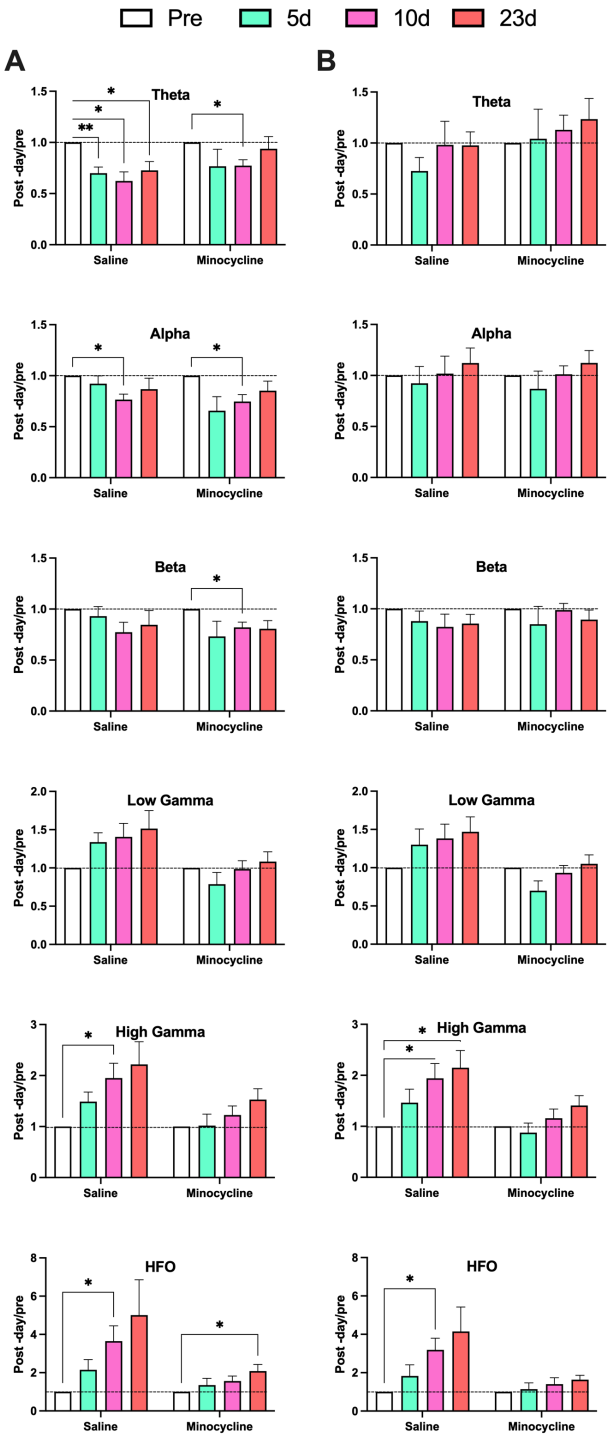

Figure 3. Spectral power after minocycline treatment is attenuated compared to saline. Spectral frequency bands show decreased resting EEG power in the lower frequencies and increased power in the AC (A) and only increased power in the higher frequency ranges in the FC (B). *, $p<0.05$; **, $p<0.01$.

Mixed-effects Two-way ANOVA

AC	Main Effect of Treatment	p	Main Effect of Time	p
Theta (3 – 7 Hz)	F (1, 17) = 1.421	0.2496	F (2.036, 30.54) = 5.239	**0.0107**
Alpha (8 – 13 Hz)	F (1, 17) = 0.9926	0.3331	F (1.669, 25.03) = 4.349	**0.0297**
Beta (14 – 29 Hz)	F (1, 17) = 0.3209	0.5785	F (1.743, 26.14) = 2.817	0.0843
Low Gamma (30 – 59 Hz)	F (1, 17) = 7.630	**0.0133**	F (1.759, 26.39) = 2.906	0.0782
High Gamma (60 – 100 Hz)	F (1, 17) = 5.610	**0.0300**	F (2.181, 32.71) = 7.763	**0.0013**
HFO (101 – 250 Hz) *	F (1, 17) = 5.497	**0.0315**	F (1.535, 23.03) = 8.223	**0.0315**

*=significant interaction of treatment and time

FC	Main Effect of Treatment	p	Main Effect of Time	p
Theta	F (1, 17) = 1.376	0.2570	F (1.795, 26.93) = 0.5683	0.5550
Alpha	F (1, 17) = 0.001622	0.9683	F (1.744, 26.16) = 1.478	0.2459
Beta	F (1, 17) = 0.2763	0.6060	F (1.573, 23.60) = 0.9623	0.3769
Low Gamma	F (1, 17) = 14.49	**0.0014**	F (1.498, 22.47) = 2.212	0.1427
High Gamma	F (1, 17) = 10.90	**0.0042**	F (1.867, 28.01) = 7.236	**0.0035**
HFO*	F (1, 17) = 10.47	**0.0049**	F (1.931, 28.96) = 6.882	**0.0039**

Table 1. Full statistics for each frequency band spectral power comparing treatment of saline versus minocycline, over time.

Bonferroni's Multiple Comparisons Test

AC	*Saline* Pre vs 5d	*Saline* Pre vs 10d	*Saline* Pre vs 23d	*Mino* Pre vs 5d	*Mino* Pre vs 10d	*Mino* Pre vs 23d
Theta (3 – 7 Hz)	**0.0055**	**0.0125**	**0.0464**	0.5784	**0.0104**	>0.9999
Alpha (8 – 13 Hz)	0.9493	**0.0102**	0.7225	0.1024	**0.0145**	0.4478
Beta (14 – 29 Hz)	>0.9999	0.1460	0.8589	0.3152	**0.0203**	0.1157
Low Gamma (30 – 59 Hz)	0.0767	0.1531	0.1769	0.5951	>0.9999	>0.9999
High Gamma (60 – 100 Hz)	0.0965	**0.0387**	0.0813	>0.9999	0.7002	0.1072
HFO (101 – 250 Hz)	0.1840	**0.0382**	0.1827	>0.9999	0.1918	**0.0360**

FC	*Saline* Pre vs 5d	*Saline* Pre vs 10d	*Saline* Pre vs 23d	*Mino* Pre vs 5d	*Mino* Pre vs 10d	*Mino* Pre vs 23d
Theta	0.2123	>0.9999	>0.9999	>0.9999	>0.9999	0.8301
Alpha	>0.9999	>0.9999	>0.9999	>0.9999	>0.9999	0.9990
Beta	0.7326	0.5571	0.4129	>0.9999	>0.9999	0.8584
Low Gamma	0.5139	0.2201	0.1279	0.1328	>0.9999	>0.9999
High Gamma	0.3449	**0.0417**	**0.0333**	>0.9999	>0.9999	0.1834
HFO *	0.5401	**0.0262**	0.1178	>0.9999	0.7592	0.0604

Table 2. Bonferroni's multiple comparisons test for each treatment over time.

iv. Auditory cortex ITPC mean is enhanced in saline and minocycline treated groups, but FC remains reduced over time.

A 40Hz pulsed noise stimulus was presented at 90 dB SPL to generate an auditory steady state response (ASSR). This stimulus was used to measure how temporal processing was affected after NIHL and drug treatment. The intertrial phase coherence (ITPC) measured the cortex's ability to consistently respond to the stimulus across trials, with mean ITPC compared between timepoints and drug condition groups.

In the AC, there was a main effect of time ($F(3, 48) = 7.193$, $p=0.0004$) with an increase from pre-levels (Figure 4A) in both the saline (Dunnett's: pre vs 23d, $p=0.0373$) and minocycline groups (Dunnett's: pre vs 10d, $p=0.0131$; pre vs 23d, $p=0.0045$). The ITPC mean in the FC (Figure 4B) showed a main effect of time ($F(3, 48) = 5.188$, $p=0.0035$) where there was a decrease in ITPC mean at 5 days in the saline group (Dunnett's: pre vs 5d, $p=0.0038$). Taken together, NIHL affected the AC with an enhancement in ITPC in both minocycline and saline treated groups. The FC did not show the same enhancement.

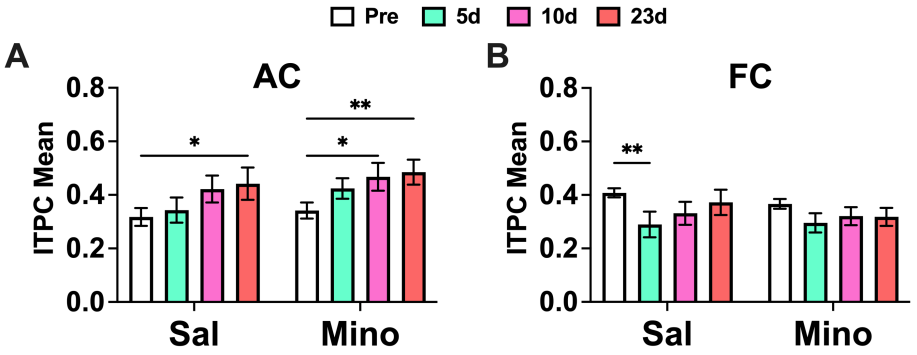

Figure 4. There was an increase in ITPC mean in the AC, but not in the FC for both saline and minocycline treatment groups in response to a 40-Hz ASSR stimulus. A) The AC showed an increase in ITPC for the saline group at 23 days after NIHL. The minocycline group had significant increases at 10- and 23 days after NIHL. B) There was a significant decrease at 5 days in the saline group from baseline, but no other ITPC mean changes were seen in either group in the FC.

v. Gap-ASSR ITPC mean is enhanced past baseline across all gap-durations in the AC

Gap-ASSR was used to measure temporal processing in the AC and FC, measuring the cortex's ability to follow and respond consistently to varying gap widths across trials. It was elicited by introducing varying gap widths in continuous noise. The longer the gap width, the better the cortex's ability to consistently entrain a response at 40 Hz across repeated presentations. This was quantified using ITPC, with the mean ITPC across trials are shown in the data below. Mixed effect 2-way ANOVA was used to compare treatment (saline vs minocycline) and time points. The 3 ms gap duration was not used in further comparisons.

In the AC, there was a main effect of time for each gap duration (4-9 ms), but no effect of treatment or interaction between the two factors (Fig 5). Both saline and minocycline had significantly elevated ITPC means compared to pre-NIHL by 23-days

post-NIHL, indicating that it was not the drug treatment that affected response consistency in the AC (See Table 3 and Table 4 for full statistics).

The FC had a main effect of time from the 4-9 ms gap durations. However, only the 8 ms and 9 ms gaps had an effect of treatment as well, but no interactions (See Table 3 for full statistics). There were significant elevations at the longer gap durations, 8 ms in the saline group and at 9 ms for the minocycline treated group (Figure 6, See Table 4 for full post-hoc analysis). Taken together, there is a cortical-region specific difference in response consistency over time, but little effect of minocycline.

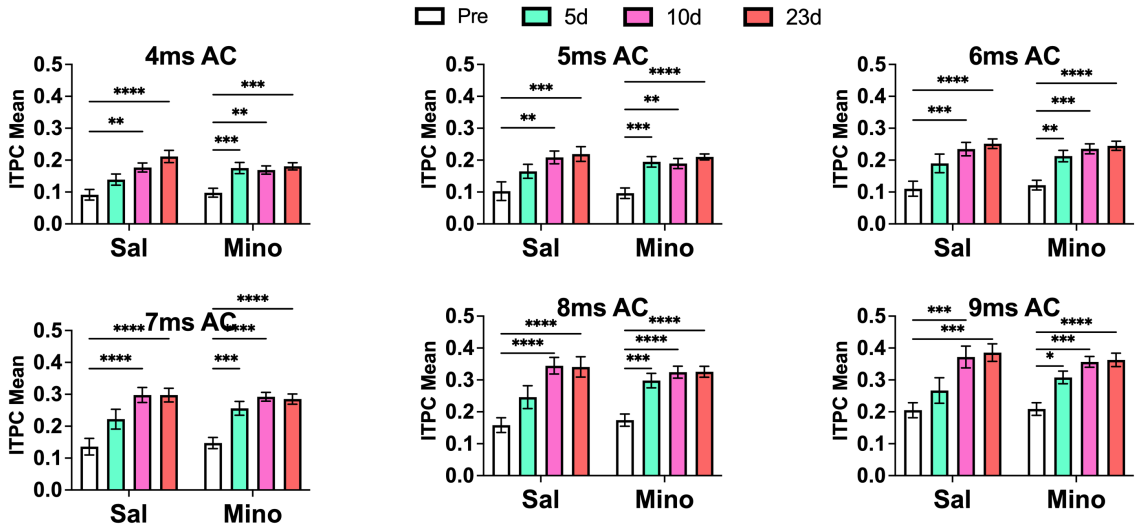

Figure 5. ITPC mean is enhanced in both the saline and minocycline treated groups in the AC. ITPC mean was averaged from the same mice at each timepoint (with +/- SEM) for each gap width (3-9 ms). All gap durations show an enhancement of ITPC across up to 23 days after NIHL in the AC. *, p<0.05; **, p<0.01; ***, p<0.001; ****, p < 0.0001.

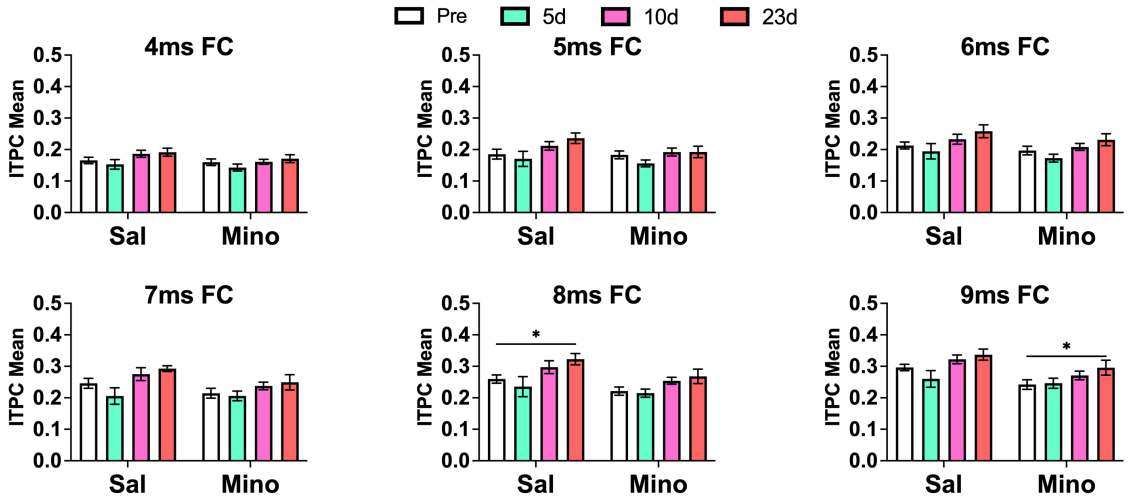

Figure 6. ITPC mean was not enhanced in either treatment groups in the FC. There were no significant differences in the FC at any time points for the shorter gap durations for either treatment group. At 8- and 9-ms, there were enhancements at 23 days in the saline and minocycline groups, respectively. *, p<0.05.

Mixed-effects Two-way ANOVA

AC	Main Effect of Treatment	p	Main Effect of Time	p
4 ms	F (1, 57) = 0.008945	0.9250	F (3, 57) = 15.68	**<0.0001**
5 ms	F (1, 57) = 0.008407	0.9273	F (3, 57) = 14.49	**<0.0001**
6 ms	F (1, 57) = 0.2630	0.6100	F (3, 57) = 18.60	**<0.0001**
7 ms	F (1, 57) = 0.1928	0.6622	F (3, 57) = 21.85	**<0.0001**
8 ms	F (1, 57) = 0.2182	0.6422	F (3, 57) = 21.11	**<0.0001**
9 ms	F (1, 57) = 0.008829	0.9255	F (3, 57) = 18.24	**<0.0001**

FC	Main Effect of Treatment	p	Main Effect of Time	p
4 ms	F (1, 16) = 2.557	0.1294	F (3, 41) = 3.489	**0.0241**
5 ms	F (1, 16) = 1.946	0.1820	F (3, 41) = 4.708	**0.0065**
6 ms	F (1, 16) = 2.511	0.1326	F (3, 41) = 5.670	**0.0024**
7 ms	F (1, 16) = 2.771	0.1154	F (3, 41) = 6.566	**0.0010**
8 ms	F (1, 16) = 5.447	0.0330	F (3, 41) = 7.335	**0.0005**
9 ms	F (1, 16) = 4.888	0.0420	F (3, 41) = 6.678	**0.0009**

Table 3. Two-way ANOVA comparing ITPC with minocycline verses saline treatment over time.

Dunnett's Multiple Comparisons Test

AC	*Saline* Pre vs 5d	*Saline* Pre vs 10d	*Saline* Pre vs 23d	*Mino* Pre vs 5d	*Mino* Pre vs 10d	*Mino* Pre vs 23d
4 ms	0.1005	**0.0015**	**<0.0001**	**0.0009**	**0.0023**	**0.0003**
5 ms	0.0767	**0.0014**	**0.0008**	**0.0008**	**0.0011**	**<0.0001**
6 ms	**0.0195**	**0.003**	**<0.0001**	**0.0019**	**0.0001**	**<0.0001**
7 ms	**0.0231**	**<0.0001**	**<0.0001**	**<0.0001**	**<0.0001**	**<0.0001**
8 ms	0.0439	**<0.0001**	**<0.0001**	**0.0007**	**<0.0001**	**<0.0001**
9 ms	0.2458	**0.0002**	**0.0001**	**0.0121**	**0.0001**	**<0.0001**

FC	*Saline* Pre vs 5d	*Saline* Pre vs 10d	*Saline* Pre vs 23d	*Mino* Pre vs 5d	*Mino* Pre vs 10d	*Mino* Pre vs 23d
4 ms	0.7627	0.04478	0.3228	0.5231	0.9991	0.7614
5 ms	0.8253	0.4819	0.0764	0.3671	0.9250	0.9151
6 ms	0.7357	0.7211	0.1508	0.5100	0.8772	0.2042
7 ms	0.1992	0.4944	0.1567	0.9657	0.5445	0.2366
8 ms	0.6186	0.3269	**0.0496**	0.9837	0.3160	0.0957
9 ms	0.2508	0.5434	0.2310	0.9817	0.3033	**0.0231**

Table 4. Adjusted p-values with Dunnett's multiple comparisons test for treatment and time.

Discussion

The present study examined the effects of minocycline administration on ABR and sound evoked responses following NIHL. Threshold shifts were induced following noise exposure. Key findings were as follows: 1) minocycline did not alter ABR thresholds after NIHL, 2) minocycline enhanced ERP amplitudes in the AC and FC, 3) minocycline attenuated exaggerated resting EEG spectral power compared to saline, 4) enhanced ITPC for 40 Hz ASSR only in the AC for both saline and minocycline treated groups, 5) increased ITPC for gap-ASSR across all gap-widths in AC for saline and minocycline treated groups over time, but not in the FC. We interpret the enhancements of ERP amplitudes to be a drug effect, but phase locking consistency increases are likely due to deafferentation and

compensatory cortical amplification. The attenuation of higher frequency resting EEG power suggests that minocycline rescues aberrant spontaneous activity. Taken together, minocycline treatment may assist with sound evoked response recovery and hyperactivity after noise-exposure, but temporal processing effects are due to gain recovery after NIHL. Future studies need to be done on permanent and full hearing loss to assess minocycline's true effects.

Few studies have investigated minocycline treatment after NIHL, though there is a consensus that administration attenuates and protects against hearing loss. A study using a rat model found that 5 days of minocycline treatment attenuated ABR thresholds and outer hair cell loss (Zhang, Song, Tian, & Qiu, 2017) after noise exposure. They reported that although click ABR thresholds of minocycline treated rats were still elevated 14 days post noise exposure, the thresholds were still significantly lower than saline treated rats. This is inconsistent with our ABR threshold shifts, but that may be due to species differences. To our knowledge, our study is the first investigation of central processing and minocycline administration following NIHL in mice. The present study reports both saline and minocycline treated groups had the same pattern of hearing loss – increased thresholds, indicating that minocycline did not influence ABR thresholds.

Spontaneous activity has been theorized to underlie tinnitus and hyperacusis. A series of Eggermont studies have purported that noise exposure in cats leads to increased firing rates and burst firing (Huetz, Guedin, & Edeline, 2014; A. J. Noreña & Eggermont, 2003; Seki & Eggermont, 2003) as well as altered inhibition (Arnaud J. Noreña, Tomita, & Eggermont, 2003). Although the mechanistic changes are not well understood, central

gain is thought to be due to abnormal excitatory/inhibitory balance (Resnik & Polley, 2017) leading to enhanced and exaggerated responses in higher auditory centers (Chambers et al., 2016; Radziwon et al., 2019b; Salvi et al., 2017b). Our resting EEG data suggests that NIHL leads to enhanced spectral power in the higher frequency ranges (80-250 Hz), which are purported to be linked to spiking activity (Ray & Maunsell, 2011) as seen by the saline treated results. However, when minocycline was administered for 5 days, the enhancement of spectral power was reduced in AC and FC. This suggests that minocycline influences spontaneous activity, particularly on attenuating central gain. It may have an alternate effect on sound detection, seen in the amplification of ERP amplitudes in both cortical regions. This rescuing may come at the expense of temporal processing abilities.

NIHL has also been shown to increase neuroinflammation, which can be a secondary mediator in molecular changes, like PNN degradation, and circuit imbalance. Microglial activation increases (Zinsmaier, Wang, Zhang, Hossainy, & Bao, 2020) after NIHL as well as proinflammatory cytokine markers in the AC (Wang et al., 2019). Targeting upregulated MMP-9 and inflammatory lends credence to minocycline's potential usage as a therapeutic treatment. Additional studies have looked at minocycline's protective role in ototoxic drug induced hearing loss. In gerbils, minocycline protected spiral ganglion neurons from deteriorating along with lower threshold increases after receiving intratympanic neomyocin (Robinson, Vujanovic, & Richter, 2015). Cisplatin treatment increased threshold shift in gerbils, but this change was reduced with minocycline administration (Lee, Shin, & Cho, 2011). Even in cochlear cultures, minocycline reduced the amount of gentamicin induced hair cell damage from neonatal

rats (Corbacella, Lanzoni, Ding, Previati, & Salvi, 2004). In a human study with minocycline treatment, residual hearing was preserved after cochlear implantation compared to age-matched individuals who did not receive minocycline. Future studies can be done to parse out minocycline's role in molecular changes after NIHL, investigating whether neuroinflammatory markers are reduced along with PNN fidelity.

Conclusions

Minocycline has some enhancing effects on sound detection and attenuating effects on spontaneous activity, but no effect on temporal processing after NIHL. With higher ABR thresholds, peripheral sound detection is altered and may lead to compensatory changes in the central auditory regions. With both cortical regions showing higher ERP amplitudes, there may be a compensatory amplification with minocycline treatment to improve sound detection centrally. However, temporal processing is not impacted by minocycline treatment in either AC or FC suggesting that recovery of spontaneous activity and sound detection at the expense of temporal processing. Conversely, spontaneous activity is attenuated with minocycline administration suggesting central gain can be reduced with a therapeutic treatment. Future studies should be performed to investigate minocycline's impact on permanent and full hearing loss.

1. Auerbach, B. D., Radziwon, K., & Salvi, R. (2019). Testing the Central Gain Model: Loudness Growth Correlates with Central Auditory Gain Enhancement in a Rodent Model of Hyperacusis. *Neuroscience*, *407*, 93–107. https://doi.org/10.1016/j.neuroscience.2018.09.036

2. Bilousova, T. V., Dansie, L., Ngo, M., Aye, J., Charles, J. R., Ethell, D. W., & Ethell, I. M. (2009). Minocycline promotes dendritic spine maturation and improves behavioural performance in the fragile X mouse model. *Journal of Medical Genetics*, *46*(2), 94–102. https://doi.org/10.1136/jmg.2008.061796

3. Chambers, A. R., Resnik, J., Yuan, Y., Whitton, J. P., Edge, A. S., Liberman, M. C., & Polley, D. B. (2016). Central Gain Restores Auditory Processing following Near-Complete Cochlear Denervation. *Neuron*, *89*(4), 867–879. https://doi.org/10.1016/j.neuron.2015.12.041

4. Chen, S. Der, Yin, J. H., Hwang, C. S., Tang, C. M., & Yang, D. I. (2012). Anti-apoptotic and anti-oxidative mechanisms of minocycline against sphingomyelinase/ceramide neurotoxicity: implication in Alzheimer's disease and cerebral ischemia. *Free Radical Research*, *46*(8), 940–950. https://doi.org/10.3109/10715762.2012.674640

5. Corbacella, E., Lanzoni, I., Ding, D., Previati, M., & Salvi, R. (2004). Minocycline attenuates gentamicin induced hair cell loss in neonatal cochlear cultures. *Hearing Research*, *197*(1–2), 11–18. https://doi.org/10.1016/J.HEARES.2004.03.012

6. Dansie, L. E., Phommahaxay, K., Okusanya, A. G., Uwadia, J., Huang, M., Rotschafer, S. E., … Ethell, I. M. (2013). Long-lasting Effects of Minocycline on Behavior in Young but not Adult Fragile X Mice. *Neuroscience*, *246*, 186–198. https://doi.org/10.1016/J.NEUROSCIENCE.2013.04.058

7. Dziembowska, M., Pretto, D. I., Janusz, A., Kaczmarek, L., Leigh, M. J., Gabriel, N., … Tassone, F. (2013). High MMP-9 activity levels in fragile X syndrome are lowered by minocycline. *American Journal of Medical Genetics, Part A*, *161*(8), 1897–1903. https://doi.org/10.1002/ajmg.a.36023

8. Eggermont, J. J., & Komiya, H. (2000). Moderate noise trauma in juvenile cats results in profound cortical topographic map changes in adulthood. *Hearing Research*, *142*(1–2), 89–101. https://doi.org/10.1016/S0378-5955(00)00024-1

9. Elewa, H. F., Hilali, R., Hess, D. C., Machado, L. S., & Fagan, S. C. (2006). Minocycline for Acute Neuroprotection. *Pharmacotherapy*, *26*(4), 515. https://doi.org/10.1592/PHCO.26.4.515

10. Huetz, C., Guedin, M., & Edeline, J. M. (2014). Neural correlates of moderate

hearing loss: Time course of response changes in the primary auditory cortex of awake guinea-pigs. *Frontiers in Systems Neuroscience*, *8*(APR). https://doi.org/10.3389/fnsys.2014.00065

11. Lee, C. K., Shin, J. I., & Cho, Y. S. (2011). Protective Effect of Minocycline Against Cisplatin-induced Ototoxicity. *Clinical and Experimental Otorhinolaryngology*, *4*(2), 77. https://doi.org/10.3342/CEO.2011.4.2.77

12. Lin, F., Zheng, Y., Pan, L., & Zuo, Z. (2020). Attenuation of noisy environment-induced neuroinflammation and dysfunction of learning and memory by minocycline during perioperative period in mice. *Brain Research Bulletin*, *159*, 16–24. https://doi.org/10.1016/J.BRAINRESBULL.2020.03.004

13. Lovelace, J. W., Ethell, I. M., Binder, D. K., & Razak, K. A. (2018). Translation-relevant EEG phenotypes in a mouse model of Fragile X Syndrome. *Neurobiology of Disease*, *115*, 39–48. https://doi.org/10.1016/j.nbd.2018.03.012

14. Lovelace, J. W., Ethell, I. M., Binder, D. K., & Razak, K. A. (2020). Minocycline Treatment Reverses Sound Evoked EEG Abnormalities in a Mouse Model of Fragile X Syndrome. *Frontiers in Neuroscience*, *14*(August), 1–16. https://doi.org/10.3389/fnins.2020.00771

15. Machado, L. S., Kozak, A., Ergul, A., Hess, D. C., Borlongan, C. V., & Fagan, S. C. (2006). Delayed minocycline inhibits ischemia-activated matrix metalloproteinases 2 and 9 after experimental stroke. *BMC Neuroscience*, *7*(1), 1–7. https://doi.org/10.1186/1471-2202-7-56/FIGURES/4

16. Mishra, M. K., & Basu, A. (2008). Minocycline neuroprotects, reduces microglial activation, inhibits caspase 3 induction, and viral replication following Japanese encephalitis. *Journal of Neurochemistry*, *105*(5), 1582–1595. https://doi.org/10.1111/J.1471-4159.2008.05238.X

17. Modheji, M., Olapour, S., Khodayar, M. J., Jalili, A., & Yaghooti, H. (2016). Minocycline is More Potent Than Tetracycline and Doxycycline in Inhibiting MMP-9 in Vitro. *Jundishapur Journal of Natural Pharmaceutical Products 2016 11:2*, *11*(2), 27377. https://doi.org/10.17795/JJNPP-27377

18. Nguyen, A., Khaleel, H. M., & Razak, K. A. (2017). Effects of noise-induced hearing loss on parvalbumin and perineuronal net expression in the mouse primary auditory cortex. *Hearing Research*, *350*, 82–90. https://doi.org/10.1016/j.heares.2017.04.015

19. Noreña, A. J., & Eggermont, J. J. (2003). Changes in spontaneous neural activity immediately after an acoustic trauma: Implications for neural correlates of tinnitus. *Hearing Research*, *183*(1–2), 137–153. https://doi.org/10.1016/S0378-

5955(03)00225-9

20. Noreña, Arnaud J., Tomita, M., & Eggermont, J. J. (2003). Neural changes in cat auditory cortex after a transient pure-tone trauma. *Journal of Neurophysiology*, *90*(4), 2387–2401. https://doi.org/10.1152/JN.00139.2003/ASSET/IMAGES/LARGE/9K1033365014.JPEG

21. Parthasarathy, A., Cunningham, P. A., & Bartlett, E. L. (2010). Age-related differences in auditory processing as assessed by amplitude-modulation following responses in quiet and in noise. *Frontiers in Aging Neuroscience*, *2*(DEC), 1–10. https://doi.org/10.3389/fnagi.2010.00152

22. Radziwon, K., Auerbach, B. D., Ding, D., Liu, X., Chen, G. Di, & Salvi, R. (2019a). Noise-Induced loudness recruitment and hyperacusis: Insufficient central gain in auditory cortex and amygdala. *Neuroscience*, *422*, 212–227. https://doi.org/10.1016/J.NEUROSCIENCE.2019.09.010

23. Radziwon, K., Auerbach, B. D., Ding, D., Liu, X., Chen, G. Di, & Salvi, R. (2019b). Noise-Induced loudness recruitment and hyperacusis: Insufficient central gain in auditory cortex and amygdala. *Neuroscience*, *422*, 212–227. https://doi.org/10.1016/j.neuroscience.2019.09.010

24. Ray, S., & Maunsell, J. H. R. (2011). Different origins of gamma rhythm and high-gamma activity in macaque visual cortex. *PLoS Biology*, *9*(4). https://doi.org/10.1371/journal.pbio.1000610

25. Resnik, J., & Polley, D. B. (2017). Fast-spiking GABA circuit dynamics in the auditory cortex predict recovery of sensory processing following peripheral nerve damage. *ELife*, *6*. https://doi.org/10.7554/eLife.21452

26. Resnik, J., & Polley, D. B. (2021). Cochlear neural degeneration disrupts hearing in background noise by increasing auditory cortex internal noise. *Neuron*, *109*(6), 984-996.e4. https://doi.org/10.1016/J.NEURON.2021.01.015

27. Robinson, A. M., Vujanovic, I., & Richter, C. P. (2015). Minocycline protection of neomycin induced hearing loss in gerbils. *BioMed Research International*, *2015*. https://doi.org/10.1155/2015/934158

28. Rumschlag, J. A., & Razak, K. A. (2021). Age-related changes in event related potentials, steady state responses and temporal processing in the auditory cortex of mice with severe or mild hearing loss. *Hearing Research*, *412*, 108380. https://doi.org/10.1016/j.heares.2021.108380

29. Salvi, R., Sun, W., Ding, D., Chen, G.-D., Lobarinas, E., Wang, J., … Auerbach, B. D. (2017a). Inner Hair Cell Loss Disrupts Hearing and Cochlear Function Leading to Sensory Deprivation and Enhanced Central Auditory Gain. *Frontiers in Neuroscience*, *10*(JAN), 621. https://doi.org/10.3389/fnins.2016.00621

30. Salvi, R., Sun, W., Ding, D., Chen, G.-D., Lobarinas, E., Wang, J., … Auerbach, B. D. (2017b). Inner Hair Cell Loss Disrupts Hearing and Cochlear Function Leading to Sensory Deprivation and Enhanced Central Auditory Gain. *Frontiers in Neuroscience*, *10*(JAN). https://doi.org/10.3389/fnins.2016.00621

31. Schmidt, E. K. A., Raposo, P. J. F., Torres-Espin, A., Fenrich, K. K., & Fouad, K. (2021). Beyond the lesion site: minocycline augments inflammation and anxiety-like behavior following SCI in rats through action on the gut microbiota. *Journal of Neuroinflammation*, *18*(1), 1–16. https://doi.org/10.1186/S12974-021-02123-0/FIGURES/7

32. Seki, S., & Eggermont, J. J. (2003). Changes in spontaneous firing rate and neural synchrony in cat primary auditory cortex after localized tone-induced hearing loss. *Hearing Research*, *180*(1–2), 28–38. https://doi.org/10.1016/S0378-5955(03)00074-1

33. Switzer, J. A., Hess, D. C., Ergul, A., Waller, J. L., MacHado, L. S., Portik-Dobos, V., … Fagan, S. C. (2011). Matrix Metalloproteinase-9 in an Exploratory Trial of Intravenous Minocycline for Acute Ischemic Stroke. *Stroke*, *42*(9), 2633–2635. https://doi.org/10.1161/STROKEAHA.111.618215

34. Umbricht, D., Vyssotky, D., Latanov, A., Nitsch, R., Brambilla, R., D'Adamo, P., & Lipp, H. P. (2004). Midlatency auditory event-related potentials in mice: Comparison to midlatency auditory ERPs in humans. *Brain Research*, *1019*(1–2), 189–200. https://doi.org/10.1016/j.brainres.2004.05.097

35. Wang, W., Zhang, L. S., Zinsmaier, A. K., Patterson, G., Leptich, E. J., Shoemaker, S. L., … Bao, S. (2019). Neuroinflammation mediates noise-induced synaptic imbalance and tinnitus in rodent models. *PLoS Biology*, *17*(6). https://doi.org/10.1371/journal.pbio.3000307

36. Yokota, Y., & Naruse, Y. (2015). Phase coherence of auditory steady-state response reflects the amount of cognitive workload in a modified N-back task. *Neuroscience Research*, *100*, 39–45. https://doi.org/10.1016/J.NEURES.2015.06.010

37. Zhang, J., Song, Y. L., Tian, K. Y., & Qiu, J. H. (2017). Minocycline attenuates noise-induced hearing loss in rats. *Neuroscience Letters*, *639*, 31–35. https://doi.org/10.1016/J.NEULET.2016.12.039

38. Zinsmaier, A. K., Wang, W., Zhang, L., Hossainy, N. N., & Bao, S. (2020).

Resistance to noise-induced gap detection impairment in FVB mice is correlated with reduced neuroinflammatory response and parvalbumin-positive neuron loss. https://doi.org/10.1038/s41598-020-75714-1

Chapter 5

Genetic reduction of MMP-9 in the *Fmr1* KO mouse partially rescues prepulse inhibition of acoustic startle response

Abstract

Sensory processing abnormalities are consistently associated with autism, but the underlying mechanisms and treatment options are unclear. Fragile X Syndrome (FXS) is the leading known genetic cause of intellectual disabilities and autism. One debilitating symptom of FXS is hypersensitivity to sensory stimuli. Sensory hypersensitivity is seen in both humans with FXS and FXS mouse model, the *Fmr1* knock out (*Fmr1* KO) mouse. Abnormal sensorimotor gating may play a role in the hypersensitivity to sensory stimuli. Humans with FXS and *Fmr1* KO mice show abnormalities in acoustic startle response (ASR) and prepulse inhibition (PPI) of startle, responses commonly used to quantify sensorimotor gating. Recent studies have suggested regulation of matrix metalloproteinase-9 (MMP-9), which is abnormally high in FXS, as a potential mechanism of sensory abnormalities in FXS. Here we tested the hypothesis that genetic reduction of MMP-9 in *Fmr1* KO mice rescues ASR and PPI phenotypes in adult *Fmr1* KO mice. We measured MMP-9 levels in the inferior colliculus (IC), an integral region of the PPI circuit, of WT and *Fmr1* KO mice at P7, P12, P18, and P40. MMP-9 levels were higher in the IC of *Fmr1* KO mice during early development (P7, P12), but not in adults. We compared ASR and PPI responses in young (P23-25) and adult (P50-80) *Fmr1* KO mice to their age-matched wildtype (WT) controls. We found that both ASR and PPI were reduced in the young *Fmr1*

KO mice compared to age-matched WT mice. There was no genotype difference for ASR in the adult mice, but PPI was significantly reduced in the adult *Fmr1* KO mice. The adult mouse data are similar to those observed in humans with FXS. Genetic reduction of MMP-9 in the *Fmr1* KO mice resulted in a rescue of adult PPI responses to WT levels. Taken together, these results show sensorimotor gating abnormalities in *Fmr1* KO mice, and suggest the potential for regulating MMP-9 as a therapeutic target to reduce sensory hypersensitivity.

Introduction

Fragile X syndrome (FXS) is a leading genetic cause of intellectual disability and autism. In conjunction with learning, anxiety, communication, and social deficits (Hatton et al., 2006), individuals with FXS are often hypersensitive to sensory stimuli. FXS is linked to a genetic mutation in the X chromosome with varying degrees of severity, due to the expansion of CGG repeats in the Fragile X mental retardation-1 (*Fmr1*) *gene* (Snow et al., 1993). If the repeated sequence exceeds ~200 repeats, this can lead to a full mutation and methylation of the *Fmr1* gene which in turn causes transcriptional suppression of the *Fmr1 gene* and the loss of Fragile X mental retardation protein (FMRP). Loss of FMRP has been associated with abnormal protein synthesis, particularly those involved with synaptic plasticity and maturation (Huber et al., 2002; Sidorov et al., 2013).

Debilitating sensory hypersensitivity is a common symptom in humans with FXS (Tsiouris and Brown, 2004), manifesting as intolerance to even mild sensory inputs. An animal model of FXS, the *Fmr1* knock out (*Fmr1* KO) mouse, shows many of the core abnormalities of FXS including sensory hypersensitivity (Rais et al., 2018; Sinclair et al.,

2017). Sensorimotor gating is a low-level (pre-attentive) sensory filtering mechanism to reduce sensory overload reaching cortical areas. Abnormal sensorimotor gating may contribute to hypersensitivity in autism spectrum disorders (Scott et al., 2018), including FXS (Sinclair et al., 2017). Acoustic startle response (ASR) and prepulse inhibition (PPI) of ASR are behavioral outcomes used to test sensorimotor gating in humans and rodents. The circuits underlying these behaviors are present in the brainstem and midbrain of the auditory system. FMRP, the protein product of *Fmr1* gene, is expressed across all levels of the central auditory system, including strong expression in the cochlear nucleus and other regions of the brainstem (Zorio et al., 2017). Abnormal functions of these regions in *Fmr1* KO mice have been reported (Garcia-Pino et al., 2017; Mott and Wei, 2014; Wang et al., 2018) and both humans with FXS and *Fmr1* KO mice show altered ASR and PPI responses (human: Frankland et al., 2004; Yuhas et al., 2011; Hessl et al., 2009; mouse: Chen and Toth, 2001; Nielsen et al., 2002; Renoux et al., 2014; Yun et al., 2006).

One of FMRP's translational targets is matrix metalloproteinase-9 (MMP-9), an endopeptidase important in CNS development through extracellular matrix remodeling and synaptic plasticity (Reinhard et al., 2015). Increased MMP-9 levels are seen in the *Fmr1* KO mouse and FXS human brains (Bilousova et al., 2009; Dziembowska et al., 2013; Sidhu et al., 2014). Genetic reduction of MMP-9 levels in the *Fmr1* KO mouse restored auditory cortex responses to WT levels (Lovelace et al., 2016; Wen et al., 2018), rescued dendritic spine abnormalities in the hippocampus and reduced anxiety-like behaviors (Sidhu et al., 2014). Beneficial effect of MMP reduction on synaptic arborization is seen in the drosophila model of FXS (Siller and Broadie, 2011). Inhibition of MMP-9 with

minocycline reduces multiple symptoms in the *Fmr1* KO mice and humans with FXS (Bilousova et al., 2009; Dziembowska et al., 2013; Schneider et al., 2013). However, it is not known if MMP-9 levels are high in circuits involved in sensorimotor gating (Li et al., 1998) and if reduction of MMP-9 in FXS reduces sensorimotor gating abnormalities. In this study, we focused on the IC because the pre-pulse activates the IC, which then initiates a long duration inhibition of the ASR circuit, resulting in the PPI of startle (Fendt et al., 2001). We found increased MMP-9 levels in the IC during development, but not in adults. The second aim was to determine if ASR and PPI responses in *Fmr1* KO mice were different from WT mice from a young age. We found reduced PPI in the *Fmr1* KO mice compared to WT mice in both age groups tested: young (P23-25) and adult. A genotype difference in ASR was found only in the young age group. Finally, we tested the hypothesis that genetic reduction of MMP-9 in *Fmr1* KO mice would alleviate PPI abnormalities in the *Fmr1* KO mice. For this purpose, we generated *Fmr1* KO mice, which were heterozygous for MMP-9 and found that these mice show ASR and PPI responses that are comparable to the WT mice.

Methods

Mice.

FVB.129P2 – Pde6b+Tyr$^{c\text{-}ch}$/AntJ controls (WT) and FVB.129P2 – *Fmr1tm1Cgr*/J (*Fmr1* KO) mice were received from Jackson Laboratories and housed on a 12:12 light/dark cycle, with standard lab chow and water given *ad libitum* in the vivarium. To generate the *Mmp9* $^{+/-}$/*Fmr1* KO mice, FVB.Cg–*Mmp–9tm1Tvu*/J mice were backcrossed with *Fmr1* KO mice. These mice had a reduced expression of MMP-9 in the

auditory cortex (Sidhu et al.., 2014 and Wen et al.., 2018). Genotypes of mice were verified by sending tail samples to Transnetyx (Cordova, TN). There were two age groups tested: young ("Y", PND 23-25) and adult ("A", PND 50-80). Table 1 provides information about the age and average weight of each group. Weights between genotypes were not significantly different in either the young ($t(16)=1.792$, $p=0.092$) or adult ($F(2,24)=0.71$, $p=0.502$) groups. All procedures were approved by the Institutional Animal Care and Use Committee at the University of California, Riverside. Each experimental group consisted of n=9 mice. All mice tested were males.

Apparatus

Acoustic Startle. The Coulbourn Animal Acoustic Startle System (Coulbourn Instruments, Whitehall, PA) was used to measure the ASR. The apparatus consisted of a single subject anechoic startle chamber with a ventilating fan built into the ceiling to provide background noise (68dB SPL). A weight-sensitive startle platform was centered inside of the chamber. The A10-21B Startle Controller Software was used to generate the PPI protocol and measure ASR peak magnitude. Each mouse was placed into individual ventilated holding cages.

Procedures.

Mice habituated for 20 minutes in their home cages after being transported to the lab. Afterwards, each mouse was weighed, and allowed to habituate for 10 additional minutes in the holding cage, before being placed in the startle chamber. A five-minute delay was built into the program to allow the animal to acclimate to the chamber prior to the stimulus presentation. The built-in fan provided background noise of 68dB SPL,

measured with a digital sound level meter (BK Precision, Model 732A). Table 2 provides information on the various trials used. Trial type 1 consisted of the initial six and final five trials, which presented only 115dB SPL startle stimulus. These trials were used to calculate the ASR and habituation. Between the stimulus alone trials, eight of each prepulse trials were presented in pseudorandom order, with the prepulse – 75, 85, or 95dB SPL – preceding the startle stimulus by 100ms. Duration of the prepulse sound was 20ms and duration of the startle pulse was 40ms. Additional prepulse trials were excluded from analysis, due to being of similar sound levels to the startle stimulus (105dB). The inter-trial interval ranged from 15-25s to minimize anticipation of the startle stimulus delivery.

Gelatin Zymography.

Inferior colliculus (IC) tissue samples were taken from P7, P12, P18, and P40 mice. The mice were euthanized with isoflurane, the IC was dissected and immediately flash frozen over dry ice then stored at -80°C. The gelatin zymography protocol was performed as previously described in Wen et al., 2018. The zymography buffer used to resuspend the IC included 100 µL of 100 mM Tris-HCl (pH = 7.6), 150 mM NaCl, 5 mM $CaCl_2$, 0.05% Brij35, 0.02% Na_3N, 1% Triton X-100, 100 µM PMSF and protease inhibitor cocktail (Sigma, catalog# P8340). Gelatin agarose beads (Sigma, catalog# G5384) were added to the sample lysates to pull down MMP-9 on 10% Tris-Glycine gel with 0.1% gelatin as the substrate (Life Technologies). Once pulled down, the gels were placed in renaturing buffer (Life Technologies, catalog# LC2670) for 90 minutes and developing buffer (Life Technologies, catalog# LC2671) for 96 hours. Gels were then stained with Commassie blue overnight and de-stained for subsequent analysis. Total protein concentration was

measured per lysate using the BCA colorimetric protein assay (Pierce, 23 235). Levels of MMP-9 protein were analyzed using Photoshop CS4. All samples were normalized to the WT values per each individual age group (n=3-7).

Data analysis.

Weight comparisons were done by independent t-tests to compare the young groups and one-way ANOVA was used to compare the adult groups. One-tailed unpaired t-test was used to compare WT and *Fmr1* KO MMP-9 levels. ASR was calculated by averaging the peak magnitude of the startle stimulus alone responses and across the 11 Trial Type 1 responses. Percent habituation was calculated as %Habituation=100 x (average last five Trial Type 1 responses/average first five Trial Type 1 response). Percent PPI was calculated as %PPI=1-(average startle amplitude from prepulse trial/average startle amplitude from startle stimulus alone trial) x 100. To compare PPI across genotypes, a two-way ANOVA was used with prepulse intensity (75, 85, 95 dB) and genotype (KO, WT) as factors. One-way ANOVA was used for comparison of ASR across genotypes separately for each age group tested. Standard error is shown by the error bars in all figures. Age was not tested as a factor in any analysis. Post-hoc tests are as described in the Results section.

Results

Genotype	Number of mice	Age (Postnatal days)	Average weight (g)	Average standard error
WT Adult	9	53-55	28.5	0.98
Fmr1 KO Adult	9	53-54	28.5	0.82
MMP9 +/- *Fmr1* KO Adult	9	65-67	27.3	0.715
WT Young	9	24-25	17.4	0.72
Fmr1 KO Young	9	23-24	15.6	0.70

Table 1. Summary of genotype and age studied.

Trial Type	Prepulse Intensity (dB)	Startle Stimulus (dB)
1	0	115
2	75	115
3	85	115
4	95	115
5	105	115
6	0	115

Table 2. Trial types for acoustic startle and prepulse inhibition. In trials looking at prepulse inhibition, the inter-stimulus interval was 100ms. The inter-trial interval ranged from 15-25 seconds.

i. Gelatin Zymography for MMP-9 levels in the inferior colliculus

Gelatin zymography was used to measure MMP-9 levels in the IC of WT and *Fmr1* KO mice at four different ages: postnatal day (P) 7, 12, 18, and 40. As seen in Figure 1, at P7 ($t(4)=-2.47$, $p=0.0345$) and P12($t(7)=-2.054$, $p=0.0395$), *Fmr1* KO mice showed greater MMP-9 levels compared to WT. There was no genotype difference in MMP9 levels at P18 ($t(8)=-0.267$, $p=0.398$) and P40 ($t(8)=-0.299$, $p=0.772$). These results show that as in the forebrain (Lovelace et al., 2016), loss of FMRP in the midbrain also causes an increase in MMP-9 levels.

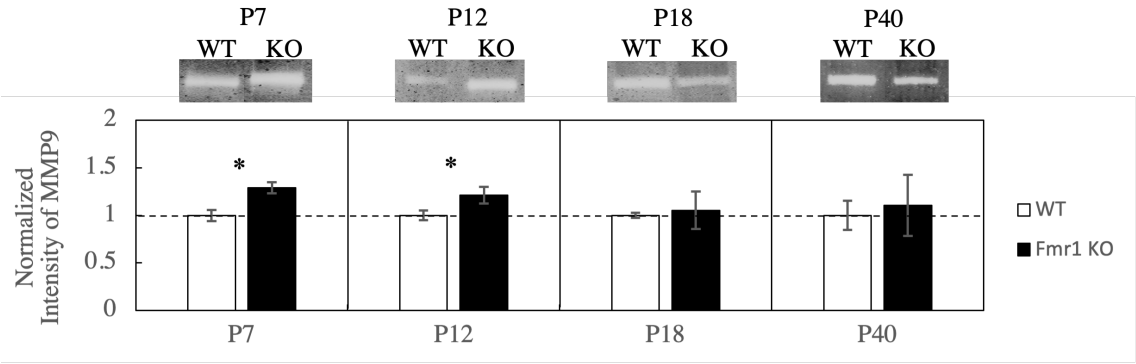

Figure 1. MMP-9 levels in IC differ between WT and adult *Fmr1* KO mice at P7 and P12, but not P18 or P40. There was an increase in MMP-9 levels in *Fmr1* KO mice earlier in development (P7: $t(4)=-2.47$, $p=0.0345$); P12: $t(7)=-2.054$, $p=0.0395$). However, at later ages there was no difference between the two genotypes (P18: P18 ($t(8)=-0.267$, $p=0.398$); P40 ($t(8)=-0.299$, $p=0.772$). Standard error is shown in the bar graphs.

ii. Acoustic startle response and prepulse inhibition

The ASR was measured in young and adult mice. Young (P23-25) *Fmr1* KO mice showed a significant reduction in ASR compared to age-matched WT mice (one-way ANOVA, $F(1,16)=6.190$, $p=0.024$) (Figure 2A). To examine PPI, two-way ANOVA was used with prepulse intensity and genotype as factors. PPI was significantly reduced in

young *Fmr1* KO mice compared to WT mice (Genotype: $F(1,48)=9.226$, p=0.004) (Figure 2B). While prepulse intensity affected PPI (Intensity: $F(2,48)=3.267$, p=0.047; Tukey HSD, 75dB vs 85dB, p=0.596; 75dB vs 95dB, p=0.038; 85dB vs 95dB, p=0.273), there were no significant interactions between genotype and prepulse intensity (Genotype*Intensity: $F(2,48)=0.499$, p=0.610). This suggests that the genotype difference in PPI is not due to change in any specific intensity tested.

The ASR was not different between adult (P50-80) WT, *Fmr1* KO, and MMP-9$^{+/-}$ /*Fmr1* KO mice (one-way ANOVA, $F(2,24)=1.019$, p=0.376) (Figure 3A). A two-way ANOVA with genotype and prepulse intensity as factors showed that there was a main effect of genotype ($F(2,72)=5.583$, p=0.006), and prepulse intensity ($F(2,72)=8.156$, p=0.001), but no significant interactions ($F(4,72)=0.401$, p=0.807) (Figure 3B). Post hoc Tukey HSD analyses revealed that *Fmr1* KO PPI was significantly reduced compared to WT (WT vs. *Fmr1* KO, p=0.004) as seen in the young mice. There was no difference in PPI responses between WT and MMP-9$^{+/-}$ /*Fmr1* KO (WT vs. MMP-9$^{+/-}$ /*Fmr1* KO, p=0.427) or between MMP-9$^{+/-}$ /*Fmr1* KO and *Fmr1* KO mice (*Fmr1* KO vs. MMP-9$^{+/-}$ /*Fmr1* KO, p=0.106). Additionally, prepulse intensity post hoc analysis revealed that as the sound intensity increased, the PPI increased as well (75dB vs 85dB, p=0.044; 75dB vs 95dB, p=0.000431, 85dB vs 95dB, p=0.267). One potential methodological concern is that the mice could have shown startle response to the pre-pulse, particularly at 85 and 95dB SPL (Valsamis et al., 2011). However, because the ASR itself was not different at this age, it is unlikely that the genotype PPI differences were due to startle to the pre-pulse. In addition, the biggest genotype effects are seen for the 75dB prepulse, which is unlikely to

cause startle by itself. Indeed a one-way ANOVA analyses of PPI just for the 75dB prepulse ($F(2,24)=3.446$, p=0.048) shows that the MMP-9$^{+/-}$/*Fmr1* KO mice were similar to WT (WT vs. MMP-9$^{+/-}$/*Fmr1* KO, p=0.720), and both showed higher PPI than the Fmr1 KO mice. Taken together, these data suggest that genetic reduction of MMP-9 in the *Fmr1* KO mice, provides a rescue of the PPI deficit, without impacting the baseline ASR.

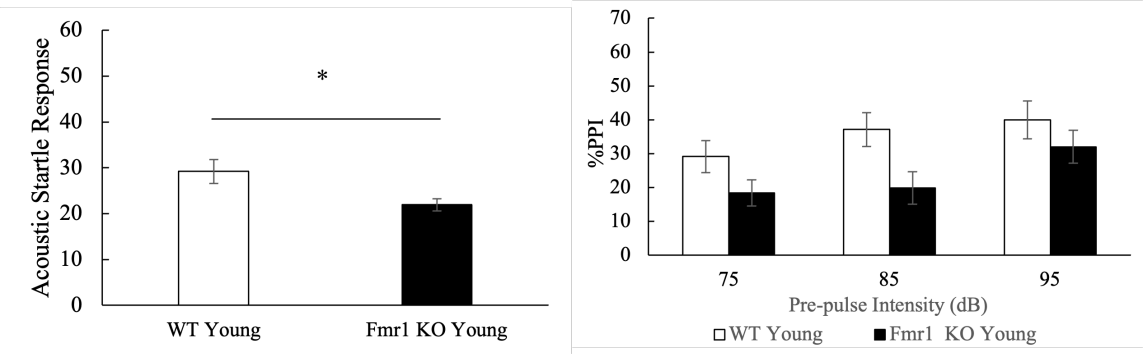

Figure 2. Startle is reduced in *Fmr1* KO mice at young, but PPI is not different from WT. A) The baseline acoustic startle response was significantly different between young WT and *Fmr1* KO mice (one-way ANOVA - $F(1,16)=6.190$, p=0.024). B) Two-way ANOVA with prepulse intensity and genotype as factors in the young mice revealed that PPI increased with sound intensity (Intensity – $F(2,48)=3.267$, p=0.047; Tukey HSD - 75dB vs 85dB, p=0.596; 75dB vs 95dB, p=0.038; 85dB vs 95dB, p=0.273) and was reduced in *Fmr1* KO compared to WT mice (Genotype – $F(1,48)=9.226$, p=0.004). There were no significant interactions between genotype and prepulse intensity (Genotype*Intensity – $F(2,48)=0.499$, p=0.610). Standard error is shown in the bar graphs.

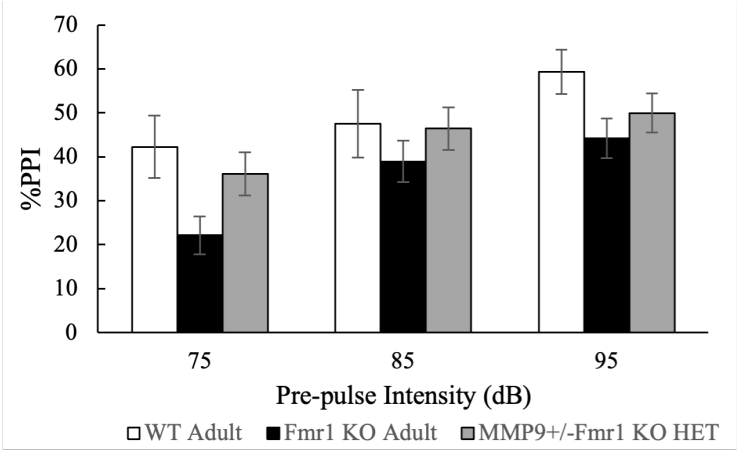

Figure 3. Genetic reduction of MMP-9 in *Fmr1* KO mice partially rescues the PPI deficit. A) In adult mice, there was no statistical difference in baseline startle across the three genotypes (one way ANOVA - $F(2,24)=1.019$, p=0.376). B) Two way ANOVA with genotype and prepulse intensity as factors shows that in adult mice, there was a significant effect of genotype ($F(2,72)=5.583$, p=0.006; Tukey HSD – WT vs *Fmr1* KO, p=0.004; WT vs MMP9+/-*Fmr1* KO, p=0.427; *Fmr1*KO vs MMP9+/-*Fmr1* KO, p=0.106) and intensity ($F(2,72)=8.156$, p=0.001; Tukey HSD – 75dB vs 85dB, p=0.044; 75dB vs 95dB, p=0.000431; 85dB vs 95dB, p=0.267) alone, but no interactions (Genotype*Intensity - $F(4,72)=0.401$, p=0.807). Standard error is shown in the bar graphs.

iii. Habituation

Habituation of electrophysiological response to repeated stimulation is reduced in both humans with FXS and the *Fmr1* KO mice (Ethridge et al., 2016; Lovelace et al., 2016; Schneider et al., 2013). Genotype differences in ASR may arise due to differences in habituation to startle stimuli. Therefore, we examined whether ASR habituation is altered in the *Fmr1* KO mice. Habituation was calculated by dividing the average of the final five ASR values by the average first five ASR values (see Methods). There was no genotype difference in habituation in young ($F(1,16)=0.316$, $p=0.582$) (Figure 4A) or adult ($F(2,24)=0.368$, $p=0.696$) (Figure 4B) mice. This suggests that in the young mouse, genotype differences in ASR do not occur because of altered habituation.

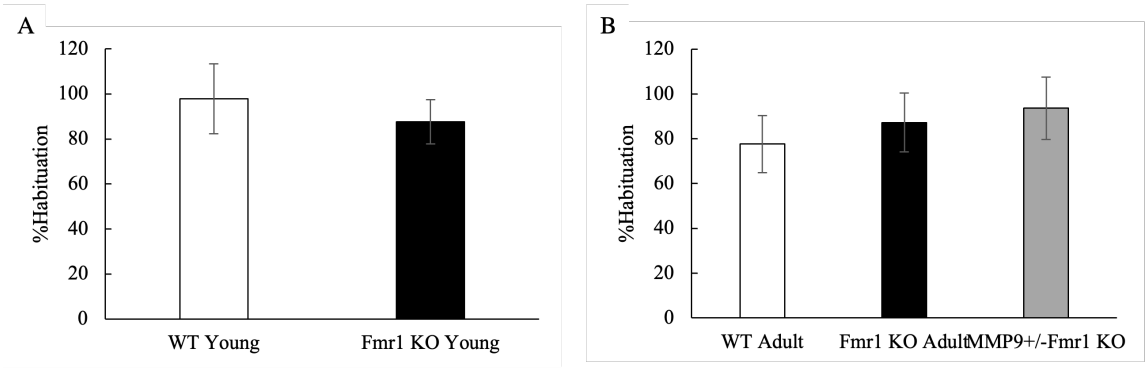

Figure 4. Habituation to ASR stimuli is normal in both young and adult *Fmr1* KO mice. A) Young WT and *Fmr1* KO mice did not show any significant difference in habituation from the beginning of the protocol to the end ($F(1,16)=0.316$, $p=0.582$). B) There was no significant difference in percent habituation between any of the adult age groups ($F(2,24)=0.368$, $p=0.696$). Standard error is shown in the bar graphs.

Discussion

We found that in young, but not in adult *Fmr1* KO mice, there was a significant reduction in ASR amplitude compared to age matched WT mice. In both age groups, PPI was significantly reduced in the *Fmr1* KO mice compared to WT mice, suggesting that sensorimotor gating abnormalities present in young *Fmr1* KO mice are maintained into adulthood. We also found increased MMP-9 levels in the IC of the developing, but not adult, *Fmr1* KO mice. This suggests that abnormal MMP-9 levels in the IC may be associated with reduced PPI. While WT and *Fmr1* KO mice were significantly different from each other in terms of PPI, the MMP-$9^{+/-}$ /*Fmr1* KO mice were not different from either WT or *Fmr1* KO mice. We interpret this to mean that there was a partial rescue of the PPI phenotype when MMP-9 was reduced in the *Fmr1* KO mice. It is not possible to interpret any intensity specific effects because there was no interaction between genotype and prepulse intensity. The partial correction implies other mechanisms in the ASR/PPI

pathway such as abnormal ion channel function may be involved in sensorimotor gating dysfunction in FXS (Deng et al., 2013; Zaman et al., 2017). The adult mouse data are consistent with data from humans with FXS who show no differences in ASR and reduced PPI suggesting that these sensorimotor gating measures can be used as potential biomarkers (Frankland et al., 2004; Hessl et al., 2009). Together these results strongly suggest that increased MMP-9 in FXS underlies abnormal sensorimotor gating and may cause sensory hypersensitivity. This conclusion is consistent with studies which over-expressed MMP-9 in mice and found FXS-like symptoms (Gkokas et al., 2014).

ASR in *Fmr1* KO mice has been examined by a number of groups, but the results are mixed in a manner indicating sensitivity of measures to variations in stimulus parameters, age, and genetic background. Chen and Toth (2001) showed that ASR is significantly reduced in 7-10 weeks old *Fmr1* KO mice compared to WT mice on the FVB background. Yun et al. (2006) showed reduced ASR in *Fmr1* KO mice compared to WT in FVB strain mice older than 4 weeks, but ASR was not different in mice younger than 3 weeks. In the C57B6/J genetic background, ASR was shown to be higher in the *Fmr1* KO mice compared to WT for stimuli in the 70-80 dB range (Nielson et al., 2002). However, when a 120dB startle stimulus was used, the WT mice showed stronger ASR than the *Fmr1* KO mice. Frankland et al. (2004) tested C57B6/J mice and found no difference in ASR for stimuli <90dB SPL. However, for >95dB SPL, ASR was stronger in the WT mice compared to *Fmr1* KO mice. Ding et al. (2014) and Veeraragavan et al. (2011) showed no genotype difference in ASR. Together the preponderance of evidence suggest that ASR is either not different between the genotypes, or decreased in *Fmr1* KO mice compared to

WT. Our data are consistent with this trend, with young *Fmr1* KO mice showing reduced ASR and adults showing no genotype difference, although the mechanisms for age-dependent genotype differences in ASR are unclear. There were no significant differences in average weight of mice between the two genotypes in either young or adult ages, suggesting that this is not a factor in the age effect on genotype difference in ASR. It is possible that the muscle tone is different in young mice. Largo and Schinzel (1985) suggested a developmental delay in motor function, with boys with FXS showing reduced muscle tone. But, very little is known about development of muscle function in the *Fmr1* KO mice. Future studies should examine electromyographic responses in these mice to determine potential delays in muscle function. The difference between young and adult ASR responses should, however, not be surprising because developmentally transient genotype differences appear to a prominent feature in FXS (see Meredith et al., for a review).

Several studies have examined PPI in *Fmr1* KO mice, also with mixed results. Chen and Toth (2001) showed PPI was increased in *Fmr1* KO mice compared to WT (FVB background) at both 75dB and 85dB SPL prepulse intensities. The differences with our PPI result may arise from different protocols used in the two studies. We included all prepulse intensities in one session, whereas, Chen and Toth (2001) tested the lower intensity a month prior to testing the higher intensity. Nielson et al. (2002), Frankland et al. (2004), and Ding et al. (2014) also reported increased PPI in *Fmr1* KO mice on the C57B6/J background. Veeraragavan et al. (2011) reported no difference and De Vrij et al. (2008) used eye-blink response and reported decreased PPI in the *Fmr1* KO mice. Despite this evidence

suggesting increased PPI in the *Fmr1* KO mouse, humans with FXS show significantly reduced PPI (Frankland et al., 2004 and Hessl et al., 2009), which is consistent with our results.

A novel finding of this paper is that abnormal MMP-9 activity may underlie sensorimotor gating abnormalities in FXS. MMP-9 is one of the targets of FMRP, so with the absence of FMRP, there is an upregulation of MMP-9 (Dziembowska et al., 2013) in several regions of the brain in FXS. The ASR pathway consists of the auditory nerve input to the ventral cochlear nucleus, which connects to the caudal pontine reticular nucleus, from there synapsing onto the motor neurons of the spinal cord whose activity elicits the startle response (Koch and Schnitzler, 1997). We show here that MMP-9 levels are increased in the IC of *Fmr1* KO mice as well. The IC is a major hub of both the ascending and descending auditory pathway, and is critically involved in PPI (Fendt et al., 2001). The activation of the IC by the prepulse sound is rapidly relayed as a long duration inhibition of the neurons of the pontine reticular nucleus neurons, which are involved in the ASR. The inhibition generated by the IC reduces ASR, leading to the classic PPI of startle response. Interestingly we found increased MMP-9 in the IC at P7 and P12, but not at P18 or P40. We found reduced PPI at ~P23 and ~P50, when MMP-9 levels in the IC are similar to WT. This suggests that MMP-9 plays a crucial role in the development of IC, and any abnormalities in early development are sustained into adulthood, even though MMP-9 levels are normalized. This makes the crucial prediction that any pharmacological treatment through MMP-9 manipulation to reduce sensorimotor gating abnormalities

would be more effective if given during the P7-P12 window, rather than in adulthood. Future studies will test this prediction.

Conclusions

In findings similar to those seen in humans with FXS, we provide evidence for reduced PPI in the *Fmr1* KO mice. PPI, may therefore, be developed as biomarker for pursuit of translation-relevant therapeutic avenues in FXS. Reduced PPI was seen in both adult and young *Fmr1* KO mice, suggesting early developmental origin of sensorimotor gating abnormalities in FXS and the necessity to provide treatment early in development. Finally, our data suggest a potential target for reducing sensory hypersensitivity in FXS through a reduction of MMP-9 levels using specific inhibitors and at specific developmental time points.

1. Bilousova, T.V., Dansie, L., Ngo, M., Aye, J., Charles, J.R., Ethell, D.W., Ethell, I.M., 2009. Minocycline promotes dendritic spine maturation and improves behavioural performance in the fragile X mouse model. *J. Med. Genet.* 46, 94–102. https://doi.org/10.1136/jmg.2008.061796

2. Chen, L., Toth, M., 2001. Fragile X mice develop sensory hyperreactivity to auditory stimuli. *Neuroscience* 103, 1043–1050. https://doi.org/10.1016/S0306-4522(01)00036-7

3. Cho, Y., Gong, T.-W.L., Stöver, T., Lomax, M.I., Altschuler, R.A., 2002. Gene Expression Profiles of the Rat Cochlea, Cochlear Nucleus, and Inferior Colliculus. JARO *J. Assoc. Res. Otolaryngol.* 3, 54–67. https://doi.org/10.1007/s101620010042

4. de Vrij, F.M.S., Levenga, J., van der Linde, H.C., Koekkoek, S.K., De Zeeuw, C.I., Nelson, D.L., Oostra, B.A., Willemsen, R., 2008. Rescue of behavioral phenotype and neuronal protrusion morphology in Fmr1 KO mice. *Neurobiol. Dis.* 31, 127–132. https://doi.org/10.1016/j.nbd.2008.04.002

5. Deng, P.Y., Rotman, Z., Blundon, J.A., Cho, Y., Cui, J., Cavalli, V., Zakharenko, S.S. and Klyachko, V.A., 2013. FMRP regulates neurotransmitter release and synaptic information transmission by modulating action potential duration via BK channels. *Neuron*, 77(4), 696-711.

6. Ding, Q., Sethna, F., Wang, H., 2014. Behavioral analysis of male and female Fmr1 knockout mice on C57BL/6 background. *Behav. Brain Res.* 0, 72–78. https://doi.org/10.1016/j.bbr.2014.05.046

7. Dziembowska, M., Pretto, D.I., Janusz, A., Kaczmarek, L., Leigh, M.J., Gabriel, N., Durbin-Johnson, B., Hagerman, R.J., Tassone, F., 2013. High MMP-9 activity levels in fragile X syndrome are lowered by minocycline. *Am. J. Med. Genet. A.* 161, 1897–1903. https://doi.org/10.1002/ajmg.a.36023

8. Ethridge, L.E., White, S.P., Mosconi, M.W., Wang, J., Byerly, M.J., Sweeney, J.A., 2016. Reduced habituation of auditory evoked potentials indicate cortical hyper-excitability in Fragile X Syndrome. *Transl. Psychiatry* 6, e787. https://doi.org/10.1038/tp.2016.48

9. Fendt, M., Li, L. and Yeomans, J.S., 2001. Brain stem circuits mediating prepulse inhibition of the startle reflex. *Psychopharmacology,* 156(2-3), pp.216-224. https://doi.org/10.1007/s002130100794

10. Frankland, P.W., Wang, Y., Rosner, B., Shimizu, T., Balleine, B.W., Dykens, E.M., Ornitz, E.M., Silva, A.J., 2004. Sensorimotor gating abnormalities in young males with fragile X syndrome and Fmr1-knockout mice. *Mol. Psychiatry* 9, 417–425. https://doi.org/10.1038/sj.mp.4001432

11. Garcia-Pino, E., Gessele, N., Koch, U., 2017. Enhanced Excitatory Connectivity and Disturbed Sound Processing in the Auditory Brainstem of Fragile X Mice. *J. Neurosci*. 37, 7403–7419. https://doi.org/10.1523/JNEUROSCI.2310-16.2017

12. Gkogkas, C.G., Khoutorsky, A., Cao, R., Jafarnejad, S.M., Prager-Khoutorsky, M., Giannakas, N., Kaminari, A., Fragkouli, A., Nader, K., Price, T.J. and Konicek, B.W., 2014. Pharmacogenetic inhibition of eIF4E-dependent Mmp9 mRNA translation reverses fragile X syndrome-like phenotypes. *Cell reports*, 9(5), pp.1742-1755. https:// 10.1016/j.celrep.2014.10.064

13. Hatton, D.D., Sideris, J., Skinner, M., Mankowski, J., Bailey, D.B., Roberts, J., Mirrett, P., 2006. Autistic behavior in children with fragile X syndrome: Prevalence, stability, and the impact of FMRP. *Am. J. Med. Genet. A*. 140A, 1804–1813. https://doi.org/10.1002/ajmg.a.31286

14. Hessl, D., Berry-Kravis, E., Cordeiro, L., Yuhas, J., Ornitz, E.M., Campbell, A., Chruscinski, E., Hervey, C., Long, J.M., Hagerman, R.J., 2009. Prepulse inhibition in fragile X syndrome: Feasibility, reliability, and implications for treatment. *Am. J. Med. Genet. B Neuropsychiatr. Genet*. 150B, 545–553. https://doi.org/10.1002/ajmg.b.30858

15. Huber, K.M., Gallagher, S.M., Warren, S.T., Bear, M.F., 2002. Altered synaptic plasticity in a mouse model of fragile X mental retardation. *Proc. Natl. Acad. Sci*. 99, 7746–7750. https://doi.org/10.1073/pnas.122205699

16. Koch, M., Schnitzler, H.-U., 1997. The acoustic startle response in rats—circuits mediating evocation, inhibition and potentiation. *Behav. Brain Res*. 89, 35–49. https://doi.org/10.1016/S0166-4328(97)02296-1

17. Largo, R.H. and Schinzel, A., 1985. Developmental and behavioural disturbances in 13 boys with fragile X syndrome. *European Journal of Pediatrics,* 143(4), pp.269-275. https://doi.org/10.1007/BF00442299

18. Li, L., Korngut, L.M., Frost, B.J., Beninger, R.J., 1998. Prepulse inhibition following lesions of the inferior colliculus: prepulse intensity functions. *Physiol. Behav*. 65, 133–139. https://doi.org/10.1016/S0031-9384(98)00143-7

19. Lovelace, J.W., Wen, T.H., Reinhard, S., Hsu, M.S., Sidhu, H., Ethell, I.M., Binder, D.K., Razak, K.A., 2016. Matrix metalloproteinase-9 deletion rescues auditory evoked potential habituation deficit in a mouse model of Fragile X Syndrome. *Neurobiol. Dis*. 89, 126–135. https://doi.org/10.1016/j.nbd.2016.02.002

20. Meredith, R.M., Dawitz, J., Kramvis, I., 2012. Sensitive time-windows for susceptibility in neurodevelopmental disorders. *Trends Neurosci*. 35, 335–344. https://doi.org/10.1016/j.tins.2012.03.005

21. Mott, B., Wei, S., 2014. Firing Property of Inferior Colliculus Neurons Affected by FMR1 Gene Mutation. *J. Otol*. 9, 86–90. https://doi.org/10.1016/S1672-2930(14)50020-7

22. Nielsen, D.M., Derber, W.J., McClellan, D.A., Crnic, L.S., 2002. Alterations in the auditory startle response in Fmr1 targeted mutant mouse models of fragile X syndrome. *Brain Res*. 927, 8–17. https://doi.org/10.1016/S0006-8993(01)03309-1

23. Rais, M., Binder, D.K., Razak, K.A., Ethell, I.M., 2018. Sensory Processing Phenotypes in Fragile X Syndrome. *ASN NEURO* 10. https://doi.org/10.1177/1759091418801092

24. Reinhard, S.M., Razak, K., Ethell, I.M., 2015. A delicate balance: role of MMP-9 in brain development and pathophysiology of neurodevelopmental disorders. *Front. Cell. Neurosci*. 9. https://doi.org/10.3389/fncel.2015.00280

25. Renoux, A.J., Sala-Hamrick, K.J., Carducci, N.M., Frazer, M., Halsey, K.E., Sutton, M.A., Dolan, D.F., Murphy, G.G., Todd, P.K., 2014. Impaired sensorimotor gating in Fmr1 knock out and Fragile X premutation model mice. *Behav. Brain Res*. 267, 42–45. https://doi.org/10.1016/j.bbr.2014.03.013

26. Schneider, A., Leigh, M.J., Adams, P., Nanakul, R., Chechi, T., Olichney, J., Hagerman, R., Hessl, D., 2013. Electrocortical changes associated with minocycline treatment in fragile X syndrome. *J. Psychopharmacol.* (Oxf.) 27, 956–963. https://doi.org/10.1177/0269881113494105

27. Scott KE, Schormans AL, Pacoli K , De Oliveira C, Allman BL, Schmid S., 2018. Altered auditory processing, filtering, and reactivity in the Cntnap2 knockout rat model for neurodevelopmental disorders.

28. Setz, C., Brand, Y., Radojevic, V., Hanusek, C., Mullen, P.J., Levano, S., Listyo, A., Bodmer, D., 2011. Matrix metalloproteinases 2 and 9 in the cochlea: expression and activity after aminoglycoside exposition. *Neuroscience* 181, 28–39. https://doi.org/10.1016/j.neuroscience.2011.02.043

29. Sidhu, H., Dansie, L.E., Hickmott, P.W., Ethell, D.W., Ethell, I.M., 2014. Genetic Removal of Matrix Metalloproteinase 9 Rescues the Symptoms of Fragile X Syndrome in a Mouse Model. *J. Neurosci.* 34, 9867–9879. https://doi.org/10.1523/JNEUROSCI.1162-14.2014

30. Sidorov, M.S., Auerbach, B.D., Bear, M.F., 2013. Fragile X mental retardation protein and synaptic plasticity. *Mol. Brain* 6, 15. https://doi.org/10.1186/1756-6606-6-15

31. Siller, S.S., Broadie, K., 2011. Neural circuit architecture defects in a Drosophila model of Fragile X syndrome are alleviated by minocycline treatment and genetic removal of matrix metalloproteinase. *Dis. Model. Mech.* 4, 673–685. https://doi.org/10.1242/dmm.008045

32. Sinclair, D., Oranje, B., Razak, K.A., Siegel, S.J., Schmid, S., 2017. Sensory processing in autism spectrum disorders and Fragile X syndrome—From the clinic to animal models. *Neurosci. Biobehav. Rev.* 76, 235–253. https://doi.org/10.1016/j.neubiorev.2016.05.029

33. Snow, K., Doud, L.K., Hagerman, R., Pergolizzi, R.G., Erster, S.H., Thibodeau, S.N., 1993. Analysis of a CGG sequence at the FMR-1 locus in fragile X families and in the general population. *Am. J. Hum. Genet.* 53, 1217–1228.

34. Tsiouris, J.A., Brown, W.T., 2004. Neuropsychiatric Symptoms of Fragile X Syndrome. *CNS Drugs* 18, 687–703. https://doi.org/10.2165/00023210-200418110-00001

35. Valsamis, B. and Schmid, S., 2011. Habituation and prepulse inhibition of acoustic startle in rodents. *JoVE (Journal of Visualized Experiments)*, (55), p.e3446. doi: 10.3791/3446

36. Veeraragavan, S., Bui, N., Perkins, J.R., Yuva-Paylor, L.A., Carpenter, R.L., Paylor, R., 2011. Modulation of behavioral phenotypes by a muscarinic M1 antagonist in a mouse model of fragile X syndrome. *Psychopharmacology (Berl.)* 217, 143. https://doi.org/10.1007/s00213-011-2276-6

37. Wang, X., Zorio, D.A.R., Schecterson, L., Lu, Y., Wang, Y., 2018. Postsynaptic FMRP Regulates Synaptogenesis In Vivo in the Developing Cochlear Nucleus. *J. Neurosci*. 38, 6445–6460. https://doi.org/10.1523/JNEUROSCI.0665-18.2018

38. Wen, T.H., Afroz, S., Reinhard, S.M., Palacios, A.R., Tapia, K., Binder, D.K., Razak, K.A., Ethell, I.M., 2018. Genetic Reduction of Matrix Metalloproteinase-9 Promotes Formation of Perineuronal Nets Around Parvalbumin-Expressing Interneurons and Normalizes Auditory Cortex Responses in Developing Fmr1 Knock-Out Mice. *Cereb. Cortex* 28, 3951–3964. https://doi.org/10.1093/cercor/bhx258

39. Yuhas, J., Cordeiro, L., Tassone, F., Ballinger, E., Schneider, A., Long, J.M., Ornitz, E.M., Hessl, D., 2011. Brief Report: Sensorimotor Gating in Idiopathic Autism and Autism Associated with Fragile X Syndrome. *J. Autism Dev. Disord.* 41, 248–253. https://doi.org/10.1007/s10803-010-1040-9

40. Yun, S.-W., Platholi, J., Flaherty, M.S., Fu, W., Kottmann, A.H., Toth, M., 2006. Fmrp is required for the establishment of the startle response during the critical period of auditory development. *Brain Res.* 1110, 159–165. https://doi.org/10.1016/j.brainres.2006.06.086

41. Zaman T, De Oliveira C, Smoka M, Narla C, Poulter M, Schmid S., 2017. BK channels mediate synaptic plasticity underlying habituation in rats. *J. Neurosci*, 37 (17): 4540-4551.

42. Zorio DA, Jackson CM, Liu Y, Rubel EW, Wang Y. (2017) Cellular distribution of the fragile X mental retardation protein in the mouse brain. *J Comp Neurol* 525:818–849. doi: 10.1002/cne.24100

Chapter 6

Conclusions

The central NIHL changes at the molecular and population activity levels builds upon previous research on central gain. These studies aimed to identify mechanistic changes higher auditory centers and specific time course that is modulated by NIHL.

In chapter 2, to test the hypothesis that there is enhanced central gain and cortical activity at the expense of temporal processing, electroencephalography (EEG) screw electrodes were implanted over the dura to measure the trajectory of changes in resting EEG spectral power, evoked response potentials (ERPs), and the auditory steady state response (ASSR) in the auditory and frontal cortices. The strength of this approach was a longitudinal measurement of EEG changes pre- and post-NIHL (10-, 23-, and 45 days) in the same animals. We found that all mice had a persistent elevated threshold shift past 90 dB SPL up, which was the sound level that all sounds were tested at. During resting measurements, higher frequency power was elevated in RR group, potentially indicating elevated spontaneous activity. For sound evoked responses, there was recovery in both AC and FC which indicates recovered and potentially amplified sound detection from residual hearing. There was a cortical region-specific difference in how temporal processing recovered in the AC, which may be indicative of central gain at the expense of a major cognitive region. Changes in temporal processing are not identical between the AC and FC, where there is recovery in the first region that potentially occurs at the expense of the

latter. This aligns with the literature following diminished cognition as it relates to hearing loss and enhanced or recovered central gain in the AC.

In chapter 3, to test the hypothesis that MMP-9 activity increased 1-day post NIHL after noise exposure and PNN degradation lasted over time, we measured these molecular components at specific time points. We did not find any changes from their respective control groups in either MMP-9 activity or PNN measurements. This may indicate that the time points we chose to measure at were too late to capture the specific molecular changes occurring post-NIHL. For MMP-9, if neuroinflammation occurs immediately after NIHL we may have to examine MMP-9 activity within a day after noise exposure. Alternatively, neuroinflammation may be acting as a secondary mediator and investigating proinflammatory cytokine regulations may elucidate their role in the AC following NIHL. Our PNN data align with our lab's previous study, though in a different mouse model, that PNN intensity has recovered over time. We tested PNN density and intensity at 23- and 45-65 days post-NIHL, indicating that PNN degradation likely recovered between 10-23 days after noise exposure. MMP-9 abundance and activity may regulate multiple regions within the central auditory pathway that influence behavioral and potentially neuronal circuitry. With our findings post-NIHL, however, we may not have targeted the correct time to see any enhancements in MMP-9 activity. Neuroinflammation markers are upregulated around 12-hours after noise exposure, which may indicate that MMP-9 activity also fluctuates around this time and returns to baseline by 1-day post-NIHL.

In chapter 4, to test the hypothesis that minocycline can reverse the effects of NIHL, sound evoked and ASSR EEG recordings were measured after NIHL. Our data found that,

after threshold shifts, minocycline increased ERP amplitudes in AC and FC compared to pre-NIHL up to 23-days post-NIHL. However, with temporal processing there was also a cortical region-specific difference to where both minocycline and saline treated groups had enhanced ITPC means by 23-days post-NIHL to 40 Hz ASSR stimulus. For the gap-ASSR analysis, there were also cortical differences – AC had enhanced ITPC at every gap duration by 23-days post-NIHL, but FC had an effect of treatment at 8- and 9 ms. With these findings, minocycline enhanced sound evoked responses, but may not have been the influencing factor in enhanced temporal processing to mice with hearing loss. Minocycline can still be used to target MMP-9 in a permanent hearing threshold model. We would expect to see similar cortical region-specific recovery in temporal processing with only minocycline treatment and a stronger enhancement of central gain.

I carried out an investigation of whether genetically reduced MMP-9 in a Fragile X Syndrome knock-out (KO) mouse influences behavioral outcomes before beginning the investigation of the central effects of NIHL. Specifically, we measured their acoustic startle response (ASR) and pre-pulse inhibition (PPI) compared to wild type and full knock-out age matched mice. We found that in young KO mice, ASR and PPI were reduced. However, adult KO mice PPI was significantly reduced from both WT and heterozygous MMP-9/KO mouse. This indicated that MMP-9 reduction rescued a behavioral phenotype in a FXS mouse model and could act as a therapeutic target.